# FOUR-DIMENSIONAL CARDIOVASCULAR MAGNETIC RESONANCE FLOW ANALYSIS AND VELOCITY MAPPING OF ALTERATIONS OF RIGHT HEART FLOW PATTERNS AND MAIN PULMONARY ARTERY HEMODYNAMICS IN PATIENTS WITH REPAIRED TETRALOGY OF FALLOT


## Dr. KARMAKAR DEEPMALA KALYANKUMAR

**DM CARDIOVASCULAR IMAGING AND VASCULAR**

**INTERVENTIONALRADIOLOGY**


**(2021-2023)**



**SREE CHITRA TIRUNAL INSTITUTE FOR MEDICAL SCIENCES**

**AND TECHNOLOGY, TRIVANDRUM**

An Institution of National Importance established by an Act of the Indian Parliament

(Act No.52 of 1980)

Dept. of Science and Technology, Govt. of Indiawww.sctimst.ac.in

# FOUR-DIMENSIONAL CARDIOVASCULAR MAGNETIC RESONANCE FLOW ANALYSIS AND VELOCITY MAPPING OF ALTERATIONS OF RIGHT HEART FLOW PATTERNS AND MAIN PULMONARY ARTERY HEMODYNAMICS IN PATIENTS WITH REPAIRED TETRALOGY OF FALLOT

A THESIS SUBMITTED BY

**Dr. KARMAKAR DEEPMALA KALYANKUMAR**

TO

**SREE CHITRA TIRUNAL INSTITUTE FOR MEDICAL**

**SCIENCES ANDTECHNOLOGY, TRIVANDRUM.**

IN PARTIAL FULFILMENT OF THE REQUIREMENTS

FOR THE AWARD OF

**DM CARDIOVASCULAR IMAGING AND VASCULAR**

**INTERVENTIONALRADIOLOGY**

(2021-2023)

## DECLARATION BY THE STUDENT

## CERTIFICATE

I, **Dr Karmakar Deepmala Kalyankumar** hereby certify that I had personally carried out the work depicted in the thesis titled, "**Four-Dimensional Cardiovascular Magnetic Resonance flow analysis and velocity mapping of alterations of right heart flow patterns and main pulmonary artery hemodynamics in patients with repaired Tetralogy of Fallot"**

No part of this thesis has been submitted for the award of any other degree or diploma prior to this date.

Deepmala

Dr Karmakar Deepmala Kalyankumar

Date: 19th August 2023

श्री चित्रा तिरुनाल आयुर्विज्ञान और प्रौद्योगिकी संस्थान, त्रिवेन्द्रम
तिरुवनन्तपुरम - ६९५०११, केरल, इंडिया
SREE CHITRA TIRUNAL INSTITUTE FOR MEDICAL SCIENCES AND TECHNOLOGY, TRIVANDRUM
Thiruvananthapuram - 695 011, Kerala, India
*(An Institute of National Importance under Govt. of India)*
Grams : Chitramet, Phone : +91-471-2443152, Fax : +91-471-2550728 / 2446433, E-mail : sct@sctimst.ac.in, Website : www.sctimst.ac.in

## CERTIFICATE BY THE RESEARCH GUIDE

Name of the Guide: **Dr Anoop A**

Division/Department: **Imaging Sciences and Interventional Radiology**

This is to certify that **Dr Karmakar Deepmala Kalyankumar,** department of **Imaging Sciences and Interventional Radiology** of this institute has fulfilled the requirements prescribed for the **DM Cardiovascular Imaging and Vascular Interventional Radiology** degree of the Sree Chitra Tirunal Institute for Medical Sciences and Technology, Trivandrum.

The thesis entitled, "**Four Dimensional Cardiovascular Magnetic Resonance flow analysis and velocity mapping of alterations of right heart flow patterns and main pulmonary artery hemodynamics in patients with repaired Tetralogy of Fallot'** was carried out under my direct supervision. No part of the thesis was submitted for the award of any degree or diploma prior to this date.

*Clearance was obtained from the Institutional Ethics Committee for carrying out the study.

**Dr. Anoop A**

Associate Professor

Department of Imaging Sciences and Interventional Radiology, SCTIMST, Trivandrum

Date: 21st July 2023

श्री चित्रा तिरुनाल आयुर्विज्ञान और प्रौद्योगिकी संस्थान, त्रिवेन्द्रम
तिरुवनन्तपुरम - ६९५०११, केरल, इंडिया
SREE CHITRA TIRUNAL INSTITUTE FOR MEDICAL SCIENCES AND TECHNOLOGY, TRIVANDRUM
Thiruvananthapuram - 695 011, Kerala, India
*(An Institute of National Importance under Govt. of India)*
Grams : Chitramet, Phone : +91-471-2443152, Fax : +91-471-2550728 / 2446433, E-mail : sct@sctimst.ac.in, Website : www.sctimst.ac.in

## CERTIFICATE BY THE RESEARCH CO-GUIDE

Name of the Guide: **Dr Jineesh V**

Division/Department: **Imaging Sciences and Interventional Radiology**

This is to certify that **Dr Karmakar Deepmala Kalyankumar,** department of **Imaging Sciences and Interventional Radiology** of this institute has fulfilled the requirements prescribed for the **DM Cardiovascular Imaging and Vascular Interventional Radiology** degree of the Sree Chitra Tirunal Institute for Medical Sciences and Technology, Trivandrum.

The thesis entitled, "**Four Dimensional Cardiovascular Magnetic Resonance flow analysis and velocity mapping of alterations of right heart flow patterns and main pulmonary artery hemodynamics in patients with repaired Tetralogy of Fallot'** was carried out under my direct supervision. No part of the thesis was submitted for the award of any degree or diploma prior to this date.

*Clearance was obtained from the Institutional Ethics Committee for carrying out the study.

**Dr. Jineesh V**

Associate Professor

Department of Imaging Sciences and Interventional Radiology, SCTIMST, Trivandrum

Date: 19th August 2023

श्री चित्रा तिरुनाल आयुर्विज्ञान और प्रौद्योगिकी संस्थान, त्रिवेन्द्रम
तिरुवनन्तपुरम - ६९५०११, केरल, इंडिया
SREE CHITRA TIRUNAL INSTITUTE FOR MEDICAL SCIENCES AND TECHNOLOGY, TRIVANDRUM
Thiruvananthapuram - 695 011, Kerala, India
*(An Institute of National Importance under Govt. of India)*
Grams : Chitramet, Phone : +91-471-2443152, Fax : +91-471-2550728 / 2446433, E-mail : sct@sctimst.ac.in, Website : www.sctimst.ac.in

## CERTIFICATE BYTHE RESEARCH CO-GUIDE

Name of the Guide: Dr Sabarinath Menon

Division/Department: Cardiovascular and Thoracic Surgery

This is to certify that Dr **Karmakar Deepmala Kalyankumar**, department of **Imaging Sciences and Interventional Radiology** of this institute has fulfilled the requirements prescribed for the DM Cardiovascular Imaging and Vascular Interventional Radiology degree of the Sree Chitra Tirunal Institute for Medical Sciences and Technology, Trivandrum.

The thesis entitled, **"Four Dimensional Cardiovascular Magnetic Resonance flow analysis and velocity mapping of alterations of right heart flow patterns and main pulmonary artery hemodynamics in patients with repaired Tetralogy of Fallot'** was carried out under my direct supervision. No part of the thesis was submitted for the award of any degree or diploma prior to this date.

*Clearance was obtained from the Institutional Ethics Committee for carrying out the study.

11/8/23

Dr Sabarinath Menon

Professor

Department of Cardiovascular and Thoracic Surgery, SCTIMST, Trivandrum

Date: 11th August 2023

श्री चित्रा तिरुनाल आयुर्विज्ञान और प्रौद्योगिकी संस्थान, त्रिवेन्द्रम
तिरुवनन्तपुरम - ६९५०११, केरल, इंडिया
SREE CHITRA TIRUNAL INSTITUTE FOR MEDICAL SCIENCES AND TECHNOLOGY, TRIVANDRUM
Thiruvananthapuram - 695 011, Kerala, India
*(An Institute of National Importance under Govt. of India)*
Grams : Chitramet, Phone : +91-471-2443152, Fax : +91-471-2550728 / 2446433, E-mail : sct@sctimst.ac.in, Website : www.sctimst.ac.in

## CERTIFICATE BY THE RESEARCH CO-GUIDE

Name of the Guide: Dr Deepa S Kumar

Division/Department: Cardiology

This is to certify that **Dr Karmakar Deepmala Kalyankumar**, department of Imaging Sciences and Interventional Radiology of this institute has fulfilled the requirements prescribed for the DM Cardiovascular Imaging and Vascular Interventional Radiology degree of the Sree Chitra Tirunal Institute for Medical Sciences and Technology, Trivandrum.

The thesis entitled, **"Four Dimensional Cardiovascular Magnetic Resonance flow analysis and velocity mapping of alterations of right heart flow patterns and main pulmonary artery hemodynamics in patients with repaired Tetralogy of Fallot"** was carried out under my direct supervision. No part of the thesis was submitted for the award of any degree or diploma prior to this date.

*Clearance was obtained from the Institutional Ethics Committee for carrying out the study.

Dr Deepa S Kumar

Additional Professor

Department of Cardiology, SCTIMST, Trivandrum

Date: 19th August 2023

श्री चित्रा तिरुनाल आयुर्विज्ञान और प्रौद्योगिकी संस्थान, त्रिवेन्द्रम
तिरुवनन्तपुरम - ६९५०११, केरल, इंडिया
SREE CHITRA TIRUNAL INSTITUTE FOR MEDICAL SCIENCES AND TECHNOLOGY, TRIVANDRUM
Thiruvananthapuram - 695 011, Kerala, India
*(An Institute of National Importance under Govt. of India)*
Grams : Chitramet, Phone : +91-471-2443152, Fax : +91-471-2550728 / 2446433, E-mail : sct@sctimst.ac.in, Website : www.sctimst.ac.in

# APPROVAL OF THE THESIS

The thesis entitled

**Four-Dimensional Cardiovascular Magnetic Resonance flow analysis and velocity mapping of alterations of right heart flow patterns and main pulmonary artery hemodynamics in patients with repaired Tetralogy of Fallot'**

Submitted by

Dr Karmakar Deepmala Kalyankumar

for the degree of

**DM Cardiovascular Imaging and Vascular Interventional Radiology**

of SREE CHITRA TIRUNAL INSTITUTE FOR MEDICAL SCIENCES AND TECHNOLOGY, TRIVANDRUM

is evaluated and approved by

**Dr. Anoop A**

(Name & Signature of the Guide)

(Name & Signature of thesis examiner)

## ACKNOWLEDGEMENTS

I hereby express my sincere gratitude to all my teachers & guides especially Dr Anoop A (Associate Professor), Dr. Jineesh V (Associate Professor), Department of Imaging Sciences and Interventional Radiology, Dr Sabarinath Menon (Professor), Department of Cardiovascular and Thoracic Surgery, Dr. Deepa S Kumar (Additional Professor), Department of Cardiology for their constant unwavering support, insightful criticism, expert supervision, and immense patience throughout this study.

I would specially like to acknowledge my gratitude to my past and present colleagues and the technologists of the Department of IS and IR and the advanced radiology technology trainees of the department for their valuable assistance at all times during this study.

I would also like to extend my heartfelt gratitude to my family for being immensely supportive all through my endeavors. I could not have achieved what I have without their prayers, love, and support.

Last but not least I am eternally grateful to all my patients & their relatives who have been very understanding and generous with their cooperation all through the study.

## TABLE OF CONTENTS


| | |
|---|---|
| Introduction | 1 |
| Aim and Objectives | 3 |
| Literature Review | 4 |
| Materials and methods | 17 |
| Results and observations | 44 |
| Discussion | 76 |
| Summary and conclusion | 86 |
| References | 91 |
| Annexure: | 97 |
| Patient Information Sheet | 97 |
| Patient Consent Form | 101 |
| Institutional Ethics Committee approval | 104 |
| Curriculum Vitae | 105 |
| Plagiarism Check Report | 107 |

## LIST OF FIGURES


| Figure No | Figure Caption | Page No |
|---|---|---|
| Figure 1 | Basic acquisition of 2D PCMRI | 12 |
| Figure 2 | Basic acquisition of 4D Flow MRI | 12 |
| Figure 3 | STROBE (Strengthening the Reporting of Observational Studies in Epidemiology) flowchart of our studied population. | 19 |
| Figure 4 | Reconstructed PCMRI showing the planning for MPA proximal to the bifurcation | 23 |
| Figure 5 | Reconstructed PCMRI images showing the planning for RPA and LPA between their respective origins and bifurcations. | 23 |
| Figure 6 | Right pulmonary artery flow assessment using 2D PCMRI | 25 |
| Figure 7 | Flow chart showing basic steps in the 4D flow study | 28 |
| Figure 8 | Overview of a typical 4D flow workflow | 28 |
| Figure 9 | Steps used in pre-processing of 4D flow data | 29 |
| Figure 10 | Technique for centerline extraction in MPA, RPA and LPA | 31 |
| Figure 11 | Color coded velocity and velocity vectors in MPA of a repaired TOF patient | 32 |
| Figure 12 | 3D particle trace visualization illustrating the dynamics of main pulmonary artery in repaired TOF patients. | 33 |

| | | |
|---|---|---|
| Figure 13 | 3D particle trace visualization illustrating the dynamics of right pulmonary artery in repaired TOF patients. | 33 |
| Figure 14 | 3D particle trace visualization illustrating the dynamics of left pulmonary artery in repaired TOF patients. | 34 |
| Figure 15 | 3D particle trace visualization in a control illustrating the dynamics of main pulmonary artery. | 34 |
| Figure 16 | Color coded velocity images showing peak velocity in MPA | 35 |
| Figure 17 | RPA flow measurements at three regions | 36 |
| Figure 18 | LPA flow measurements at three regions | 37 |
| Figure 19 | 4D flow MRI with streamlines demonstrating vortical flow in LPA with measurements at two places (at the vortex and distal to the vortex) | 37 |
| Figure 20 | Technique for calculation of WSS in MPA in a repaired TOF patient | 39 |
| Figure 21 | Technique for calculation of EL in MPA in a repaired TOF patient | 40 |
| Figure 22 | Pressure visualization in MPA in a repaired TOF patient | 41 |
| Figure 23 | Pearson correlation between PR by 2DPCMRI and 4D flow | 51 |
| Figure 24 | Bland Altman plot showing the Limits of Agreement between 2D and 4D CMRI sequence for measuring PR. | 52 |
| Figure 25 | Bland Altmann plot between aortic total volume 4D and Total Pulmonary Venous flow 4D | 54 |
| Figure 26 | Boxplot comparing the Mean differences between Total pulmonary venous blood flow and MPA total volume as measured by 2D PMCRI and 4D flow | 55 |

| | | |
|---|---|---|
| Figure 27 | Scatterplot between QRS duration and WSS RVOT | 57 |
| Figure 28 | Progressive reduction in the regurgitation fraction in RPA and increase in the total volume of blood across RPA from proximal to distal aspect of the artery. | 61 |
| Figure 29 | Progressive reduction in the regurgitation fraction in LPA and increase in the total volume of blood across LPA from proximal to distal aspect of the artery. | 61 |
| Figure 30 | Boxplot comparing the Mean differences between Total pulmonary venous blood flow on 4D and RPA+LPA volume at the Vortex versus Distal to the vortex on 4D | 63 |
| Figure 31 | Boxplot showing the comparison between the subjects who had undergone Pulmonary valve replacement and those who had not with respect to PR by 4D flow | 66 |
| Figure 32 | Bland Altman plot for Total pulmonary venous flow on 4D between observer 1 and 2 | 69 |
| Figure 33 | Bland Altman plot for Aortic root total volume on 4D between observer 1 and 2 | 70 |
| Figure 34 | Bland Altman plot for Total vol RPA +LPA (at the vortex) between observer 1 and 2 | 71 |
| Figure 35 | Bland Altman plot for Total vol RPA +LPA (distal to the vortex) between observer 1 and 2 | 72 |
| Figure 36 | Pulmonary artery flow assessment using 2D PCMRI in a young adult with pulmonary regurgitation 15 years after tetralogy of Fallot repair. | 73 |
| Figure 37 | 4D flow MRI with streamlines in a repaired TOF patient with pulmonary regurgitation demonstrating vortical flow | 73 |
| Figure 38 | Right pulmonary artery flow assessment using 2D PCMRI in a repaired TOF patient | 74 |

| | | |
|---|---|---|
| Figure 39 | 4D flow MRI with streamlines in RPA in a repaired TOF patient demonstrating vortical flow | 74 |
| Figure 40 | Left pulmonary artery flow assessment using 2D PCMRI in a repaired TOF patient | 75 |
| Figure 41 | 4D flow MRI with streamlines in LPA in a repaired TOF patient demonstrating vortical flow | 75 |

# LIST OF TABLES


| Table No | Table Caption | Page No |
|---|---|---|
| Table 1 | Summary of 4D flow studies | 15 |
| Table 2 | Routine 2D sequences acquired in a repaired TOF patient | 24 |
| Table 3 | Comparison between the imaging parameters of 4D CMR and 2D PCMRI flow acquisition | 26 |
| Table 4 | Demographics of repaired TOF patients (clinical and ECG parameters) | 44 |
| Table 5 | Demographics of repaired TOF patients (CMR parameters) | 45 |
| Table 6 | Demographics of controls (clinical and ECG parameters) | 46 |
| Table 7 | Demographics of controls (CMR parameters) | 47 |
| Table 8 | Comparison of demographics (Clinical, ECG and CMR parameters) between cases and controls | 48 |
| Table 9 | Comparison of maximum and average WSS between cases and controls | 49 |
| Table 10 | Comparison of maximum and average EL between cases and controls | 50 |
| Table 11 | Spearman Rank correlation analysis between the variables RVEDVi (mL/m2) and PR by 2D PCMRI and 4D flow | 52 |
| Table 12 | Peak velocity (cm/s) in MPA, RPA and LPA with 2D PCMRI and 4D flow MRI | 53 |
| Table 13 | Correlation analysis between variables Aortic root total volume (mL) and Total Volume MPA (mL) on 2D and 4D sequences | 53 |

| | | |
|---|---|---|
| Table 14 | Correlation analysis between variables aortic total volume 4D (mL) and Total Pulmonary Venous flow 4D (mL) | 54 |
| Table 15 | Mean differences between Total pulmonary venous blood flow and MPA volumes as measured by 2D PCMRI and 4D flow. | 55 |
| Table 16 | Spearman's rank correlation between the clinical and ECG parameters and right ventricular parameters | 56 |
| Table17 | Spearman's rank correlation between the 4D flow CMR and right ventricular parameters | 56 |
| Table18 | Spearman's rank correlation between the RVOT dimension and QRS duration with WSS RVOT | 57 |
| Table19 | Spearman correlation between RVEDVi (ml/m2) and maximum and average WSS in MPA | 58 |
| Table 20 | Location of WSS in MPA among repaired TOF patients | 58 |
| Table 21 | Correlation analysis between variables RVEDVi (mL/m2) and Maximum EL and average EL in MPA | 59 |
| Table 22 | Vorticity grading in MPA, RPA and LPA | 60 |
| Table 23 | Spearman correlation between vessel diameter and respective vorticity grading in MPA, RPA and LPA | 60 |
| Table 24 | Correlation between total pulmonary venous blood flow on 4D versus total volume of RPA+LPA on 2D versus 4D sequences | 62 |
| Table 25 | Mean differences between Total pulmonary venous blood flow and RPA+LPA total volume at the Vortex versus Distal to the vortex | 63 |
| Table 26 | Correlation between the right sided pulmonary venous blood flow and RPA total volume at the Vortex versus Distal to the vortex | 64 |
| Table 27 | Correlation between the Left sided pulmonary venous blood flow and LPA total volume at the Vortex versus Distal to the vortex | 64 |

| | | |
|---|---|---|
| Table 28 | RPA/LPA ratio on 4D flow MRI in repaired TOF patients and controls | 65 |
| Table 29 | Comparison between the subjects who had undergone Pulmonary valve replacement and those who had not with respect to PR by 2D PCMRI versus 4D | 66 |
| Table 30 | Comparison between the subjects who had undergone Pulmonary valve replacement and those who had not with respect to Maximum and average EL in MPA, RPA and LPA | 67 |
| Table 31 | Comparison of PVR VS non-PVR groups with respect to RVEF and peak systolic velocity in MPA, RPA and LPA | 68 |
| Table 32 | Comparison of PVR VS non-PVR groups with respect to WSS in MPA | 68 |
| Table 33 | Interobserver variability related to Total pulmonary venous flow (ml) between Observer 1 and observer 2 | 69 |
| Table 34 | Interobserver variability related to Aortic root total volume 4D (ml) between Observer 1 and observer 2 | 70 |
| Table 35 | Interobserver variability related to Total vol RPA +LPA (at the vortex) | 71 |
| Table 36 | Interobserver variability related to Total vol RPA +LPA (distal to the vortex) | 72 |

## LIST OF ABBREVIATIONS

| S No | Abbreviation | Full Form |
|---|---|---|
| 1 | TOF | Tetralogy of Fallot |
| 2 | CHD | congenital heart disease |
| 3 | PR | Pulmonary regurgitation |
| 4 | RV | Right ventricle |
| 5 | PVR | pulmonary valve replacement |
| 6 | RVOT | right ventricular outflow tract |
| 6 | ICR | intracardiac repair |
| 7 | KE | kinetic energy |
| 8 | MRI | Magnetic Resonance Imaging |
| 9 | 2D PCMRI | Two-dimensional phase contrast MRI |
| 10 | 4D flow | four-dimensional flow |
| 11 | CMR | cardiac MR |
| 12 | VSD | ventricular septal defect |
| 13 | TR | tricuspid regurgitation |
| 14 | LV | left ventricle |
| 15 | VT | Ventricular tachycardia |
| 16 | SCD | sudden cardiac death |
| 17 | PRF | pulmonary regurgitant fraction |
| 18 | MPA | main pulmonary artery |
| 19 | RVEDVi | indexed RV end-diastolic volume |
| 20 | RVESVi | indexed RV end-systolic volume |

| | | |
|---|---|---|
| 21 | RPA | right pulmonary artery |
| 22 | LPA | left pulmonary artery |
| 23 | VENC | velocity encoding |
| 24 | ROI | region of interest |
| 25 | TE | Time to echo |
| 26 | TR | Time to repeat |
| 27 | SNR | signal to noise ratio |
| 28 | VNR | velocity to noise ratio |
| 29 | PC-MRA | phase contrast MR angiography |
| 30 | CS | compressed sensing |
| 31 | PC-VIPR | Phase contrast vastly undersampled isotropic projection reconstruction |
| 32 | WSS | Wall shear stress |
| 33 | EL | energy loss |
| 34 | STROBE | Strengthening the Reporting of Observational Studies in Epidemiology. |
| 35 | METS | metabolic equivalents |
| 36 | LGE | Late Gadolinium enhancement |
| 37 | PSIR | Phase sensitive inversion recovery |
| 38 | EF | ejection fraction |
| 39 | PSV | peak systolic velocity |

**SYNOPSIS**

"**Four-dimensional cardiovascular magnetic resonance flow analysis and velocity mapping of alterations of right heart flow patterns and main pulmonary artery hemodynamics in patients with repaired Tetralogy of Fallot.**"

Synopsis

By

**Dr. Karmakar Deepmala Kalyankumar**

for

DM CARDIOVASCULAR IMAGING AND VASCULAR

INTERVENTIONAL RADIOLOGY

of

**SREE CHITRA TIRUNAL INSTITUTE FOR MEDICAL SCIENCES AND TECHNOLOGY, TRIVANDRUM**

## SYNOPSIS

**TITLE:** "Four-dimensional cardiovascular magnetic resonance flow analysis and velocity mapping of alterations of right heart flow patterns and main pulmonary artery hemodynamics in patients with repaired Tetralogy of Fallot."

## AIMS AND OBJECTIVES

The aim and objectives of the study are:

(1) To assess whether 4-D flow MRI-derived parameters can differentiate repaired TOF patients with controls.

(2) To assess if 4D flow derived hemodynamic parameters are associated with disease severity in repaired TOF patients .

(3) To compare 2D flow versus 4D flow in repaired TOF patients

**Methods and Materials:** Ours was a single-center retrospective cross-sectional, observational study done from June 2021 to June 2023 after obtaining institutional ethics committee approval (IEC No:1790) on all patients of TOF who underwent ICR (either transannular patch repair or pulmonary annulus preserving surgery) in the institute 5 years prior to cardiac MRI, irrespective of any gender or ethnicity bias. Those persons who were referred for CMR and had normal CMR findings were taken as controls. The control group all had no prior cardiovascular disease, pulmonary disease, hypertension, or diabetes mellitus and no history of cardiac surgery. The symptomatology, QRS duration and associated results of cardiopulmonary exercise test (CPET) of the enrolled patients

were recorded. The standard clinical TOF CMR protocol consisted of scout images followed by functional assessment of the RV and LV using cine steady-state free precession (SSFP) techniques and post contrast Late Gadolinium enhancement (LGE) images using Phase sensitive inversion recovery (PSIR) sequence. This was followed by phase contrast flow study of MPA and branch pulmonary arteries and 4D flow study of whole heart. Qualitative 4D flow analysis included gross visualization of the flow, velocity vectors, streamlines, and path lines. Quantitative analysis involved flow calculation, calculation of wall shear stress (WSS), pressure difference, viscous energy loss (EL) as well as kinetic energy related parameters.

**Results:** Advanced 4D flow parameters such as maximum and average WSS were significantly elevated in repaired TOF patients in RVOT, MPA, RPA and LPA in comparison to controls (p value<0.001). When comparing maximum and average EL with controls, repaired TOF patients showed elevated values in MPA, RPA and LPA (p value <0.001) with more significant losses observed at the proximal region of the artery and bifurcation regions. A medium positive and a statistically significant correlation between QRS duration and Maximum WSS (p value=0.001) and average WSS RVOT (p value=0.002) was noted. A Pearson correlation showed a high, positive correlation between PR by 2DPCMRI and 4D flow , $r(28) = 0.87$, $p = <0.001$. A statistically significant and positive correlation was found between RVEDV and PR by 2D PCMRI (p value 0.015) and 4D flow (p value <0.001).However the correlation coefficient was higher for 4D as compared to 2D PCMRI (r=0.835 on 4D versus 0.442 on 2D). Internal validation was done between aortic root total volume and total Pulmonary venous flow on 4D. Spearman Rank correlation analysis showed a statistically significant and positive correlation between these variables (r = 0.861, p value <0.001). Correlation analysis

between aortic root total volume and total Volume of MPA blood flow on 2D and 4D sequences showed a stronger correlation (r = 851) and a much higher coefficient of determination ($R^2$ = 0.819) on 4D flow as compared to the 2D sequence (r = 670, $R^2$ = 0.508). The mean difference was significantly lower in the 4D flow, as compared to the 2D PCMRI. (Mean 2.5 ± 4.92 on 4D versus -7.2 ± 13.81 on 2D PCMRI) while assessing the total pulmonary venous blood flow via MPA total volume. While assessing the total pulmonary venous blood flow on 4D via RPA+LPA total volumes by 4D flow, the mean difference was significantly lower distal to the vortex, as compared to at the vortex (Mean -0.32 ± 5.83 versus 4.55+_13.49).There was a statistically significant difference between the PVR versus non-PVR subjects when PR was measured by 4D flow as compared to 2D PCMRI. The average value of PR by 4D flow was significantly higher in the group who had undergone PVR as compared to those who had not (Mean 57.53 versus 43.92, p value- 0.007). However, the average value of PR by 2D PCMRI was comparable in both the groups ( p value 0.09). When EL in MPA, RPA and LPA were compared between patients who underwent PVR versus no PVR, we could not find a statistically significant difference between the two groups. Our analysis showed non-PVR group to have higher EL values and peak systolic velocities in MPA, RPA and LPA. RVEF showed statistically significant difference between the two groups with PVR group showing lower mean values as compared to non-PVR group (48.30±8.20 versus 57.22 ±5.58)

## Conclusion

- 4D flow is highly applicable to repaired TOF patients in a single free-breathing 10–15 min acquisition. Particular strengths are better volumetric and velocity quantification.
- Calculations by 4D flow scores over 2D PCMRI as seen by our 4D flow analysis of total pulmonary venous blood flow and comparison between the total volume of blood in MPA on 2D PCMRI versus 4D flow. This method has the potential to compensate for the limitations of conventional PR measurements.
- Positive correlation of QRS duration with WSS in the RVOT but no significant correlation with RVEDVi may suggest that hemodynamic stress in the RVOT due to constant PR even in asymptomatic repaired TOF patients may be the initiating factor leading to subsequent RV dilation and dysfunction. Thus, alteration in the 4D flow derived hemodynamic parameters such as WSS may be associated with disease severity and may help in predicting patients who are prone to progressive RV failure, thus subjecting them to earlier interventions. More prospective, randomized, multi-centered studies are required to investigate the application of these methods in patient management.
- Identification of lower EL in the PVR group in comparison with non-PVR group was a new finding and may need better evaluation with larger samples to find if lower EL corresponds to early onset RV dysfunction.

# INTRODUCTION

Tetralogy of Fallot (TOF) is the most common form of cyanotic heart disease. TOF has an incidence of 4 in 10,000 live births constituting 5–7% of all congenital heart disease (CHD) , affecting males and females equally(Zhao et al., 2022) (Smith et al., 2019). Pulmonary regurgitation (PR) is the most common complication in repaired TOF. PR is seen especially with transannular patch repair and occurs many years after the surgery (Isorni et al., 2020) . PR induces right ventricle (RV) volume overload leading to RV dilation and dysfunction resulting in exercise intolerance, arrhythmia, and even sudden death (Tsuchiya et al., 2021) (Burchill et al., 2011). The timing of reintervention in the form of pulmonary valve replacement (PVR) continues to vary greatly.

Most of the patients present late with dilated right ventricular outflow tract (RVOT) and RV and are not good candidates for percutaneous PVR, thus resorting to surgical PVR. Hence, in light of the globally increasing number of adults with intracardiac repair (ICR), a detailed analysis of blood flow in the heart and vessels is needed in order to acquire a thorough understanding of the underlying pathomechanisms.

4D-flow is a time-averaged three-dimensional flow imaging which seems to be a promising tool providing functional information in addition to the morphological visualization of vessels(Sträter et al., 2018). It helps in assessing velocities, flow volumes and kinetic energy (KE) in RV and pulmonary artery (Robinson et al., 2019). A few studies have compared 4D (four dimensional) flow with 2D PCMRI ( Two dimensional 2D phase contrast MRI) blood flow quantification in children and young adults with repaired TOF(Jacobs et al., 2020) (Geiger et al., 2011). However, 4D flow MRI is not a validated technique with poor standardization at present. There is also a lack of definite

evidence in 4D flow MRI for repaired TOF patients to predate RV dysfunction. Current cardiac MR (CMR) risk assessment is based on volumetric and functional parameters that is rather a late expression of underlying physiological changes. As severe RV dysfunction presents late, factors other than PR such as RV KE losses may underpin functional deterioration in repaired TOF patients(Robinson et al., 2019). Our study is aimed in bridging these lacunae by assessing the relation of flow parameters in 4D flow using various parameters

# AIMS AND OBJECTIVES

The aim and objectives of the study are:

(1) To assess whether 4-D flow MRI-derived parameters can differentiate repaired TOF patients with controls.

(2) To assess if 4D flow derived hemodynamic parameters are associated with disease severity in repaired TOF patients .

(3) To compare 2D flow versus 4D flow in repaired TOF patients

# LITERATURE REVIEW

TOF is the most common form of cyanotic CHD accounting for one in 3600 live births and 5–7% of all CHD(Zhao et al., 2022). The embryological basis of TOF is antero-cephalad deviation of the developing outlet ventricular septum(or its fibrous remnant )leading to obstruction of the RVOT, override of the ventricular septum by the aortic root, ventricular septal defect (VSD) and right ventricular hypertrophy(Fratz et al., 2013). Surgical correction of TOF involves VSD closure, resection of obstructive RVOT musculature, and pulmonary valvotomy or placement of a transannular patch(Jeong et al., 2015). There is a steady increase in longevity of these post-operative patients with around 85% surviving well into adulthood (Bailliard and Anderson, 2009). Marelli et al observed that the number of adults with repaired TOF in the province of Québec (Canada) exceeds the number of children(Marelli et al., 2007). However, repaired TOF patients often have residual anatomic and hemodynamic abnormalities resulting in increasing rates of morbidity and mortality in late adulthood.

## Hemodynamics in repaired TOF patients

PR is a common complication in repaired TOF patients , especially with transannular patch repair, that may develop within few years after the primary repair owing to monocusp valve. In a large multicentre study involving patients with corrected TOF, 54% of patients had at least moderate PR(Gatzoulis et al., 2000). Progression of PR in various patients over the years is different and hence there is no clear time lines available for Pulmonary valve replacement. PR initiates a cascade of pathophysiologic events leading to RV dilatation and dysfunction. Other abnormalities that can adversely affect the

clinical course in these patients include RVOT or pulmonary artery stenosis, RVOT aneurysm, tricuspid regurgitation (TR) , residual VSD, left ventricular (LV) dysfunction, aortic valve regurgitation, and severe aortic dilatation. Adverse RV remodeling because of volume, pressure, or mixed volume and pressure overload results in varying degrees of dilatation and hypertrophy, increased wall stress, interstitial fibrosis, and dyssynchrony (both intra- and interventricular). Adverse remodelling initially involves RV but eventually affects the LV.

**Risk assessment in repaired TOF patients- issues with clinical parameters and 2D PCMRI**

Ventricular size and function in many of the repaired TOF patients may remain stable over many years with others showing progressive RV dilation and dysfunction over a short period of time. Outcome predictors can be grouped into the following 3 categories:(1) clinical factors (eg, syncope, older age at repair) (2) electrophysiological markers (eg, prolonged QRS duration, sustained atrial tachyarrhythmias, and sustained Ventricular tachycardia (VT)(Valente and Geva, 2017) and (3) imaging biomarkers of adverse ventricular remodeling (eg, RV dilation and RV or LV dysfunction)(Geva, 2011). In a study of 793 patients from 6 centres, Gatzoulis et al. found that older age at repair and QRS duration > 180 ms were independent predictors of sudden cardiac death (SCD)(Gatzoulis et al., 2000). This finding was later supported by findings from Khairy et al(Mbbs, 2008). However, these studies lacked tools to measure RV size and function. A study utilizing CMR for measuring ventricular size and function found that severe RV dilation and RV and/ or LV dysfunction were independent predictors of heart failure, sustained VT and SCD(Knauth et al., 2008).

As PR is the main contributor to dilated RVOT and RV dysfunction, accurate quantification of regurgitation is important. PR severity is reflected by the pulmonary regurgitant fraction [PRF (%)] measured on 2D PCMRI. The RVOT , main pulmonary artery (MPA) and RV are modified by the surgical procedures in a way that varies from patient to patient , creating challenges in identifying the correct acquisition planes in such complex geometries. Multiple studies have shown discrepancy between the PRF value, which can be underestimated, and symptom severity or RV function on 2D PCMRI. One reason for an underestimation of the PR is the presence of backward flow within a systole that is affected by turbulence or stagnation due to the dilation or stenosis of the MPA in repaired TOF patients (Tsuchiya et al., 2021). Moreover, 2D PCMRI doesn't allow the tracking of the valve plane, while 4D flow CMR does, thus improving reliability and accuracy of flow measurements by 4D flow (Isorni et al., 2020). Though 2D PCMRI is widely used in clinical practice , it has several limitations including prolonged breath holding, immobility during scan, and lengthy scan times requiring sedation in patients younger than 6–8 years of age and/or those with developmental delay . Each exam requires a highly trained CMR technologist familiar with pediatric CHD and oversight from a radiologist to determine scan planes and acquisition parameters(Vasanawala et al., 2015). At present, asymptomatic patients with indexed RV end-diastolic volume (RVEDVi) >150 ml/m2 and/or indexed RV end-systolic volume index (RVESVi) >80 ml/m2 qualify for PVR(Geva, 2011). Although PVR at guideline-recommended RV volume threshold values may reverse RV remodelling, the evidence for mortality benefit is less firm. Hence the indications and timing of PVR in repaired TOF patients with PR are still under debate. Thus we need better studies for assessing the parameters of early RV dysfunction in such patients.

## Need for better study in repaired TOF patients

The point of reintervention in the form of PVR continues to remain very heterogenous and the various factors leading to progressive RV dilation and dysfunction still needs to be analysed.

## 4D flow MRI

4D flow is a novel technique that provides flow-related information in all three directions. It helps in qualitative analysis in the form of vortex visualisation as well quantitative analysis of velocities, flow volumes (forward flow and reverse flow) and KE in RV and MPA and right (RPA) and left (LPA) pulmonary arteries in repaired TOF patients. Velocity information in the MRI can be achieved with either 2D PCMRI or 4D flow. In the 2D PCMRI, images are obtained with single direction encoding velocity (VENC) during breath hold. The plane should be exactly perpendicular to the flow in the vessel to obtain correct velocity information(Wymer et al., 2020). Blood flow through the cavities of the heart and great vessels is pulsatile and is subject to time and multidirectional variations. Hence, acquisition in case of complex CHD like TOF is difficult and requires scans to be repeated multiple times in multiple planes to attain true orthogonal image acquisition as well as true VENC selection in tortuous anatomy(Sträter et al., 2018). 4D flow MRI is a time-resolved, three-dimensional phase contrast MRI sequence that provides 3D volume information over a period(Azarine et al., 2019). It has three velocity images in 3 directions and one magnitude image. Field of view should be as large as necessary and as small as possible to include the region of interest (ROI). Spoiled gradient echo sequences with short echo (TE) and repetition (TR) are used for 4D flow

measurement. Due to the short TR, the signal maximum of the blood is weighted inversely with respect to the T1 relaxation time. Therefore, 4D-flow measurement does not usually require contrast agent administration(François et al., 2011). However, acquiring the 4D Flow data after the contrast study takes advantage of the enhanced signal to noise ratio (SNR) , velocity to noise ratio (VNR) and contrast between blood and surrounding tissue (François et al., 2011) (Bock et al., 2010). But contrast agents that wash out during the 4D Flow can result in time-varying blood T1 times and the effects of this variability on PC-CMR velocity data is not fully known(Sträter et al., 2018). The results of a study by Bock et al(Bock et al., 2010) and Hess et al(Hess et al., 2015) demonstrated that the application of contrast agent affected image quality of phase contrast MR angiography (PC-MRA) positively especially in smaller vessels and provided improved background suppression in 4D flow. But SNR in data with contrast agent showed significantly higher variation presumably due to different scan timing and contrast agent elimination rates. Since such variances may affect image quality, future studies should include the effect of scan timing and duration in more detail.

The advantage of 4D flow over 2D PCMRI is that the plane of velocity assessment can be retrospectively selected at any location due to its ability to make calculations perpendicular to the flow vector anywhere within the acquisition volume in the post-processing software in the 4D flow(Elsayed et al., 2021). Despite longer scan times, 4D Flow CMR may be advantageous and faster especially in cases where multiple 2D PCMRI scans would be needed especially in CHD. Further, the option of valve tracking may improve assessment of flow through heart valves. Compared to 2D PCMRI, 4D Flow CMR measures velocity in all spatial directions and has superior spatial coverage

and may therefore also be better at capturing the peak velocity of a stenotic jet (Nordmeyer et al., 2010). This is due to the segmentation technique in 4D flow calculation in an entire vessel segment rather than relying on 2D analysis planes which do not coincide with the location of the maximum systolic velocity. Studies with 2D PCMRI have shown that at least 5–6 voxels across the vessel lumen are needed for accurate flow volume quantification(Hofman et al., 1995)

A high spatial resolution is required for accurate determination of flow parameters and to be able to record even small flow phenomena. However, the smaller the voxel size, the longer the scan time and the lower the SNR. Therefore, a compromise must be made on an individual basis for each patient. A voxel size with an isotropic edge length of 2.5 – 3.0 mm for the heart has been established(Dyverfeldt et al., 2015). The highest possible temporal resolution of approximately 40 ms per 3D dataset is needed to be able to record even brief flow phenomena(François et al., 2013).

4D Flow CMR data processing usually involves the use of automated or semi-automated corrections of known artefacts as several sources of error can compromise its analysis. Similar to 2D PCMRI, the major sources of errors include eddy current effects (switching of time-varying magnetic field gradients result in changes in magnetic flux), concomitant gradient field effects (Maxell terms- spatially varying background phase offsets) , gradient field nonlinearity and phase wraps resulting in velocity aliasing(Dyverfeldt et al., 2015). Correction factors for the concomitant gradient field correction can be directly derived from the gradient waveforms used for the data acquisition. However, not all eddy current effects can be compensated for and there currently is no definite solution to remove all eddy current induced background phase offsets(Bissell et al., 2023) . During

flow analysis, it is not always possible to predict the maximum velocity. Hence the use of a phase-unwrapping algorithm in 4D flow helps in identification of abrupt phase shifts in the temporal domain. Though 2D PCMRI also provides the option of background and phantom correction, it is not robust and may lead to additional errors.

Quality control is important for every clinical and research study. Screening of 4D Flow CMR source images can reveal phase wraps, background phase offsets (by using narrow color-window), fold-over, and other image artifacts(Bissell et al., 2023) (Dyverfeldt et al., 2015). 4D Flow CMR offers several opportunities for internal data consistency due to its volumetric coverage which is not possible with 2D PCMRI. For flow volume quantification, the conservation-of-mass principle can be employed to assess pulmonary vs. systemic flow volume ratios and flow volume in vs. out of the ventricles. Similarly quality control of pathlines analysis can be done as the number of pathlines that enter and leave a specified ROI should be the same (e.g., ventricles). Other advantages of 4D flow MRI over 2D PCMRI is to screen data for streamlines or pathlines that abruptly change direction or slowly drift out of the lumen, which can be indicative of phase wraps or uncompensated background phase offsets, respectively. Similarly, the presence of uncompensated background phase offsets can be suspected if pathlines emitted from the chest or back move in a non-random fashion. Hence, preprocessing step is of utmost importance during 4D flow analysis.

However, as compared to 2D PC-CMR which is widely available and a standardised technique, 4D flow CMR currently remains technically challenging and is rarely used in clinical routine settings, mainly due to the long scan time which is further increased by the need for respiratory motion compensation(Neuhaus et al., 2019). A whole heart and

an aortic acquisition takes approximately 15 min by using standard parallel imaging techniques on a typical clinical CMR system. Therefore, a range of acceleration techniques that exploit spatio-temporal correlations have been applied to 4D flow of the heart and/or surrounding vessels including k-t BLAST, k-t GRAPPA or k-t PCA allowing for acceleration factors in the order of 5 to 8. Acceleration techniques based on compressed sensing (CS) − often combined with non-Cartesian sampling, with and without exploitation of spatio-temporal correlations − have also been applied to 4D flow CMR achieving similar acceleration rates (Carlsson et al., 2011) (Schnell et al., 2014) (Giese et al., 2014). One major disadvantage of most proposed CS techniques is their relatively long off-line reconstruction time, being in the range of 45 to 60 min(Valvano et al., 2017) (Cheng et al., 2016). A study by Neuhaus et al (Neuhaus et al., 2019) demonstrated a six- to eightfold acceleration of 4D flow CMR using CS in patients with aortopathies. However, the magnitude images visually suffer from increased artefacts for higher CS factors. The main benefits are scan-time savings and direct on-line reconstruction.

Radial 4D Flow MRI (PC-VIPR- ,vastly undersampled isotropic projection reconstruction ) is another promising approach for accelerated PC MRI. With this approach, data points in k-space are recorded on a radial trajectory. In contrast to traditional Cartesian sampling with parallel lines in k-space, spatial resolution is preserved even if fewer radial lines are acquired than dictated by the Nyquist limit(Markl et al., 2012). Instead of a compromised resolution, the tradeoffs for scan time reductions are streak artifacts and a loss of SNR.

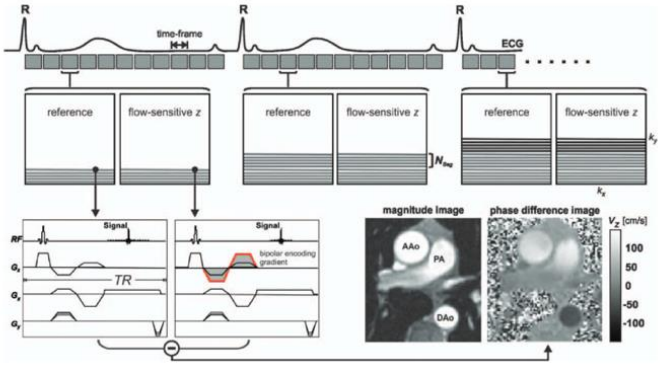


Figure 1Basic acquisition of 2D PCMRI (Image courtesy (Markl et al., 2012))

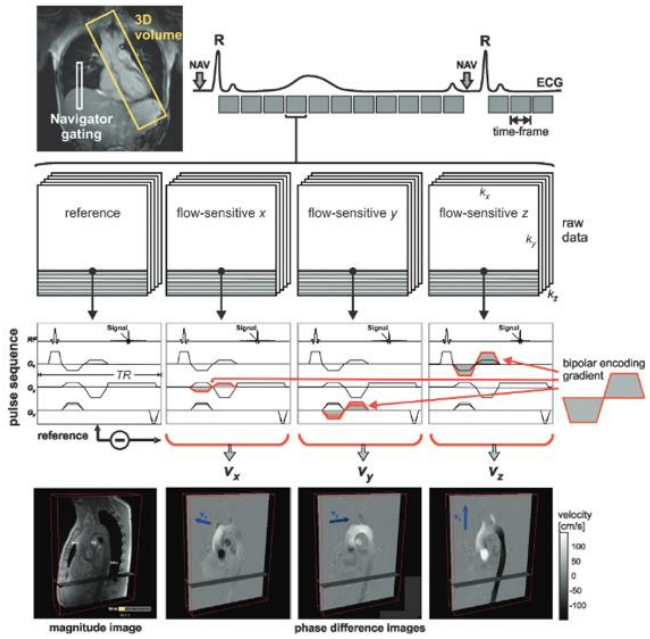


Figure 2 Basic acquisition of 4D flow MRI (Image courtesy (Markl et al., 2012))

**Analysis of the 4D flow:**

It involves qualitative and quantitative analysis. The qualitative analysis includes gross

visualization of the flow, velocity vectors, streamlines, and path lines. Quantitative analysis involves flow calculation, calculation of wall shear stress (WSS), pressure difference, viscous energy loss (EL) as well as KE related parameters.

**Evidence for 4D flow MRI in repaired TOF patients – current scenario**

Studies conducted by Van der Hulst et al(Van Der Hulst et al., 2010), Hsiao et al(Hsiao et al., 2011), Tariq et al(Tariq et al., 2013), Giese et al(Giese et al., 2014), Gabbour et al(Gabbour et al., 2013), Hirtler et al(Hirtler, 2016) have shown that 4D flow MRI helps in accurate flow quantification and provides information regarding intracardiac and vascular vorticity and helps in better outcome predictions as compared to 2D PCMRI. In all the above mentioned studies, strong correlations between the 2D and 4D flow MRI measurements of PRF were observed with 4D flow giving more accurate effective flow measurements. Ha et al(Ha et al., 2016) demonstrated helical or vortical streamlines in repaired TOF patients due to acceleration of blood flow in the RV, MPA, RPA and LPA. This causes turbulence resulting in high-velocity jet impinging focally on the wall. Turbulent kinetic energy is the energy stored in the turbulent flow and this is dissipated as heat. Blood flow turbulence is expressed as rapid velocity fluctuations within a single imaging voxel(Robinson et al., 2019). Isorni et al(Isorni et al., 2020), Jacobs et al(Jacobs et al., 2020), Lee et al(Lee et al., 2019), Fredriksson et al(Fredriksson et al., 2018) have evaluated the 4D flow patterns in MPA, RPA, LPA and RV. These studies indicate altered flow patterns with higher intravascular vorticity and increased KE losses in the RV. Robinson et al (Robinson et al., 2019) demonstrated increased KE in MPA in repaired TOF children vs. controls across the entire cardiac cycle (12.5 mJ/m2 vs. 8.2 mJ/m2, $P<0.01$ in systole; and 2.3 mJ/m2 vs. 1.4mJ/m2, $P<0.01$ in diastole ). Jeong et al (Jeong

et al., 2015) showed that greater ventricular KE was necessary to generate flow in the pulmonary and aortic circulations in repaired TOF patients with higher peak systolic KE in RV and LV (6.06±2.27mJ and 3.55±2.12mJ, respectively) than healthy volunteers (5.47±2.52mJ and 2.48±0.75mJ, respectively). Francois et al(François et al., 2012) also showed increased vortical flow patterns in the right atrium (RA) and in the RV during diastole, and increased helical or vortical flow features in the MPA in repaired TOF subjects. Regarding other advanced 4D flow parameters, Francois et al (François et al., 2012) showed increased WSS in the MPA of repaired TOF patients, consistent with the Bedard et al(Bédard et al., 2009) observation of the histological abnormalities present in the pulmonary trunk of such patients. However, one major limitation of these studies was limited number of cases. Few of the studies have been summarised in the table below

Table 1 Summary of 4D flow studies

| Author | Parameter Studied | Study Characteristics | Key Results |
|---|---|---|---|
| Nordmeyer et al(Nordmeyer et al., 2010) | To validate the quantitative use of flow sensitive 4-D velocity encoded cine MRI for simultaneously acquired venous and arterial blood flow in healthy volunteers and for abnormal flow in patients with CHD. | 19 patients and 7 healthy volunteers | 4-D flow MRI is accurate in arterial, venous, and pathological flow. |
| Robinson et al(Robinson et al., 2019) | 4-D flow MRI-derived measures of blood KE between repaired TOF patients and controls and whether these parameters were associated with disease severity | Pediatric patients post TOF repair (n=21) and controls (n=24) | Increased KE in pulmonary artery (PA) in children post TOF vs. controls across the entire cardiac cycle 12.5 mJ/m2 vs. 8.2 mJ/m2, P<0.01 in systole; and 2.3 mJ/m2 vs. 1.4mJ/m2, P<0.01 in diastole ). KE had a direct, non-linear relationship with traditional measures of disease progression. |
| Jeong et al(Jeong et al., 2015) | To assess differences in ventricular KE with 4D Flow MRI between patients with repaired TOF and healthy volunteers. | 10 subjects with repaired TOF and 9 healthy volunteers | Peak systolic KE (RV) and KE (LV) were higher in repaired TOF subjects (6.06±2.27mJ and 3.55±2.12mJ, respectively) than healthy volunteers (5.47±2.52mJ and 2.48±0.75mJ, respectively) but not statistically significant (p= .65 and p= .47, respectively) Greater ventricular KE was necessary to generate flow in the pulmonary and aortic circulations in repaired TOF patients. |
| Geiger et al(Geiger et al., 2011) | Comprehensive analysis of haemodynamics by 4-D flow visualization and | 10 patients and 4 healthy controls | 4-D flow analysis provides valuable data on both intracardiac and pulmonary vascular flow |

| | | | |
|---|---|---|---|
| | retrospective flow quantification in patients after repair of TOF. | | |
| Francois et al(François et al., 2012) | To assess changes in right heart flow and pulmonary artery hemodynamics in patients with repaired TOF | 11 subjects and 10 normal volunteers | Right heart flow patterns in repaired TOF subjects were characterized by increased vortical flow patterns in the right atrium (RA) and in the RV during diastole, and (c) increased helical or vortical flow features in the PA. Differences in main PA retrograde flow, resistance index, peak flow, time-to-peak flow, peak acceleration, and mean wall shear stress were statistically significant. Helps in outcome prediction |

**Summary of review of literature with lacunae in literature**

2D PCMRI provides information related to the RV, LV morphological parameters including RVEDV, RVESV and PR. Treatment is also based on these anatomical parameters keeping the patient on regular clinical follow up till the threshold volume is reached. However, these anatomical parameters are not able to predict which patient can have early RV failure. Imaging of the flow dynamics like velocities and vortex analysis in RV and MPA and stress exerted on the walls of the RV, MPA, RPA and LPA by turbulent blood are not extensively studied to provide data on the deterioration of RV. In addition, many of the studies are retrospective with limited number of subjects and controls. The present cross-sectional study aimed to fill these lacunae to derive 4D flow parameters which can predict the long-term outcomes in repaired TOF patients so that timely intervention can be done in those subsets who are at high risk of early RV failure.

# 3 MATERIALS AND METHODS

**Study type:**

Ours was a single-center retrospective cross-sectional, observational study done from June 2021 to June 2023 after obtaining institutional ethics committee approval (IEC No:1790) on all patients of TOF who underwent ICR (either transannular patch repair or pulmonary annulus preserving surgery) in the institute 5 years prior to cardiac MRI, irrespective of any gender or ethnicity bias. Informed consent was obtained from all the patients. For minor participants, written informed consent was taken from either the parents or guardian. Those persons who were referred for CMR and had normal CMR findings were taken as controls. The control group all had no prior cardiovascular disease, pulmonary disease, hypertension, or diabetes mellitus and no history of cardiac surgery

**Inclusion criteria:**

Consecutive Patients of TOF who underwent either transannular patch repair or pulmonary annulus preserving surgery in the institute with CMR done at least 5 years after the surgery.

**Exclusion criteria:**

- Associated shunt lesions including major aortopulmonary collaterals and residual VSD.
- Patients with moderate or severe TR

- Claustrophobic patients, patients with MR incompatible metallic implants, pacemakers or cochlear implants and other contraindications to CMR.
- Patients with history of renal disease and eGFR < 30mL/min/1.73 $m^2$ or other contraindications for intravenous gadolinium contrast.
- Studies with inadequate image quality.
- Patients who were unable to lie down for a prolonged period.
- Patients or relatives declining consent.

**Study design:**

**Study population**

60 post TOF ICR patients and 35 age matched controls were included in the study . After applying the elimination and exclusion criteria (Fig ) as per the STROBE guidelines (Strengthening the Reporting of Observational Studies in Epidemiology) for retrospective cohort, 30 repaired TOF patients (13 pediatric; 17 adult) and 15 age matched controls with normal ventricular function were selected to be included in the current analysis. The control group all had no prior cardiovascular disease, pulmonary disease, hypertension, or diabetes mellitus and no history of cardiac surgery.

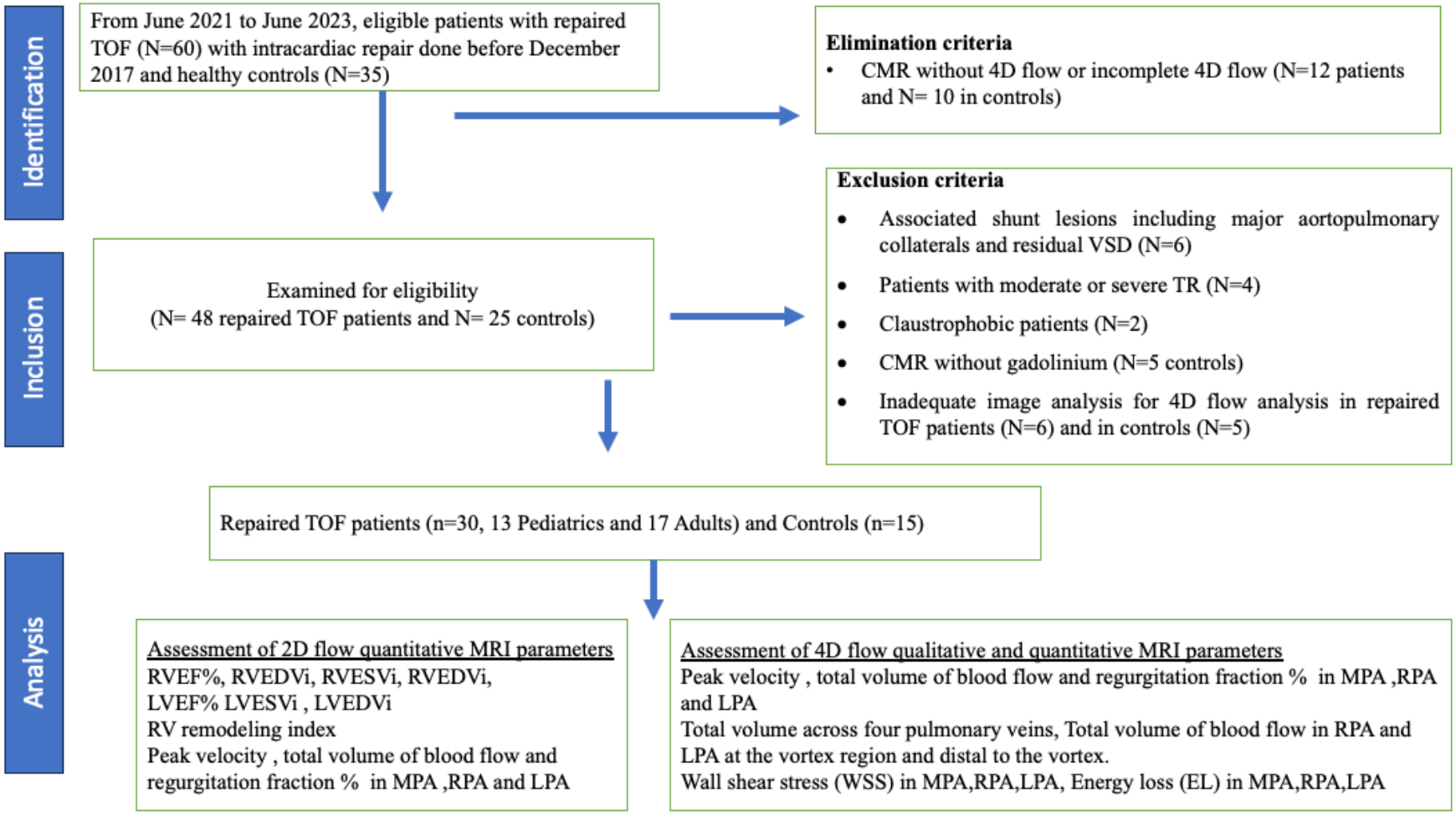


Figure 3 STROBE (Strengthening the Reporting of Observational Studies in Epidemiology) flowchart of our studied population.

**Clinical data**

The symptomatology, QRS duration and associated results of CPET of the enrolled patients were recorded. All patients underwent treadmill exercise testing as per Bruce protocol to maximal volition within one week of the CMR. Symptoms such as muscle fatigue, exhaustion, extreme dyspnea, and light-headedness were taken as end points of test termination. Cardiac arrhythmias were not an indication to stop the test unless sustained tachyarrhythmias developed. The exercise was stopped when 85% of maximum heart rate was achieved or 10.10 metabolic equivalents (METS). Patients were stratified by peak oxygen uptake (VO2) values into two groups: low risk: peak VO2 > 15 ml/kg/min; medium to high risk: peak VO2 $\leq$ 15 ml/kg/min (Farina et al., 2018).

**Cardiovascular magnetic resonance protocol**

CMR examinations were done on 1.5 T Siemens (MAGNETOM Avanto , Siemens Healthcare, Erlangen, Germany) equipped with a 36-element dedicated cardiac array. CMR was done for assessing the RV and LV functional parameters and qualitative and quantitative hemodynamic parameters of MPA, RPA, LPA and RVOT. The standard clinical TOF CMR protocol consisted of scout images followed by functional assessment of the RV and LV using cine steady-state free precession (SSFP) techniques and post contrast Late Gadolinium enhancement (LGE) images using Phase sensitive inversion recovery (PSIR) balanced SSFP sequence. This was followed by phase contrast flow study of MPA and branch pulmonary arteries and 4D flow study of whole heart.

**2D CMR sequences**

**Cine images**

Cine images were obtained using retrospective electrocardiographic (ECG)- gating in short axis, four chamber, two chamber and three chamber RV outflow tract imaging planes. A total of 25 cardiac phases were acquired during one R–R interval with temporal resolution of approximate 60 ms between phases. Bright blood imaging technique using balanced SSFP (TruFISP) sequence was applied to obtain CINE images. Short axis stack covered the heart from its base to apex, which allowed for the assessment of global and regional ventricular function, calculation of LV and RV volumes, ejection fraction (EF). Cut-off values of RV remodeling index(RVEDVi/LVEDVi ) for moderate to-severe and severe RV remodelling were 1.41 and 2.0, respectively(Zhao et al., 2022). TR was visually graded as none, mild, moderate, or severe.

**LGE sequence**

LGE images were obtained 10 minutes after administrating intravenous Gadolinium-based contrast medium (Gadoterate Meglumine, Vivere Imaging, India) intravenously at 0.1 mmol/kg body weight. Breath-hold segmented ECG gated PSIR b-SSFP sequence performed in the same orientation as the cine images. The inversion time was adjusted to completely null normal myocardium (typically 250-400 ms).

**Pulmonary artery angiogram**

Dynamic time resolved MR angiography (TWIST) acquisition was performed with contrast agent injected intravenously at 0.1 mmol/kg body weight sufficient to create enough T1-shortening during the course of data acquisition. This enabled visualization

of the passage of a contrast bolus from the venous system, across the MPA and branch pulmonary arteries.

**2D Phase contrast flow study of main pulmonary artery and branch pulmonary arteries**

VENC was adapted individually to yield images without aliasing artefacts (200-400 cm/s). Imaging plane was selected from the oblique axial and sagittal planes of dynamic contrast pulmonary MR angiogram and the point between the pulmonary valve and MPA bifurcation was selected for acquisition. The usual VENC selected was about 120–150 cm/s. The encoding velocity for branch pulmonary arteries selected was about 120-180 cm/s. The right pulmonary artery plane was selected from the oblique axial and coronal images of dynamic pulmonary MR angiogram. The imaging plane was selected between the origin and first order bifurcation. Since the left pulmonary artery has a more sagittal course, the imaging plane was selected from oblique axial and sagittal image. Patients with aorta pulmonary collaterals were excluded from the study, hence combined RPA plus LPA flow was taken as the total pulmonary artery flow (Qp).

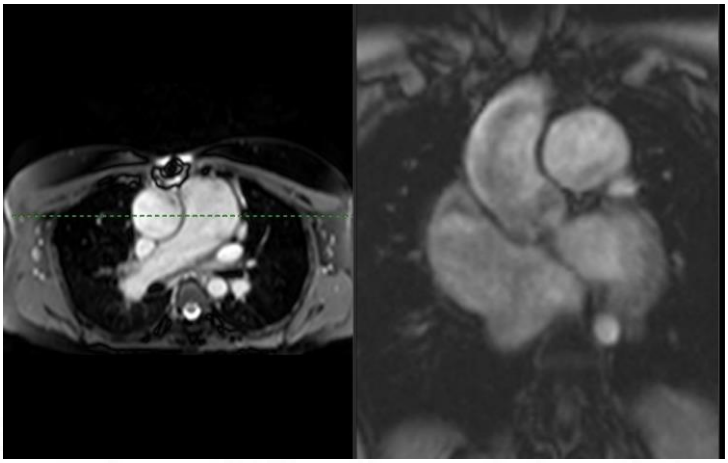

Figure 4 Reconstructed PCMRI showing the planning for MPA proximal to the bifurcation.

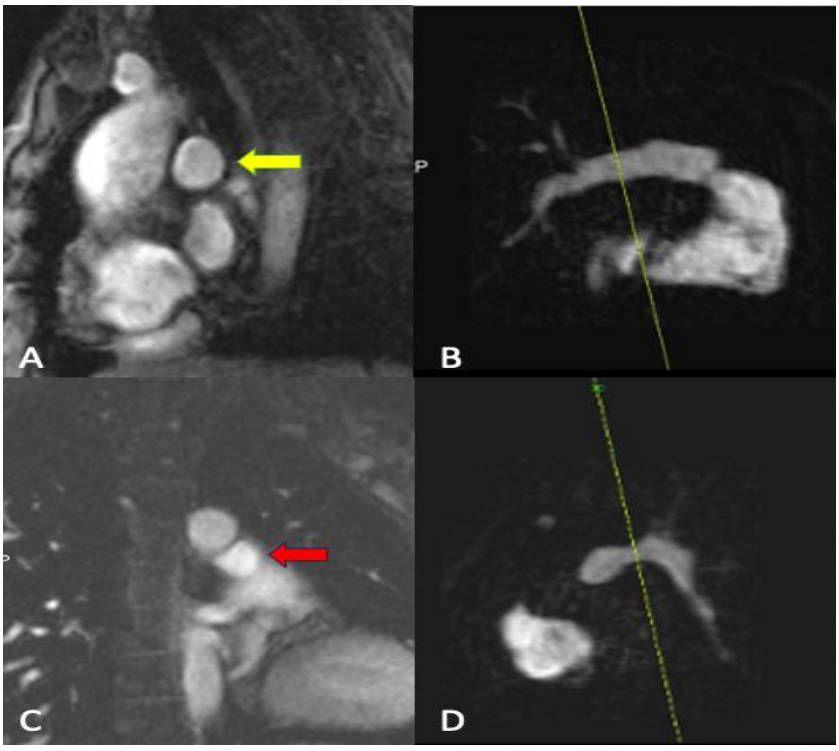


Figure 5 Reconstructed PCMRI images showing the planning for RPA (yellow arrow in A and green line in B) and LPA ( red arrow in C and green line in D) between their respective origins and bifurcations.

Table 2 Routine 2D sequences acquired in a repaired TOF patient

| **Parameter** | **Scout** | **Cine images** | **TWIST MR angiography** | **15 min LGE PSIR** |
|---|---|---|---|---|
| TE | 1.12 ms | 1.19 ms | 1 ms | 1.21 |
| TR | 269.99ms | 36.14 | 2.73 ms | 657 |
| Flip angle | 60° | 58° | 33° | 40° |
| FOV | 400x400 mm | 230x208.4 mm | 340x340 mm | 360x270 mm |
| Matrix size | 240x158 | 174x192 | 246x352 | 164x272 |
| Slice thickness | 8 | 6 mm | 1 mm | 8 mm |
| Time of inversion | - | - | - | Adjusted to null the myocardium |
| ECG gating | Prospective | Retrospective | - | Prospective |
| Breath hold | Yes | Yes | No | Yes |
| Spatial resolution | 1.7x1.7x8 mm | 1.2x1.2x6 mm | 1x1x1 mm | 1.3x1.3x8 mm |
| Interslice gap | 16 mm | 1.5 mm | - | 4 mm |
| SNR | 1 | 1 | 1 | 1 |

**Image analysis using routine 2D CMR sequences**

Absolute and indexed RV and LV volumes, LV, and RV ejection fractions, myocardial LGE, flow quantification across MPA, RPA and LPA were measured using cvi42 Version 5.13 (Circle Cardiovascular Imaging, Calgary, Alberta, Canada) by a single experienced

reader (3 years of CMR experience). Cine images were used to measure RV and LV ejection fraction and volumes by tracing the endocardial and epicardial boundaries at the end-diastole and end-systole. EF was obtained using the semi-automated technique. For flow quantification, the automatic contour detection was used for drawing the contour towards the vessel borders based on the information from all phases and the contour was forwarded to all phases. Quantification of 2D flows and flow pattern calculations (forward flow, backward flow, regurgitation fraction (RF) and net flow) were analysed as shown in Figure 6.

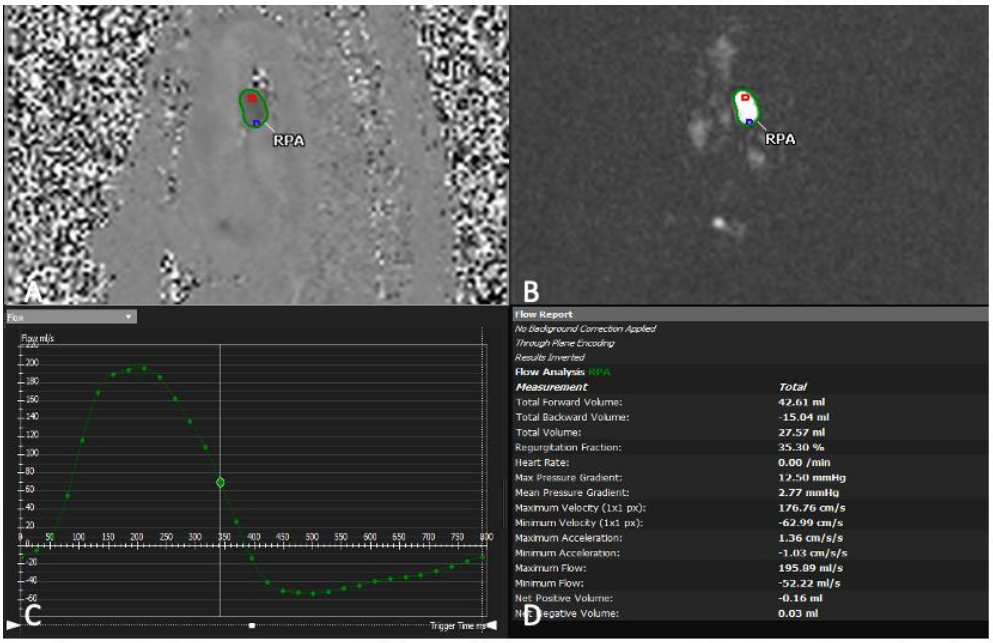


Figure 6 Right pulmonary artery flow assessment using 2D PCMRI in a young adult with pulmonary regurgitation 12 years after TOF repair. A and B phase-contrast and magnitude images of right pulmonary artery with C and D showing a regurgitation fraction of 35.30 %.

**4D flow acquisition protocol and parameters:**

Scanning was performed in the axial plane from thoracic inlet up to the diaphragm in the free-breathing mode using retrospective ECG gating to enable coverage of the entire cardiac cycle and respiratory gating techniques (respiratory navigator echo) . It included one magnitude image and 3 phase images in 3 directions. The sequence used for 4D flow was a spoiled gradient sequence with short TE and TR (Geiger et al., 2011). Scanning parameters included: Slice thickness- 2.5 mm, spatial resolution-2.5 mm, temporal resolution- 40 milliseconds, TE-2.3 milliseconds, TR-38.80 milliseconds, flip angle-15°, spatial resolution-2.4x2.4x2.5 mm, single VENC of 200 cm/s. Cartesian reconstruction algorithm was used. Contrast agent was used as part of a comprehensive CMR study for visualization of the pulmonary artery and its branches. 4D flow was acquired approximately 12 minutes after dynamic contrast MR pulmonary angiography. Scanning time ranged from 8-10 minutes. Total acquisition time including 4D flow was around 45 minutes , depending on the heart rate and breath hold.

Table3 Comparison between the imaging parameters of 4D CMR and 2D PCMRI flow acquisition

| **Parameter** | **2D PCMRI Flow study (MPA,RPA,LPA)** | **4D flow** |
|---|---|---|
| TE | 2.91 ms | 2.3 ms |
| TR | 42.16 ms | 38.80 ms |
| Flip angle | 20° | 15° |
| FOV | 340x233mm | 380x304mm |
| Matrix size | 119x192 | 90x160 |
| Slice thickness | 6 mm | 2.5 mm |

| | | |
|---|---|---|
| ECG gating | Retrospective | Retrospective |
| Breath hold | Yes | Respiratory navigator triggered |
| Spatial resolution | 1.2x1.2x 6mm | 2.4x2.4x2.5mm |
| Interslice gap | - | - |
| SNR | 1 | 1 |

All CMR images were stored in picture archiving and communication system (PACS). For the purpose of the study, CMR images were retrieved from PACS, anonymized and stored separately in numbered folders. These images were post-processed and analysed by a reader with 3 years of experience in interpreting CMR studies. The post-processing in 4D flow was reviewed by another cardiac radiologist with 9 years of experience. The calculations were checked for inter-observation discrepancies by recalculating part of the data set.

## 4D flow MRI processing:

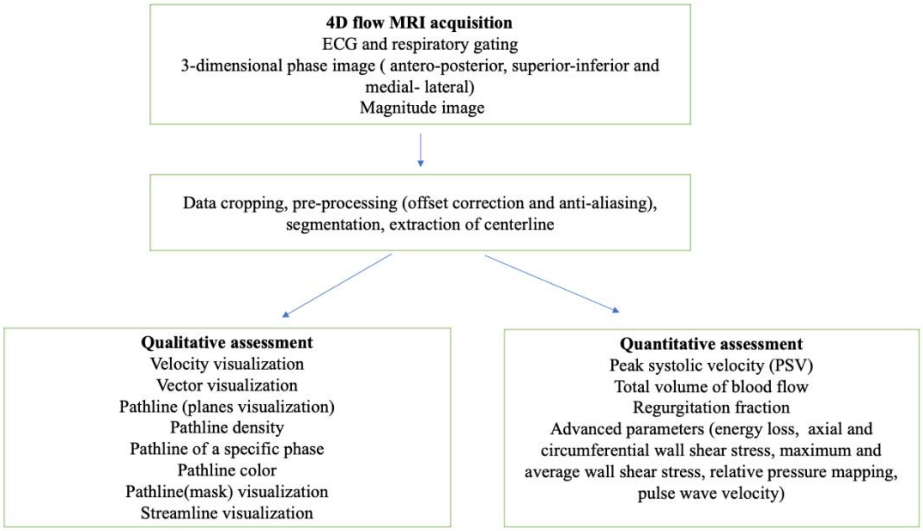


Figure 7 Flow chart showing basic steps in the 4D flow study

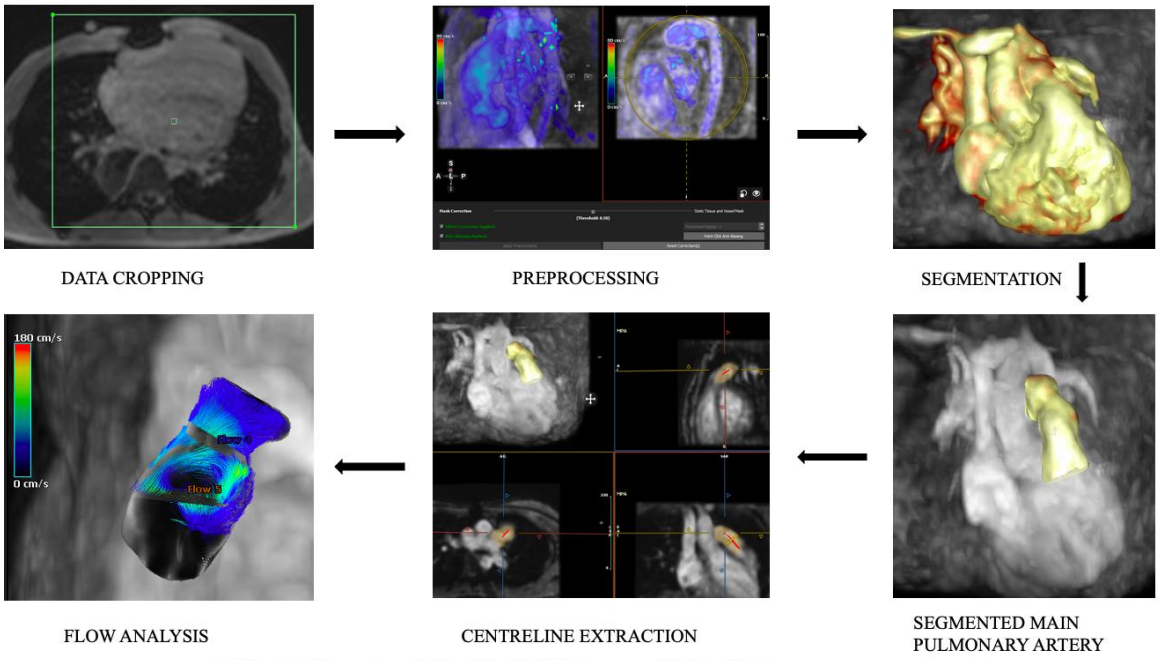


Figure 8 Overview of a typical 4D flow workflow

**Preprocessing-** After cropping the data, offset and anti-aliasing correction were applied before further processing. Velocity offset correction was verified by identifying the uniform distribution of the static tissue mask (yellow) across the image.. Voxels representing noise (air) or spatial aliasing were excluded. A polynomial surface was fitted to the velocities of static tissue voxels and then subtracted from the whole image. This was based on the assumption that there is no flow in static tissue. Anti-aliasing (phase unwrapping) were applied to correct velocities that exceeded the VENC, however it corrected only velocities upto 2x VENC. Static tissue (yellow) and noise (blue) were not altered by this correction. The threshold value for mask correction was set to 50% of the maximum value in the magnitude data.

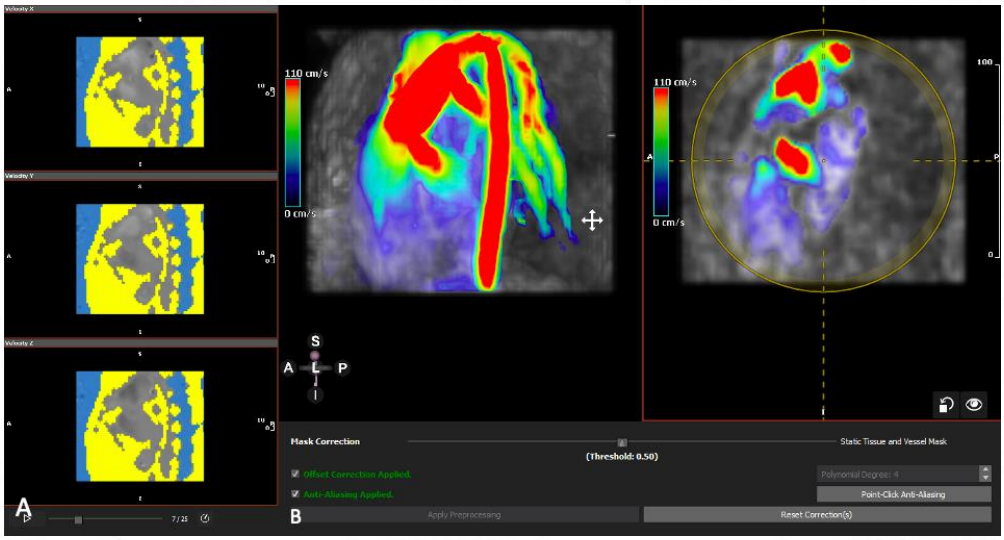


Figure 9 Steps used in pre-processing of 4D flow data

Calculation of PC-MRA was performed using the pixelwise squared absolute velocity values combined with noise masking and additional magnitude weighting. The resulting data were then averaged over time for further enhancement of vascular regions with high blood flow and suppression of the background signal.

Segmentation- The Center line in MPA was drawn from the pulmonary valve level upto its bifurcation into RPA and LPA. Similar centerline extraction was done for RPA, LPA and four pulmonary veins, starting from their respective origins upto the first branch which was verified for its true central position and modified manually for accurate measurements. High flow analysis was used for MPA, RPA and LPA. Low flow analysis was used for pulmonary veins. This was followed by qualitative and quantitative flow analysis in the segmented vessels. A visual assessment of streamlines and pathlines in MPA, RPA, LPA and RVOT was performed, paying attention to laminar flow, spiral or vortex flow. The visualization of the path line and the stream line were performed in continuous emission mode with 50 particles/10 ml and 5 particles/ml, respectively, and a speed of 20 frames/second.. The hemodynamic parameters of regurgitation, peak velocity and total volume of blood flow were calculated perpendicular to the vessel axis in MPA, avoiding areas of vortex flow.

RPA and LPA were divided into three segments each (proximal-1, mid-2, and distal-3). Quantitative parameters in RPA and LPA were taken at the following positions: at the level of vortex and distal to the vortex.

Total volume in right upper and right lower and left upper and left lower pulmonary veins was taken into consideration. As patients with aorta pulmonary collaterals were excluded from the study, combined RPA plus LPA flow was taken as the total pulmonary artery flow (Qp) and was postulated to be equal to the total volume of pulmonary venous blood flow. WSS and EL was calculated at the sites of vortical flow.

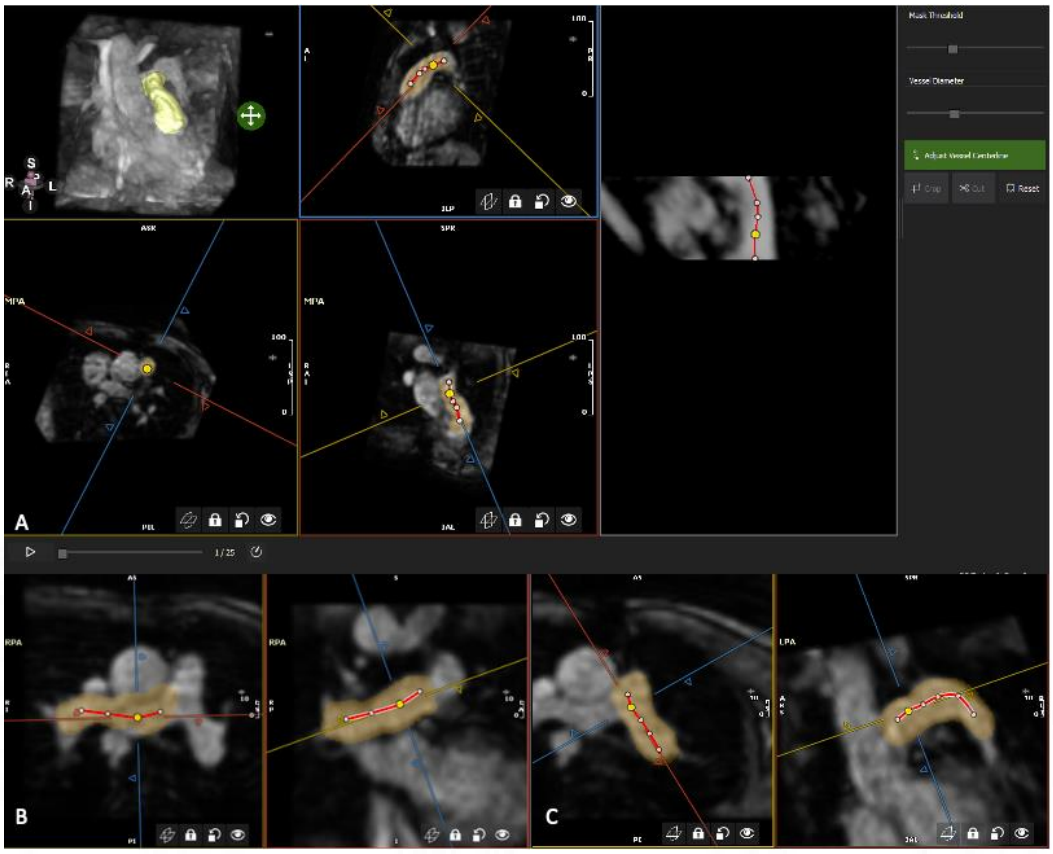


Figure 10 Technique for centerline extraction in MPA (A), RPA(B) and LPA(C)

Analysis of the 4D flow:

It involves qualitative and quantitative analysis. The qualitative analysis includesgross visualization of the flow, velocity vectors, streamlines, and path lines.

**Qualitative analysis:**

Color-coded velocity images: They provide information related to the gross visualization of the direction and velocity of the flow (Fig A)

Velocity vectors: provide information related to the speed and direction of the flow. The arrow of the vector points to the direction of flow, the color of the vector determines magnitude of flow (Fig B)

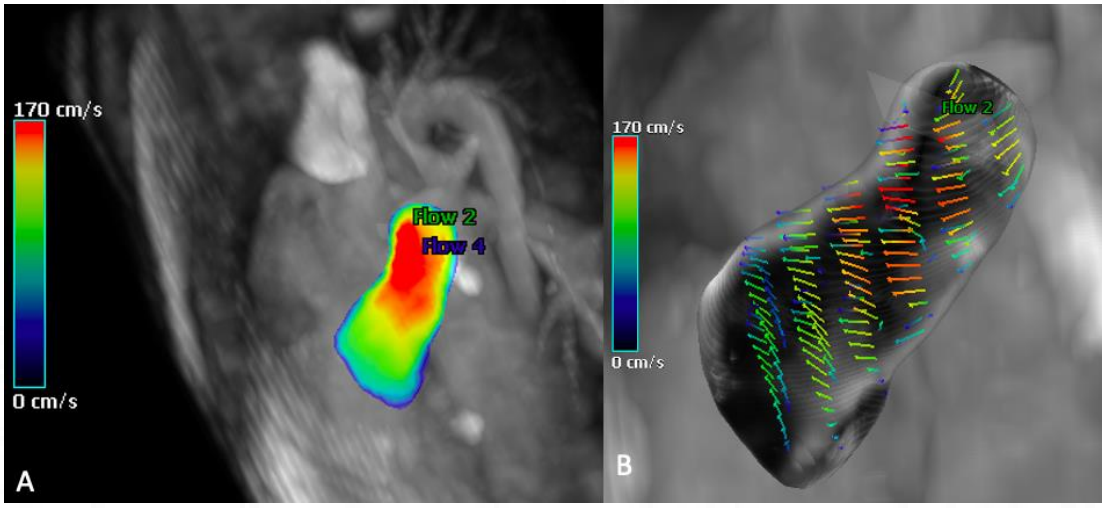


Figure 11 Color coded velocity images showing higher velocities in MPA of a repaired TOF patient (red color in A), (B) demonstrates the velocity vectors in the same patient. Peak velocity in the region of red color was 202.78 cm/s.

Streamlines determine the path a particle takes when it is released into the velocity field. Normal flow in the arteries is laminar. In vortical flow, blood will be recirculated from the main flow direction resulting in the swirling motion as in whirlpools. Vortical flow was graded as follows. Grade 0- laminar flow with no helices or vortices. Grade 1- mild helical or vortical flow (< 360 degrees of rotation), Grade 2- severe helical or vortical flow(>/= 360 degrees of rotation)(Sieren et al., 2019).

Path lines show blood flow in the 3-dimensional plane over one or more heartbeats. Normal flow in the arteries is laminar with high velocity noted in the center of the lumen as compared to the periphery(Azarine et al., 2019).

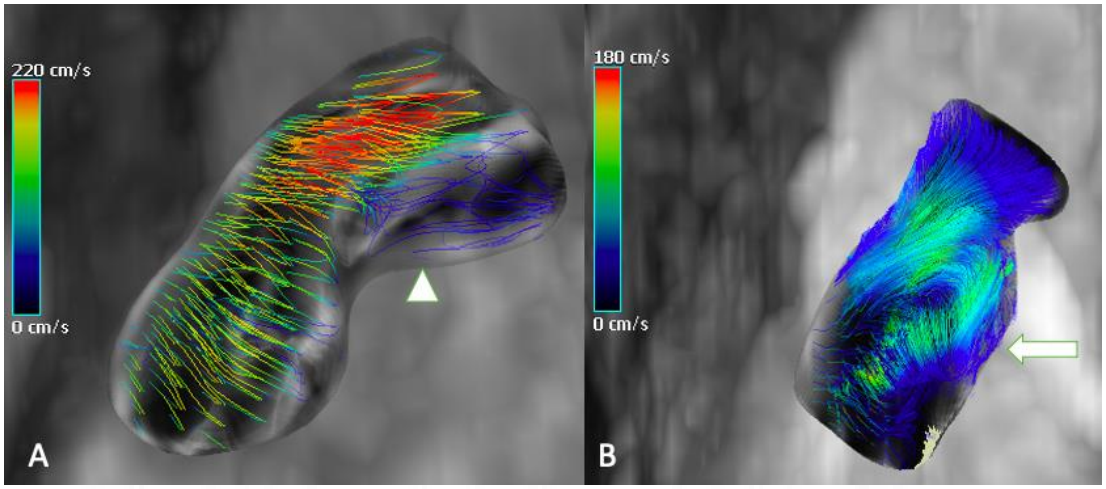


Figure 12 3D particle trace visualization illustrating the dynamics of main pulmonary artery in repaired TOF patients. White arrowhead in A shows moderate vortex (flow rotation <360°) = grade 1 and pronounced vortex (flow rotation >360°) = grade 2 (white arrow in B)

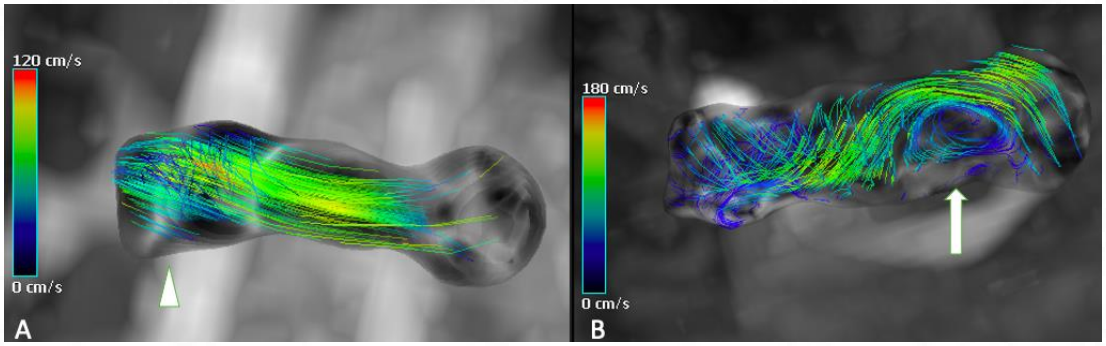


Figure 13 3D particle trace visualization illustrating the dynamics of right pulmonary artery in repaired TOF patients. White arrowhead in A shows moderate vortex (flow rotation <360°) = grade 1 and pronounced vortex (flow rotation >360°) = grade 2 (white arrow in B)

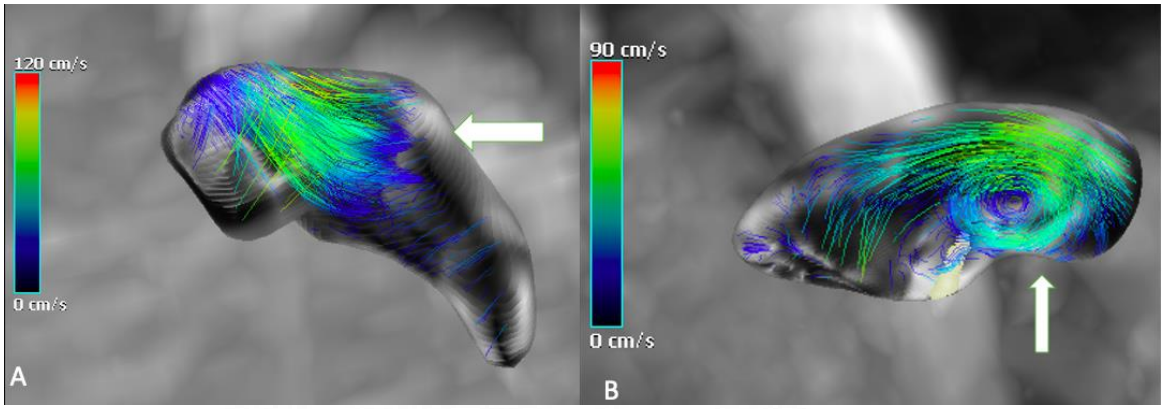


Figure 14 3D particle trace visualization illustrating the dynamics of left pulmonary artery in repaired TOF patients. White arrow in A shows moderate vortex (flow rotation <360°) = grade 1 and pronounced vortex (flow rotation >360°) = grade 2 (white arrow in B)

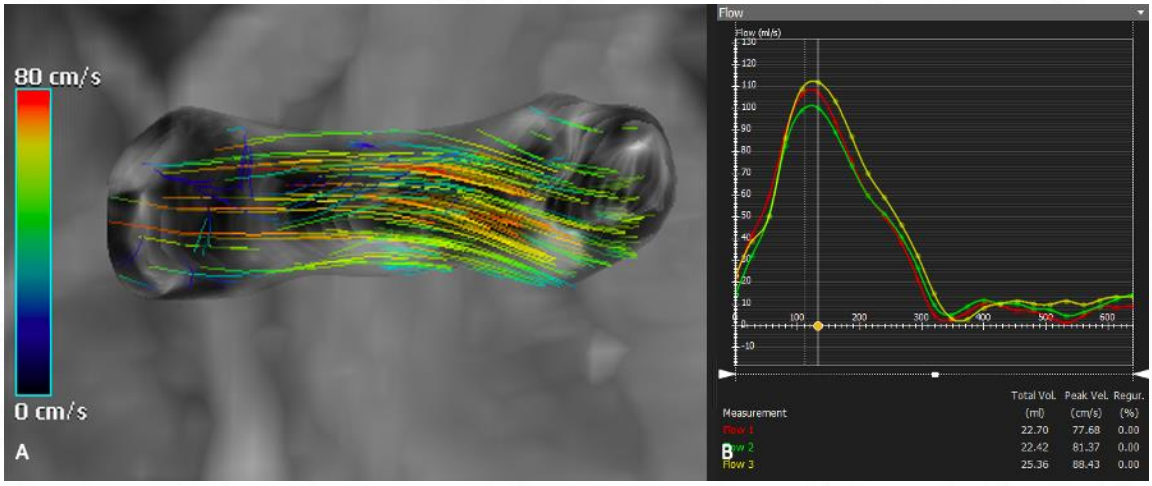


Figure 15 3D particle trace visualization in a control illustrating the dynamics of main pulmonary artery. Vortical flow was graded as Grade 0- laminar flow with no helices or vortices. PR was 0.00%.

**Quantitative analysis:**

They include

Basic quantitative parameters: After segmentation of the part where the flow information is to be studied, an ROI was drawn on the vessel of interest. The software automatically propagates the ROI in all the cardiac frames. All the frames were cross-checked to avoid measurement errors from the inclusion of nearby field. Various flow parameters obtained were forward flow (ml/beat), peak systolic velocity of that vessel (centimetres/second), reverse flow (ml/beat), and regurgitation fraction(percentage)(Azarine et al., 2019).


Figure 16 Color coded velocity images showing higher velocities in MPA (red color in A), (C) Peak velocity in the region of red color was 202.78 cm/s with PR of 64.35%.

**Flow assessment in RPA and LPA and pulmonary veins**

Internal validation was done with total volume of pulmonary venous blood flow with total volume of aortic root blood flow on 4D sequence. Similarly internal validation was done with total volume of MPA blood flow with total volume of aortic root blood flow on 2D and 4D sequences respectively.

Based on the observation of abundance of the vortices in proximal RPA and LPA, quantitative parameters in RPA and LPA were taken at the following positions: at the level of vortex (proximal aspect of artery) and distal to the vortex (could be either mid or distal aspects of artery) . Total volume of blood flow in right upper and right lower and left upper and left lower pulmonary veins was taken into consideration.

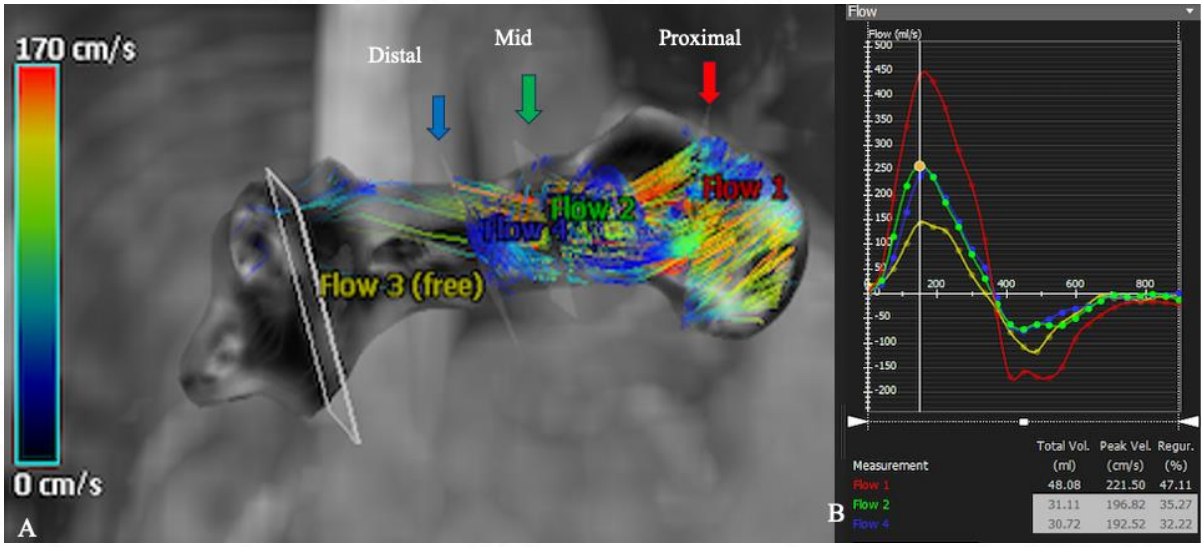


Figure 17 RPA flow measurements at three regions (proximal- red arrow, mid-green arrow and distal- blue arrow in A). Corresponding graph in B showing progressive reduction in the regurgitation fraction from proximal to distal aspect of the vessel

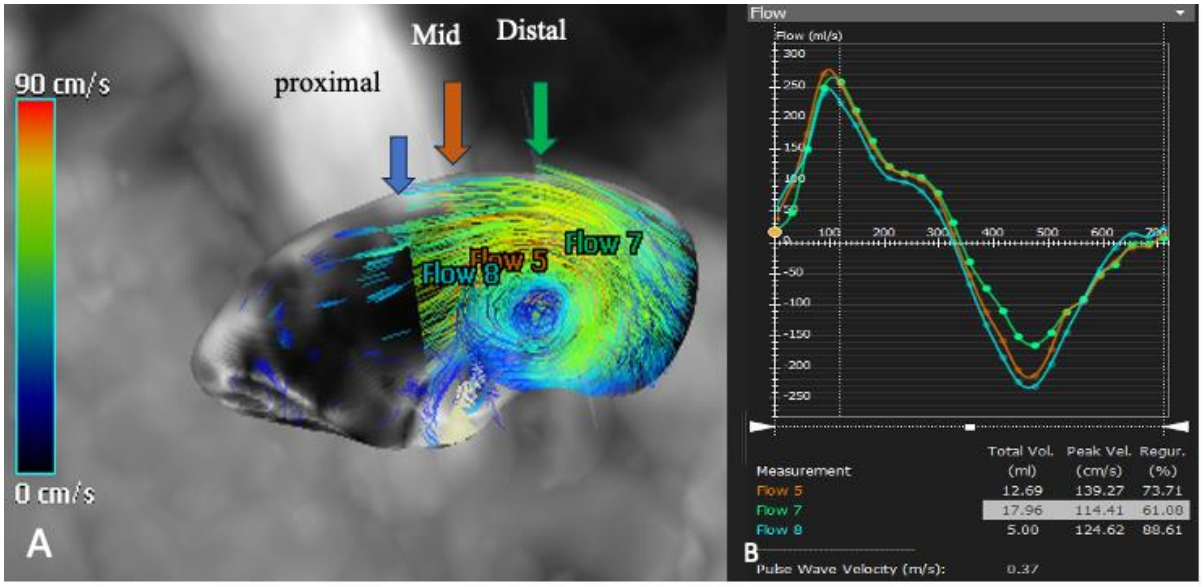


Figure 18 LPA flow measurements at three regions (proximal- blue arrow, mid- brown arrow and distal- green arrow in A). Corresponding graph in B showing progressive reduction in the regurgitation fraction from proximal to distal aspect of the vessel

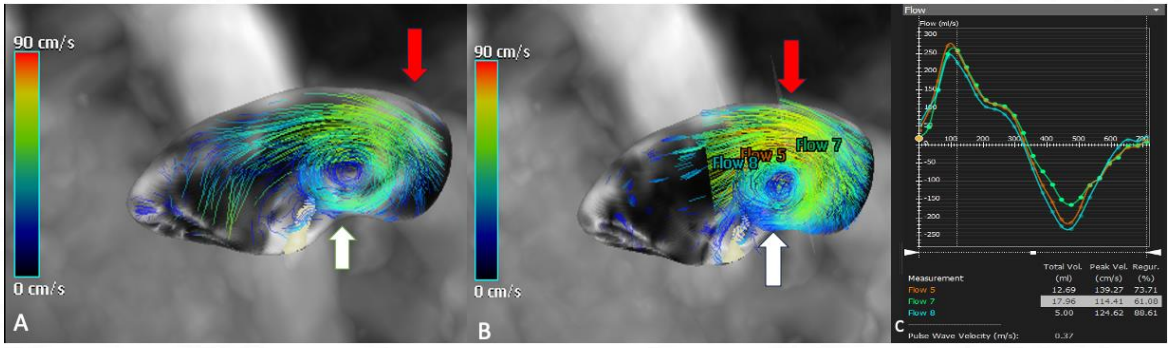


Figure 19 4D flow MRI with streamlines demonstrating vortical flow in LPA (white arrow in A and B). Flow measurements were taken at two regions (at the vortex, white arrow in A and B, flow 8 and 5 in B) and distal to the vortex (red arrow in A and B, flow 7 in B). Corresponding graphs in C

As patients with aorta pulmonary collaterals were excluded from the study, combined RPA plus LPA flow was taken as the total pulmonary artery flow (Qp) and was postulated to be equal to the total volume of pulmonary venous blood flow. Accuracy was internally

validated through employing the ‘conservation of mass’ principle, comparing volumes that are expected to be equal in absence of valvular malfunction or shunts(Elsayed et al., 2021).

Total pulmonary venous blood flow on 4D was considered as ground truth or benchmark to analyze with total volume of blood flow in MPA on 2D PCMRI versus 4D flow. The bias in this technique was measured by the difference between the values (The true value, which was Total pulmonary venous blood flow) and the measured value (MPA total volumes by 2D and 4D).

Total pulmonary venous blood flow on 4D was analyzed with the total volume of RPA+LPA on 4D at the vortex versus distal to the vortex. The bias in this technique was measured by the difference between the values. (The true value, which is Total pulmonary venous blood flow ) and the measured value (RPA+LPA volumes at the vortex or Distal to the vortex).

Differential flow to the lungs was calculated for both patients and controls using RPA/LPA flow ratio(Geiger et al., 2011). For patients, flow distal to the vortex in RPA and LPA was used for the analysis.

Wall shear stress- WSS is the shear force exerted tangentially on the vessel wall by the moving viscous blood(Fogel et al., 2012). Maximum and average WSS, average axial WSS (through plane) and average circumferential WSS(in-plane) were the parameters derived from 4D flow. WSS was measured in the following three regions: -above the pulmonary valve, mid MPA and pre bifurcation level. The highest of the three values was taken into consideration for analysis.

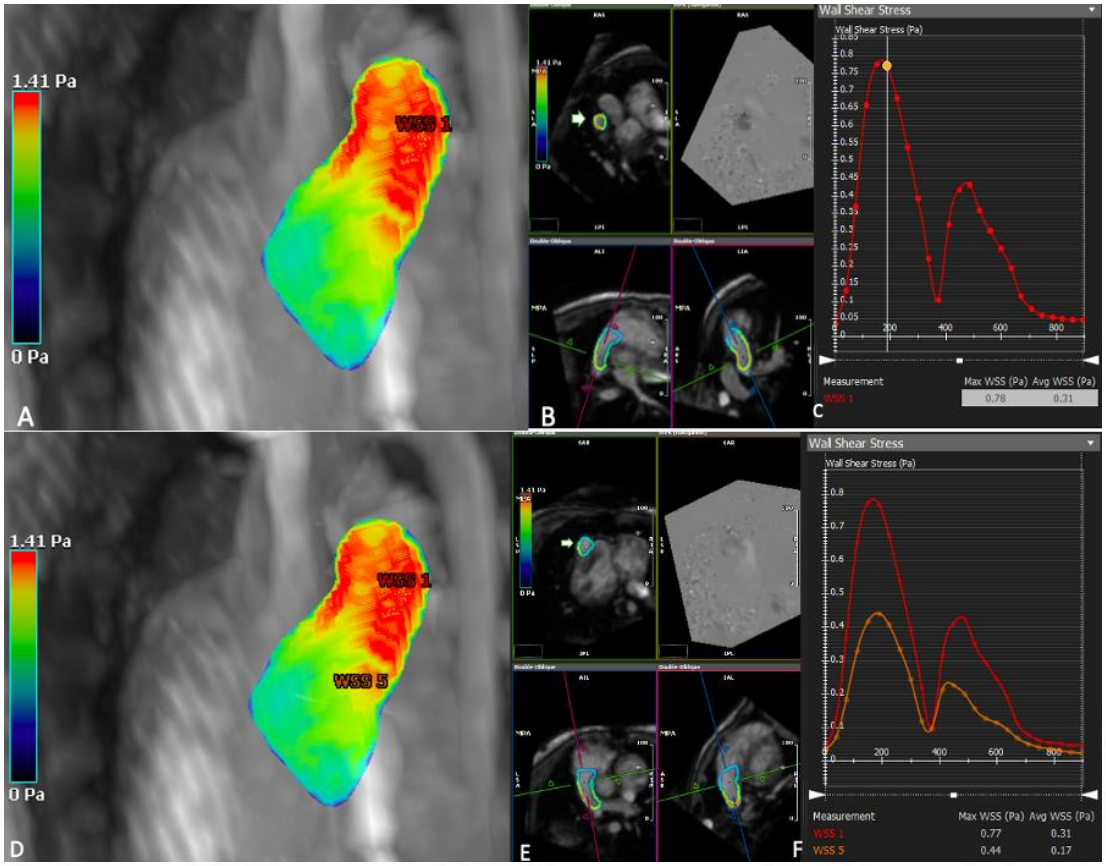


Figure 20 Technique for calculation of WSS. WSS in MPA in a repaired TOF patient with PR of 64.35 5%. (A) WSS 1 shows red color indicating turbulent flow. Axial section of MPA shows increased WSS (White arrow in B) with maximum and average values of 0.77 Pa and 0.31 Pa respectively. (D)WSS 5 in the same patient in the region of laminar flow. Axial section of MPA (White arrow in E) shows lesser values of WSS (F) with maximum and average WSS of 0.44 Pa and 0.17 Pa respectively

Energy loss across lumen: EL was calculated at the sites of vortical flow. Viscous energy loss is the non-turbulent mechanical energy converted irreversibly into heat. It is measured per volume units. Here viscous dissipation is calculated using reformulation of the viscous portion of the incompressible Navier-Stokes energy equation(Zajac et al.,

2015) (Robinson et al., 2019). EL due to complex flow can be accounted as well as regions of permanent energy loss are visualized(Zajac et al., 2015).

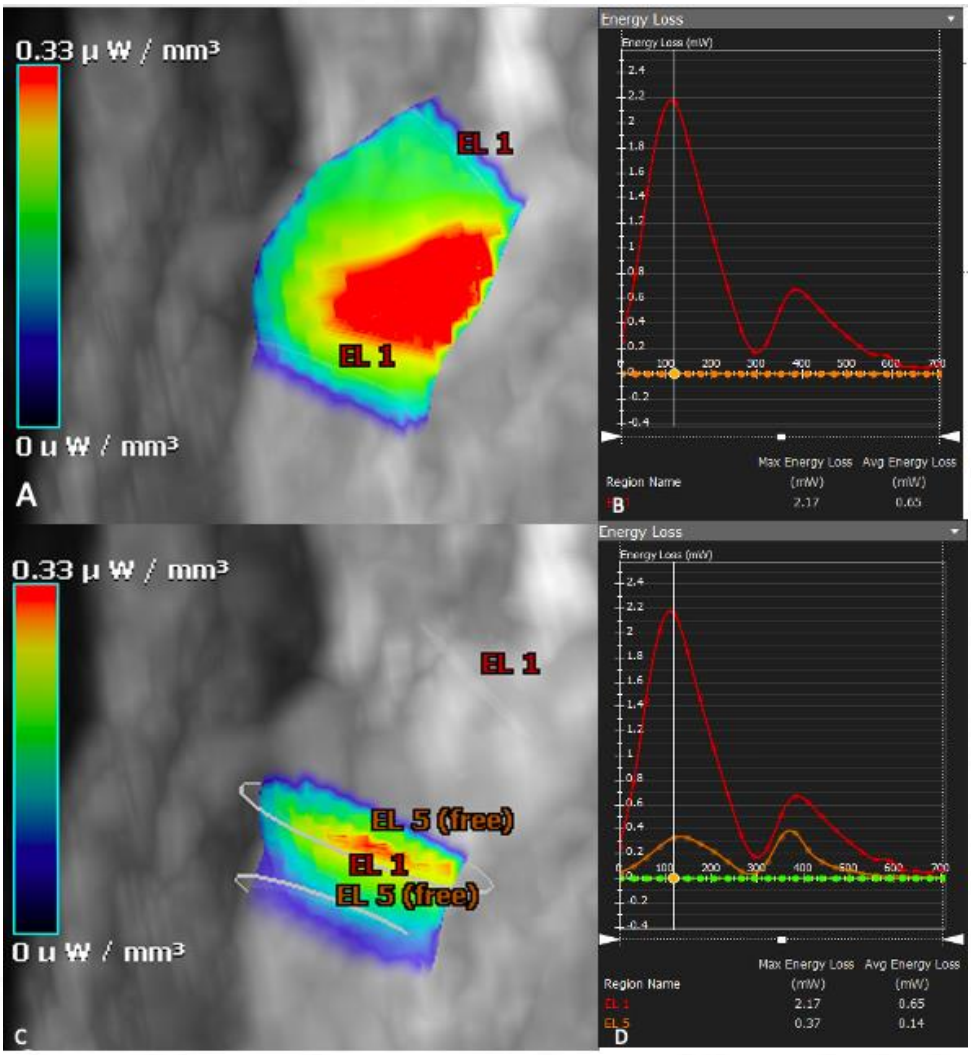


Figure 21 Technique for calculation of EL in MPA in a repaired TOF patient with PR of 47.95 %. (A) EL 1 shows red color indicating turbulent flow with increased values of maximum and average EL of 2.17 and 0.65 mW respectively in (B). EL in the same patient in a region of laminar flow (EL 5 in C) shows lesser values of EL (D) with maximum and average EL of 0.37 and 0.14 mW respectively.

Pressure loss across lumen: It is relative pressure measurements that can be achieved with the 4D flow. Color maps show distribution of pressure in the vessel during the cardiac cycle(François et al., 2012).

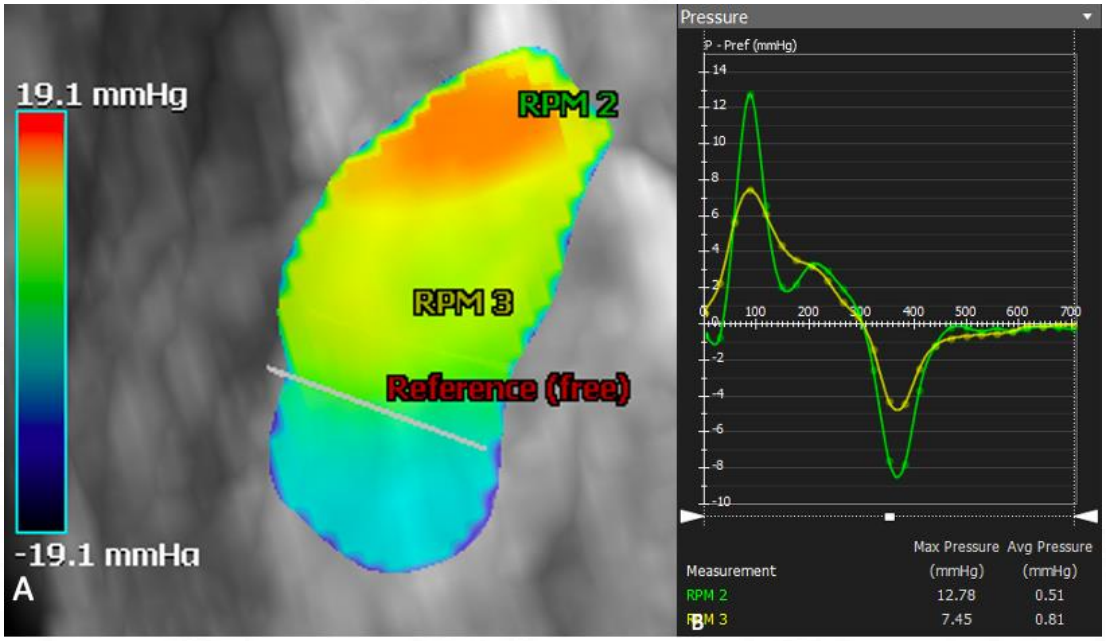


Figure 22 Pressure visualization in MPA in a repaired TOF patient with PR of 47.95 %. (A) Relatively higher values are noted in the region of turbulent flow (RPM2) as compared to areas with laminar flow. B shows the values of maximum and average pressure loss across the MPA.

**Analysis of results:**

The collected data was entered in Microsoft Excel spreadsheet and analysis was done using Epi-Info, JASP and Statistical Package for Social Sciences (SPSS) version 23.0. Continuous variables are represented as mean ± SD or medians with Inter-quartile range. Categorical variables are represented as number and percentage (%).

The variables were tested for normality with the Kolmogorov-Smirnov test for normality, Q-Q plots, visual inspection of the histograms and the z-scores for the degree of skewness and kurtosis.

Scatter diagrams were used to describe the relationship between two quantitative variables.

Comparison of EL and WSS between cases and controls was done using parametric Student's T Test if the variable was normally distributed in the various subgroups.

Not all variables met the assumptions required for parametric; therefore, non-parametric test (i.e., Mann-Whitney test) was used for all analyses for consistency.

The Bland Altman analysis was performed to ascertain the level of agreement between the 2D and 4D sequences for the measurement of PR and peak velocity in MPA, RPA and LPA.

The Spearman correlation coefficient was determined to assess the correlation between demographics (age at the time of surgery), ECG (QRS duration) and RV CMR parameters (RV remodeling Index (RVEDV/LVEDV), RVESVi and RVEDVi. The Spearman correlation coefficient was determined to assess the correlation between WSS in RVOT and RV CMR parameters, between RVOT dimension and WSS in RVOT, between QRS duration and WSS in RVOT, between PR and RVEDV, between RVEDV and EL in MPA, between total volume of aortic root blood flow and total pulmonary venous blood flow on 4D, between total volume in MPA and total volume of aortic root blood flow on 2D and 4D sequences.

For assessment of total pulmonary venous blood flow via MPA volume by 2D versus 4D flow, the mean difference was calculated using Student's Paired T test.

For assessment of total pulmonary venous blood flow via RPA+LPA volume (at the vortex versus distal to the vortex) on 4D flow, the mean difference was calculated using Student's Paired T test. Statistical significance was defined as $P < 0.05$. Appropriate graphs such as pie charts, bar diagrams and histograms have been constructed.

# RESULTS AND OBSERVATIONS

**Demographics of repaired TOF patients**

A total of 30 cases was included in our study, of which 20 (66.67%) were males and 10 (33.33%) were females(Fig ). 26 patients belonged to New York Heart Association classification (NYHA) FC I, 3 patients belonged to FC II and 1 was FC III. Pulmonary valve replacement was performed in 12 patients (40%). The mean age at the time of surgery was 3.86±3.63 years. The mean age at the time of CMR was 26.2±11.1 years.

Table 4 Demographics of repaired TOF patients (clinical and ECG parameters)

| | Mean | Standard deviation | Median |
|---|---|---|---|
| Age at the time of CMRI (Years) | 26.2 | 11.1 | 22 |
| Age at the time of surgery (years) | 3.86 | 3.63 | 2.54 |
| Bruce time (minutes) | 8.05 | 1.17 | 8.41 |
| METS | 9.7 | 1.5 | 10.1 |
| VO2 (ml/kg/min) | 29.2 | 4.7 | 29.3 |
| QRS duration | 140.86 | 26.75 | 150 |

Table 5 Demographics of repaired TOF patients (CMR parameters)

| | Mean | Standard deviation | Median |
|---|---|---|---|
| LVEF % | 57.44 | 6.97 | 57.73 |
| LVEDVi(mL/m2) | 67.28 | 16.15 | 64.60 |
| LVESVi (mL/m2) | 28.85 | 9.19 | 28.27 |
| RVEF% | 53.66 | 7.97 | 52.99 |
| RVEDVi(mL/m2) | 137.85 | 38.90 | 136.63 |
| RVESVi (mL/m2) | 65.36 | 25.58 | 60.95 |
| RV remodeling Index | 2.12 | 0.70 | 2.04 |
| RVOT (mm) | 26.60 | 5.52 | 27.20 |
| MPA Area (cm2) | 6.60 | 2.97 | 5.69 |
| MPA Diameter (mm) | 26.5 | 5.8 | 26.5 |
| Peak Velocity MPA by 2D (cm/s) | 157.17 | 36.75 | 149.64 |
| Peak Velocity MPA by 4D (cm/s) | 175.79 | 29.47 | 169.56 |
| Peak Velocity RPA 2D (cm/s) | 137.04 | 54.37 | 132.73 |
| Peak Velocity RPA 4D (cm/s) | 154.11 | 34.17 | 158.14 |
| Peak Velocity LPA 2D (cm/s) | 146.93 | 52.32 | 143.52 |
| Peak Velocity LPA 4D (cm/s) | 170.36 | 36.73 | 167.51 |
| PR% MPA by 2D | 50 | 15 | 50 |
| PR % MPA by 4D | 49.37 | 14.08 | 50.11 |

Table 6 Demographics of controls (clinical and ECG parameters)

| | Mean | Standard deviation | Median |
|---|---|---|---|
| Age at the time of CMRI (Years) | 25.13 | 6.87 | 23 |
| QRS duration | 93.2 | 10.16 | 90 |

Table 7 Demographics of controls (CMR parameters)

| | Mean | Standard deviation | Median |
|---|---|---|---|
| LVEF % | 67.48 | 6.61 | 67.91 |
| LVEDVi(mL/m2) | 65.40 | 11.37 | 61 |
| LVESVi (mL/m2) | 20.74 | 5.04 | 19 |
| RVEF% | 65.41 | 6.57 | 65.5 |
| RVEDVi(mL/m2) | 55.17 | 11.77 | 52.53 |
| RVESVi (mL/m2) | 17.66 | 5.35 | 16.35 |
| RV remodeling Index | 0.81 | 0.10 | 0.77 |
| MPA Diameter (mm) | 18.53 | 2.60 | 18.94 |
| Peak Velocity MPA by 4D (cm/s) | 96.81 | 23.39 | 96.21 |
| PR % MPA by 4D | 0.84 | 0.88 | 1 |

## COMPARISON OF CASES AND CONTROLS

### Comparison of demographics (Clinical, ECG and CMR parameters) between cases and controls

There was no significant difference between the mean ages of repaired TOF patients and controls (26.2±11.1 versus 25.13±6.87). Repaired TOF patients had significantly larger RV volumes and lower RVEF and LVEF compared with controls. Mean PR was 49.37±14.08 among repaired TOF patients. There were significant differences in CMR parameters between repaired TOF patients and controls except for LVEDV and RPA/LPA ratio

Table 8 Comparison of demographics (Clinical, ECG and CMR parameters) between cases and controls

| | Repaired TOF patients(n=30) | Controls (n=15) | P value |
|---|---|---|---|
| Age at the time of CMRI (Years) | 26.2±11.1 | 25.13±6.87 | 0.055 |
| Gender(male/female) | 20:10 | 8:7 | |
| QRS duration | 140.86±26.75 | 93.2±10.16 | **<.001** |
| LVEF % | 57.44±6.97 | 67.48±6.61 | **<.001** |
| LVEDVi(mL/m2) | 67.28±16.15 | 65.40±11.37 | 0.952 |
| LVESVi (mL/m2) | 28.85±9.19 | 20.74±5.04 | **.002** |
| RVEF% | 53.66±7.97 | 65.41±6.57 | **<.001** |
| RVEDVi(mL/m2) | 137.85±38.90 | 55.17±11.77 | **<.001** |

| | | | |
|---|---|---|---|
| RVESVi (mL/m2) | 65.36±25.58 | 17.66±5.35 | **<.001** |
| RV remodeling Index | 2.12±0.70 | 0.81±0.10 | **<.001** |
| MPA Diameter (mm) | 26.5±5.8 | 18.53±2.60 | **<.001** |
| Peak Velocity MPA by 4D (cm/s) | 175.79±29.47 | 96.81±23.39 | **<.001** |
| PR % MPA by 4D | 49.37±14.08 | 0.84±0.88 | **<.001** |
| RPA/LPA ratio on 4D | 2.08±3.86 | 1.43±0.24 | 0.549 |

**Comparison of WSS between cases and controls**

Patients with repaired TOF showed elevated maximum and average WSS values as compared to controls in RVOT, MPA, RPA and LPA with significant p value (<0.001)

Table 9 Comparison of maximum and average WSS between cases and controls

| | | Cases | Controls | P value |
|---|---|---|---|---|
| Maximum WSS RVOT | Mean (SD) | 0.23(0.06) | 0.14(0.01) | **<0.001** |
| Average WSS RVOT | Mean (SD) | 0.12 (0.03) | 0.06 (0.01) | **<0.001** |
| Maximum WSS MPA | Mean (SD) | 0.46 (0.11) | 0.22 (0.04) | **<0.001** |
| Average WSS MPA | Mean (SD) | 0.22 (0.05) | 0.08 (0.02) | **<0.001** |
| Maximum WSS RPA | Mean (SD) | 0.58(0.23) | 0.26(0.02) | **<0.001** |
| Average WSS RPA | Mean (SD) | 0.26 (0.08) | 0.12 (0.01) | **<0.001** |
| Maximum WSS LPA | Mean (SD) | 0.47 (0.08) | 0.25 (0.03) | **<0.001** |
| Average WSS LPA | Mean (SD) | 0.2 (0.05) | 0.11 (0.02) | **<0.001** |

**Comparison of EL between cases and controls**

Patients with repaired TOF showed elevated maximum and average EL values as compared to controls in MPA, RPA and LPA with significant p value (<0.001)

Table 10 Comparison of maximum and average EL between cases and controls

| | | Cases | Controls | P value |
|---|---|---|---|---|
| Maximum EL (MPA) | Mean (SD) | 2.2(0.84) | 0.26(0.09) | **<0.001** |
| Average EL (MPA) | Mean (SD) | 0.81(0.26) | 0.1(0.03) | **<0.001** |
| Maximum EL (RPA) | Mean (SD) | 1.47(1.3) | 0.08(0.02) | **<0.001** |
| Average EL (RPA) | Mean (SD) | 0.45(0.34) | 0.03(0.01) | **<0.001** |
| Maximum EL (LPA) | Mean (SD) | 1.3(0.75) | 0.08 (0.07) | **<0.001** |
| Average EL (LPA) | Mean (SD) | 0.33(0.21) | 0.03(0.03) | **<0.001** |

## CORRELATION ANALYSIS

### 2D VS 4D FLOW

#### Pulmonary regurgitation fraction between 2D and 4D sequences

A Pearson correlation showed a high, positive correlation between PR in MPA by 2DPCMRI and 4D flow , $r(28) = 0.87$, $p = <.001$.

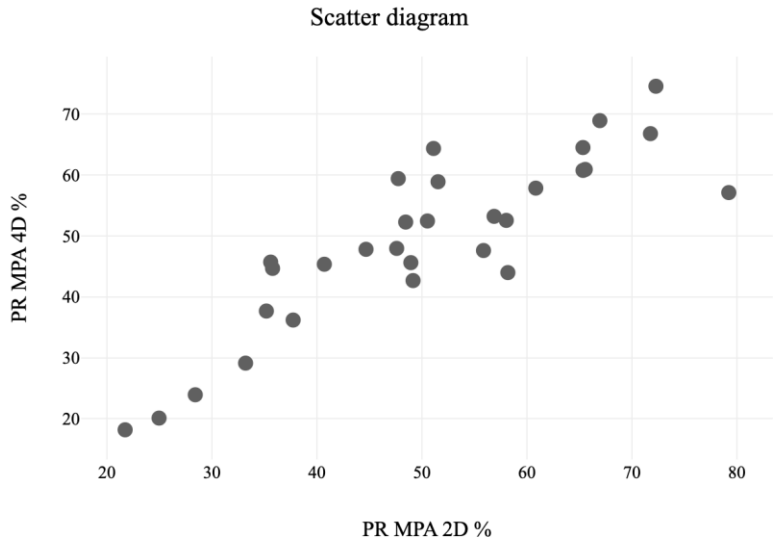


Figure 23 Pearson correlation between PR by 2DPCMRI and 4D flow

#### Level of agreement between 2D PCMRI and 4D flow with respect to PR

Using Bland Altman analysis, 4D flow reported lower value than 2D PCMRI by about 0.948%.

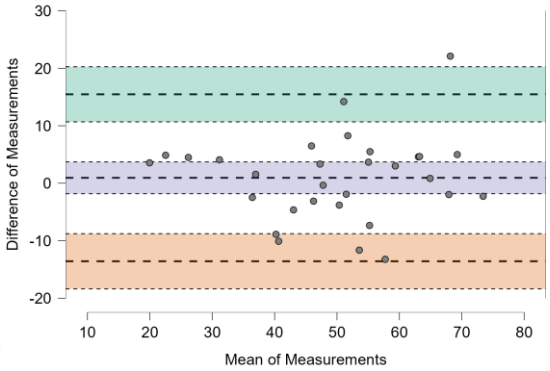


Figure 24 Bland Altman plot showing the Limits of Agreement between 2D and 4D CMRI sequence for measuring PR.

**Correlation analysis between Pulmonary regurgitation on 2D and 4D sequences with RVEDV**

A statistically significant and positive correlation was found between these two variables (p value <0.001). Thus, RVEDVi tends to have higher values with increasing values of PR. However the correlation coefficient was higher for 4D as *compared to 2D PCMRI (r=0.835 versus 0.442)*

Table 11 Spearman Rank correlation analysis between the variables RVEDVi (mL/m2) and PR by 2D PCMRI and 4D flow

| | | PR by 2D | PR by 4D |
|---|---|---|---|
| RVEDVi (mL/m2) | Correlation Coefficient | **0.442** | **0.835** |
| | P Value | **0.015** | **<.001** |

**Peak velocity (cm/s) in MPA, RPA and LPA with 2D PCMRI and 4D flow MRI**

There were significant differences between the peak velocities in MPA ( p value=0.034) ,RPA (p value=0.017) and LPA ( p value=0.049) with higher velocities seen in 4D flow as compared to 2D PCMRI

Table 12 Peak velocity (cm/s) in MPA, RPA and LPA with 2D PCMRI and 4D flow MRI

| | Peak velocity(cm/s) 2D | Peak velocity(cm/s) 4D | P value |
|---|---|---|---|
| MPA | 157.17 ± 36.75 | 175.79± 29.47 | 0.034 |
| RPA | 137.04 ± 54.37 | 154.11± 34.17 | 0.017 |
| LPA | 146.93± 52.32 | 170.36± 36.73 | 0.049 |

**Correlation analysis between variables Aortic root Total volume (mL) and Total Volume MPA (mL) on 2D and 4D sequences**

4D flow had a stronger correlation (r = 851) and a much higher coefficient of determination ($R^2$ = 0.819) as compared to the 2D sequence (r = 670, $R^2$ = 0.508).

Table 13 Correlation analysis between variables Aortic root total volume (mL) and Total Volume MPA (mL) on 2D and 4D sequences

| | | **Total Volume MPA 2D** (mL) |
|---|---|---|
| **Aortic root Total volume 2D** (mL) | Correlation Coefficient | **0.670** |
| | P Value | <0.001 |
| | | **Total Volume MPA 4D** (mL) |
| **Aortic root Total volume 4D** (mL) | Correlation Coefficient | **0.851** |
| | P Value | <0.001 |

**Correlation analysis between aortic root total volume 4D (mL) and Total Pulmonary Venous flow 4D (mL)**

Internal validation was done between aortic root total volume with total Pulmonary Venous flow on 4D. Spearman Rank correlation analysis showed a statistically significant and positive correlation between these variables (r = 0.861, p value <0.001).

Table 14 Correlation analysis between variables aortic total volume 4D (mL) and Total Pulmonary Venous flow 4D (mL)

| | | Total Pulmonary Venous flow 4D (mL) |
|---|---|---|
| Aortic root total volume 4D (mL) | Correlation Coefficient | **0.861** |
| | P Value | <0.001 |

Bland Altmann plot showed good agreement between aortic root total volume 4D (mL) and Total Pulmonary Venous flow 4D (mL)

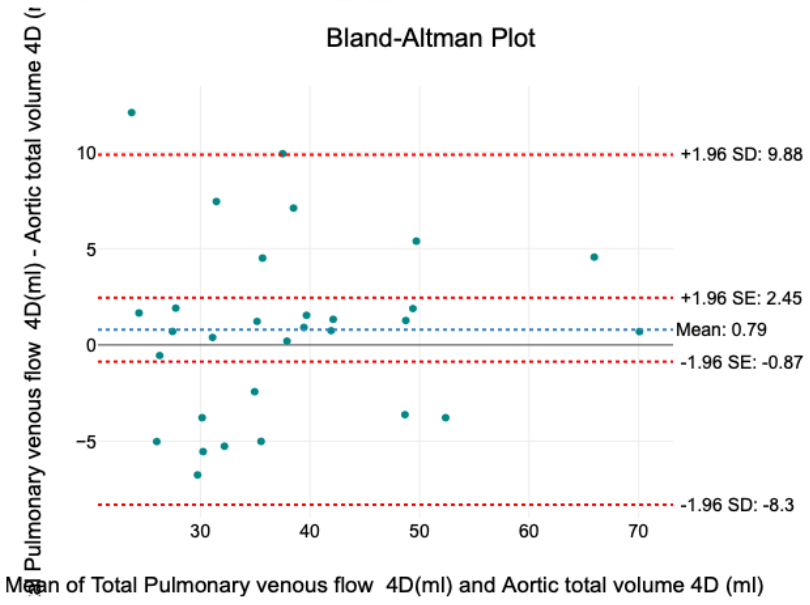


Figure 25 Bland Altmann plot between aortic root total volume 4D (mL) and Total Pulmonary Venous flow 4D (mL)

**Assessment of total pulmonary venous blood flow on 4D versus total volume of blood flow in MPA on 2D PCMRI and 4D flow sequences**

The mean difference/bias was significantly lower in the 4D flow, as compared to the 2D PCMRI. (Mean 2.5 ± 4.92 on 4D versus -7.2 ± 13.81 on 2D PCMRI) while assessing the total pulmonary venous blood flow via MPA total volume.

Table 15 Mean differences between Total pulmonary venous blood flow and MPA volumes as measured by 2D PCMRI and 4D flow.

| | Δ (PVBF-MPA 2D) | Δ (PVBF-MPA 4D) | P value |
|---|---|---|---|
| Mean± Standard Deviation | -7.20±13.81 | 2.50±4.92 | **<0.001** |
| Median | -7.55 | 3.38 | |

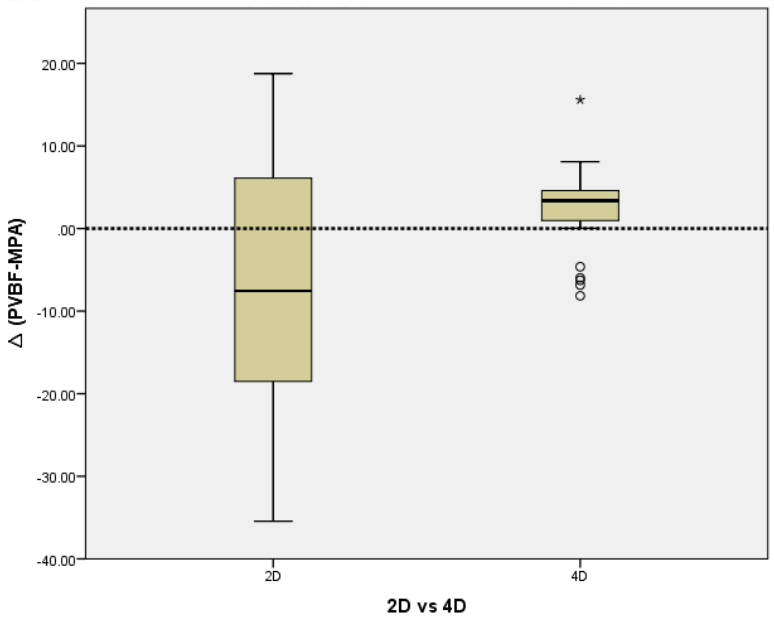


Figure 26 Boxplot comparing the Mean differences between Total pulmonary venous blood flow and MPA total volume as measured by 2D PMCRI and 4D flow.

**Correlation between the clinical and ECG parameters and RV parameters**

No significant correlation was noted between the age at the time of surgery and QRS duration with right ventricular parameters

Table 16 Spearman's rank correlation between the clinical and ECG parameters and right ventricular parameters

| Clinical and ECG parameters | | RV remodeling Index (RVEDV/LVEDV) | RVEDVi (mL/m2) | RVESVi (mL/m2) |
|---|---|---|---|---|
| Age at the time of Surgery (Years) | Correlation Coefficient | 0.150 | 0.000 | -0.071 |
| | P value | 0.427 | 0.999 | 0.711 |
| QRS Duration (ms) | Correlation Coefficient | 0.251 | 0.190 | 0.120 |
| | P value | 0.181 | 0.313 | 0.529 |

**4D flow CMR parameters in repaired TOF patients**

No significant correlation was noted between the WSS in RVOT and RV parameters

Table 17 Spearman's rank correlation between the 4D flow CMR and right ventricular parameters

| 4D CMR parameters | | RV remodeling Index (RVEDV/LVEDV) | RVEDVi (mL/m2) | RVESVi (mL/m2) |
|---|---|---|---|---|
| Average WSS RVOT | Correlation Coefficient | 0.165 | 0.046 | 0.156 |
| | P value | 0.384 | 0.808 | 0.409 |
| Maximum WSS RVOT | Correlation Coefficient | 0.028 | -0.002 | 0.15 |
| | P value | 0.884 | 0.993 | 0.937 |

**Correlation between the RVOT dimension and QRS duration with WSS RVOT**

A medium positive and a statistically significant correlation between QRS duration and Maximum WSS (p value=0.001) and average WSS RVOT (p value=0.002) was noted. Thus, higher or lower values of QRS duration are associated with respectively higher or lower values of both average as well as Maximum WSS RVOT.

Table 18 Spearman's rank correlation between the RVOT dimension and QRS duration with WSS RVOT

| | | Average WSS RVOT | Maximum WSS RVOT |
|---|---|---|---|
| RVOT (mm) | Correlation Coefficient | 0.227 | 0.008 |
| | P value | 0.228 | 0.965 |
| **QRS Duration (ms)** | Correlation Coefficient | 0.536 | 0.559 |
| | P value | **0.002** | **0.001** |

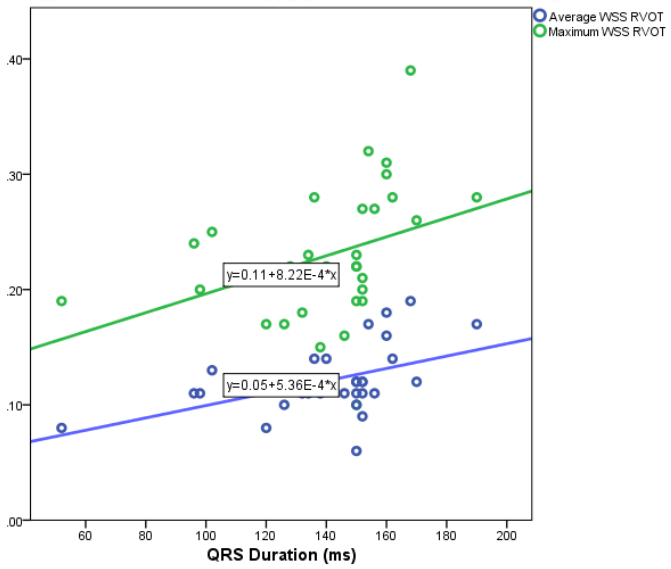


Figure 27 Scatterplot between QRS duration and WSS RVOT

**Correlation analysis between RVEDVi (ml/m2) and maximum and average WSS in MPA**

A statistically significant and positive correlation between the variables RVEDV and maximum and average WSS in MPA (p value <0.001) was noted. Thus, RVEDVi tends to have higher values with increasing values of Maximum and average WSS in MPA and vice versa.

Table 19 Spearman correlation between RVEDVi (ml/m2) and maximum and average WSS in MPA

| | | Max WSS MPA |
|---|---|---|
| RVEDVi (mL/m2) | Correlation Coefficient | 0.61 |
| | P Value | **<0.001** |
| | | Average WSS MPA |
| RVEDVi (mL/m2) | Correlation Coefficient | 0.66 |
| | P Value | **<0.001** |

**Location of WSS in MPA among repaired TOF patients**

Patients with repaired TOF had higher values of WSS in prebifurcation region of MPA (N=24, 80%) followed by proximal MPA (N=5, 16.67%).

Table 20 Location of WSS in MPA among repaired TOF patients

| Location of WSS in MPA | Number |
|---|---|
| Pre-bifurcation | 24 |
| Mid MPA | 1 |
| Proximal MPA | 5 |
| | 30 |

**Correlation analysis between variables RVEDVi (mL/m2) and Maximum EL and average EL in MPA**

A statistically significant and positive correlation between the variables RVEDV and maximum and average EL in MPA (p value <0.001) was noted. Thus, RVEDVi tends to have higher values with increasing values of Maximum and average EL in MPA and vice versa.

Table 21 Correlation analysis between variables RVEDVi (mL/m2) and Maximum EL and average EL in MPA

| | | Maximum EL in MPA |
|---|---|---|
| RVEDVi (mL/m2) | Correlation Coefficient | 0.648 |
| | P Value | **<0.001** |
| | | Average EL in MPA |
| RVEDVi (mL/m2) | Correlation Coefficient | 0.594 |
| | P Value | **<0.001** |

**Branch vessel assessments with 4D flow**

The mean vortex severity in the MPA and LPA was (average grading=1.83+_0.379) and (average grading=1.8+_0.406) respectively in the repaired TOF patients. RPA showed average grading of 1.43+_0.504. Mean vortices were maximum in MPA and LPA with less severe vortices in the RPA. Grade 2- severe helical or vortical flow(>/= 360 degrees of rotation) was seen in MPA and LPA in 25(83.33%) and 24 (80%) of repaired TOF patients respectively. Grade 1- mild helical or vortical flow (< 360 degrees of rotation) was seen in 5 (16.67%) and 6 (20%) patients in MPA and LPA respectively. RPA predominantly showed moderate vortices (grade 1) in 17 (56.67%) repaired TOF patients. None of the patients demonstrated grade 0- laminar flow with no helices or vortices in either of MPA, RPA or LPA.

Table 22 Vorticity grading in MPA, RPA and LPA

| Vessel | Vorticity grading |
|---|---|
| MPA | 1.83+_0.379 |
| RPA | 1.43+_0.504 |
| LPA | 1.8+_0.406 |

**Correlation analysis between the vessel diameter and respective vorticity grading in MPA, RPA and LPA**

No statistically significant difference was demonstrated between the vessel diameter and their respective vorticity grading in MPA, RPA and LPA.

Table 23 Spearman correlation between the variables vessel diameter and respective vorticity grading in MPA, RPA and LPA

| | | Vortex severity MPA |
|---|---|---|
| MPA diameter | Correlation | 0.29 |
| | P value | 0.11 |
| | | Vortex severity RPA |
| RPA diameter | Correlation | 0.24 |
| | P value | 0.20 |
| | | Vortex severity LPA |
| LPA diameter | Correlation | 0.08 |
| | P value | 0.66 |

**Division of RPA and LPA into three segments**

RPA and LPA were arbitrary divided into three segments each and labelled as follows (proximal-1, mid-2, and distal-3). Regurgitation fraction was calculated as depicted in Fig and Fig for RPA and LPA each respectively.

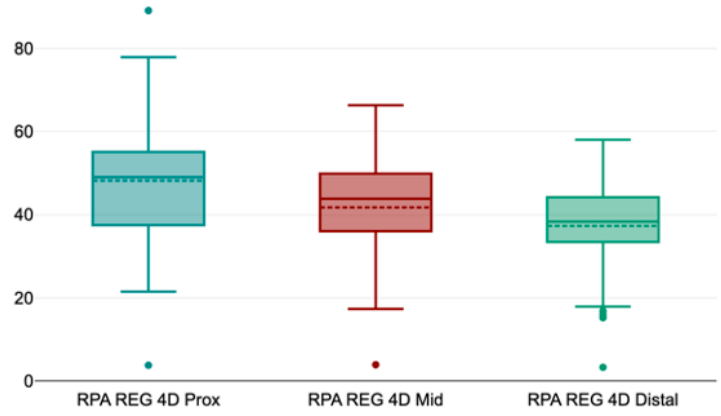


Figure 28 Progressive reduction in the regurgitation fraction in RPA and increase in the total volume of blood across RPA from proximal to distal aspect of the artery.

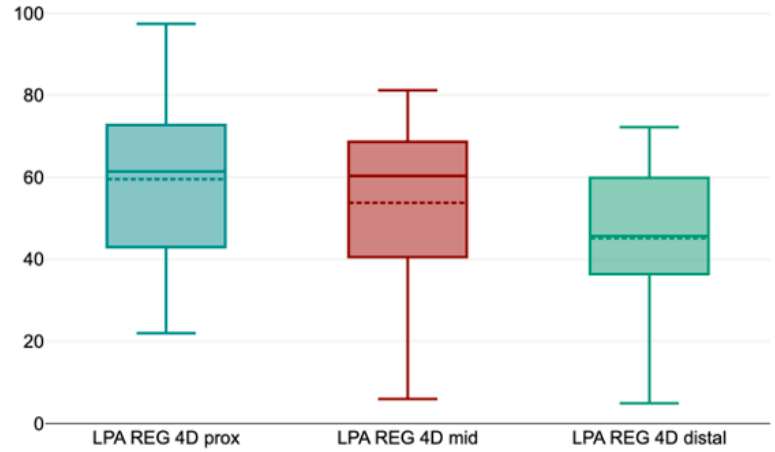


Figure 29 Progressive reduction in the regurgitation fraction in LPA and increase in the total volume of blood across LPA from proximal to distal aspect of the artery.

Table 24 Correlation between total pulmonary venous blood flow on 4D versus total volume of RPA+LPA on 2D versus 4D sequences

| | | Total pulmonary venous blood flow on 4D |
|---|---|---|
| Total volume of RPA+LPA on 2D (mL) | Correlation Coefficient | **0.37** |
| | P Value | **0.044** |
| Total volume of RPA+LPA at the vortex on 4D (mL) | Correlation Coefficient | 0.35 |
| | P Value | 0.054 |
| Total volume of RPA+LPA **distal to the vortex on 4D** (mL) | Correlation Coefficient | **0.79** |
| | P Value | **<0.001** |

**Assessment of total pulmonary venous blood flow on 4D versus total volume of RPA+LPA on 4D (at the vortex versus distal to the vortex)**

While assessing the total pulmonary venous blood flow on 4D via RPA+LPA total volumes by 4D flow, **the mean difference/bias was significantly lower distal to the vortex, as compared to at the vortex** (Mean -0.32 ± 5.83 versus 4.55+_13.49)

Table 25 Mean differences between Total pulmonary venous blood flow and RPA+LPA total volume at the Vortex versus Distal to the vortex

| | Δ (PVBF-RPA+LPA at the Vortex) | Δ (PVBF-RPA+LPA Distal to the Vortex) | P value |
|---|---|---|---|
| Mean | 4.55 | -0.32 | **0.019** |
| Standard Deviation | 13.49 | 5.83 | |
| Median | 5.30 | -1.87 | |

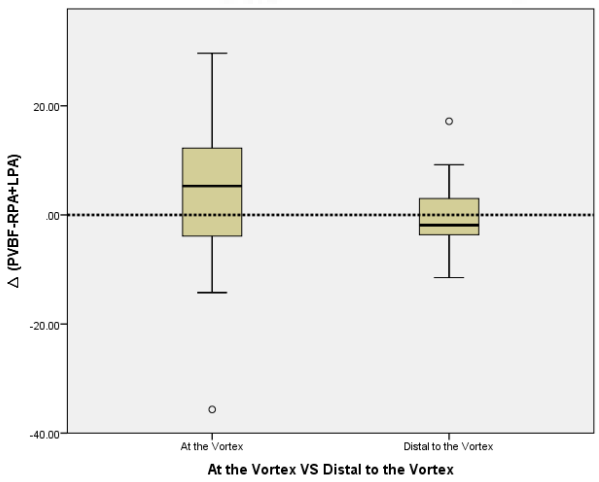


Figure 30 Boxplot comparing the Mean differences between Total pulmonary venous blood flow on 4D and RPA+LPA volume at the Vortex versus Distal to the vortex on 4D

**Assessment of right sided pulmonary venous blood flow on 4D versus total volume of blood flow in RPA (at the vortex versus distal to the vortex) on 4D**

Higher correlation was noted between right sided pulmonary venous blood flow with RPA total volume (distal to the vortex versus at the vortex)

Table 26 Correlation between the right sided pulmonary venous blood flow and RPA total volume at the Vortex versus Distal to the vortex

| | | Total volume of blood in Right sided pulmonary veins 4D (ml) |
|---|---|---|
| RPA Total vol **at the vortex** on 4D | Correlation | **0.4** |
| | P value | **0.031** |
| RPA Total vol **distal to the vortex** on 4D | Correlation | **0.59** |
| | P value | **0.001** |

**Assessment of left sided pulmonary venous blood flow on 4D versus total volume of blood flow in LPA (at the vortex versus distal to the vortex) on 4D**

Higher correlation was noted between left sided pulmonary venous blood flow with LPA total volume (distal to the vortex versus at the vortex)

Table 27 Correlation between the Left sided pulmonary venous blood flow and LPA total volume at the Vortex versus Distal to the vortex

| | | Total volume of blood in left sided pulmonary veins 4D (ml) |
|---|---|---|
| LPA total vol **at the vortex** on 4D | Correlation | **0.34** |
| | P value | **0.063** |
| LPA total vol **distal to the vortex** on 4D | Correlation | **0.83** |
| | P value | **<.001** |

**RPA/LPA ratio on 4D flow MRI in repaired TOF patients and controls**

RPA showed consistently elevated flows as compared to LPA in both cases and controls, however no statistically significant correlation was noted

Table 28 RPA/LPA ratio on 4D flow MRI in repaired TOF patients and controls

| | RPA/LPA ratio on 4D | P Value |
|---|---|---|
| Repaired TOF patients | 2.08±3.86 | 0.54 |
| Control | 1.43±0.24 | |

**Comparison of PVR VS non-PVR groups in 4D flow with respect to PR**

The average value of PR by 4D flow was significantly higher in the group who had undergone Pulmonary valve replacement as compared to those who had not (Mean 57.53 versus 43.92, p value- 0.007). However, the average value of PR by 2D PCMRI was comparable in both the groups ( p value 0.09)

Table 29 Comparison between the subjects who had undergone Pulmonary valve replacement and those who had not with respect to PR by 2D PCMRI versus 4D.

| PR by 2D PCMRI | Pulmonary Valve Replacement | | P Value |
|---|---|---|---|
| | Yes | No | |
| Mean (SD) | 55.87 (10.61) | 46.61 (15.4) | 0.09 |
| Median (IQR) | 54.0 (48.65-65.4) | 48.03 (35.34-57.5) | |
| Min-Max | 35.6-71.77 | 21.74-79.23 | |
| **PR by 4D flow** | Pulmonary Valve Replacement | | P Value |
| | Yes | No | |
| Mean (SD) | 57.53 (7.94) | 43.92 (14.25) | **0.007** |
| Median (IQR) | 60.08 (51.29-64.39) | 45.01 (36.56-52.48) | |
| Min-Max | 45.61-68.92 | 18.18-74.56 | |

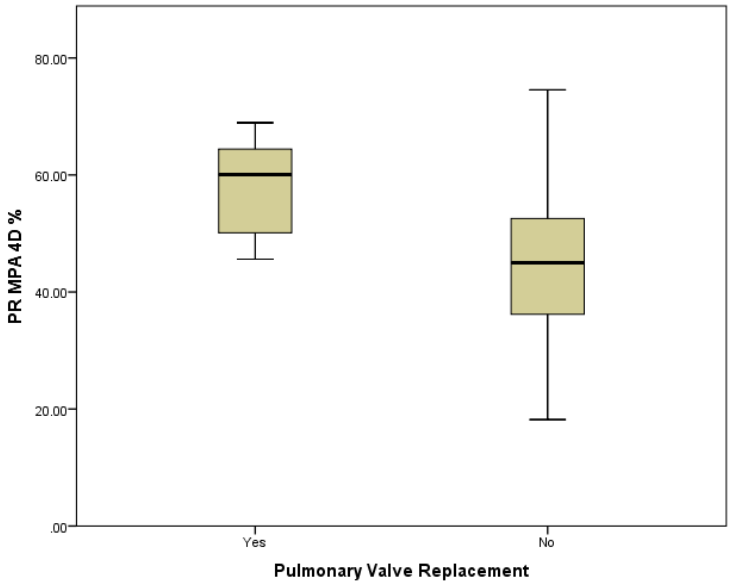


Figure 31 Boxplot showing the comparison between the subjects who had undergone Pulmonary valve replacement and those who had not with respect to PR by 4D flow

**Comparison of PVR VS non-PVR groups with respect to EL in MPA, RPA and LPA**

No statistically significant difference was found in the maximum and average values of EL in MPA, RPA and LPA between the PVR and non-PVR groups with higher EL in non-PVR group

Table 30 Comparison between the subjects who had undergone Pulmonary valve replacement and those who had not with respect to Maximum and average EL in MPA, RPA and LPA

| | | | Pulmonary Valve Replacement | | P value |
|---|---|---|---|---|---|
| | | | Yes | No | |
| MPA | Maximum EL | Mean (SD) | 2.02 (0.84) | 2.32 (0.82) | 0.354 |
| | Average EL | Mean (SD) | 0.77 (0.26) | 0.85 (0.25) | 0.435 |
| RPA | Maximum EL | Mean (SD) | 1.26 (0.6) | 1.61 (1.64) | 1.0 |
| | Average EL | Mean (SD) | 0.41 (0.21) | 0.47 (0.41) | 0.602 |
| LPA | Maximum EL | Mean (SD) | 1.2 (0.98) | 1.37 (0.6) | 0.172 |
| | Average EL | Mean (SD) | 0.31 (0.25) | 0.34 (0.19) | 0.346 |

**Comparison of PVR VS non-PVR groups with respect to RVEF and peak systolic velocity in MPA, RPA and LPA**

RVEF was significantly lower in PVR group as compared to non-PVR group(48.30±8.20 versus 57.22±5.58, p value=0.017), however the peak systolic velocity in MPA, RPA and LPA was comparable between the PVR and non-PVR groups

Table 31 Comparison of PVR VS non-PVR groups with respect to RVEF and peak systolic velocity in MPA, RPA and LPA

| | | Pulmonary Valve Replacement | | P value |
|---|---|---|---|---|
| | | Yes | No | |
| **RVEF** | Mean (SD) | 48.30(8.20) | 57.22(5.58) | **0.017** |
| MPA PSV | Mean (SD) | 166.74 (19.24) | 181.81 (33.84) | 0.226 |
| RPA PSV | Mean (SD) | 147.66 (25.71) | 158.41 (38.92) | 0.259 |
| LPA PSV | Mean (SD) | 159.85 (33.42) | 177.37(38.06) | 0.24 |

**Comparison of PVR VS non-PVR groups with respect to WSS in MPA**

Maximum and average WSS in MPA were comparable between the PVR and non-PVR groups

Table 32 Comparison of PVR VS non-PVR groups with respect to WSS in MPA

| | | | Pulmonary Valve Replacement | | P value |
|---|---|---|---|---|---|
| | | | Yes | No | |
| MPA | Maximum WSS | Mean (SD) | 0.45 (0.15) | 0.47(0.083) | 0.404 |
| | Average WSS | Mean (SD) | 0.22 (0.05) | 0.23 (0.049) | 0.264 |

**Reproducibility analysis / interobserver variation**

The segmentation and flow analysis were done by 2 observers with 3 years and 9 years of experience in cardiac CMR. The flow parameters -Total pulmonary venous flow on 4D, Aortic root total volume on 4D, Total vol RPA +LPA (at the vortex) and Total vol

RPA +LPA (distal to the vortex) were compared between the two observers. Interobserver variation was measured by Bland Altman plots

Table 33 Interobserver variability related to Total pulmonary venous flow (ml) between Observer 1 and observer 2

| | Total pulmonary venous flow (ml)-Observer 1 | Total pulmonary venous flow (ml)-Observer 2 |
|---|---|---|
| Mean | 38.52 | 38.324 |
| Standard deviation | 11.82 | 11.93 |
| Minimum | 23.5 | 24.34 |
| Maximum | 70.42 | 70.23 |

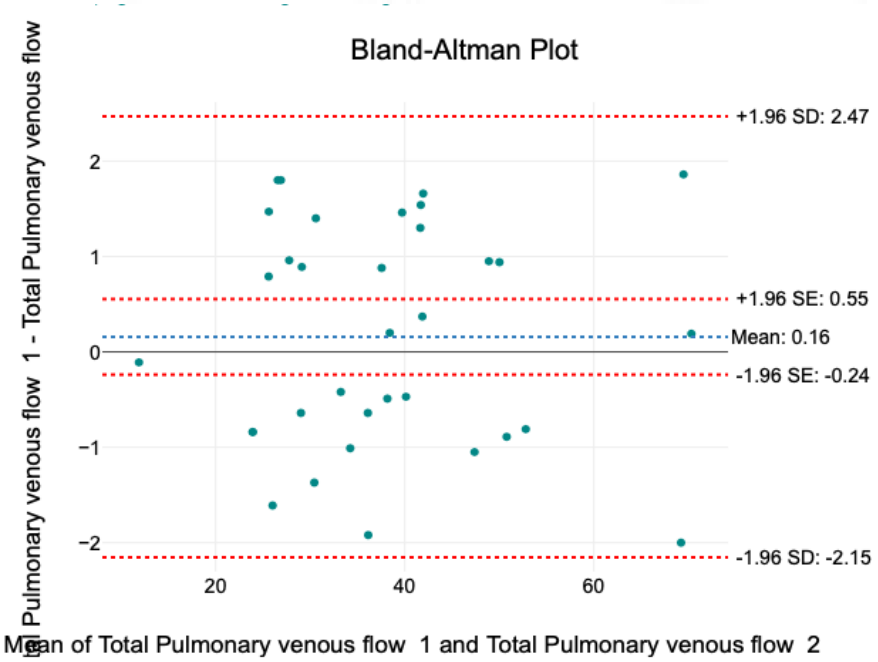


Figure 32 Bland Altman plot for Total pulmonary venous flow on 4D between observer 1 and 2

**Aortic root total volume 4D (ml):** Aortic root total volume 4D (ml) analysis was performed by the two observers and Bland Altmann plot was drawn which showed no significant interobserver variability.

Table 34 Interobserver variability related to Aortic root total volume 4D (ml) between Observer 1 and observer 2

| | Aortic root total volume 4D (ml) Observer 1 | Aortic root total volume 4D (ml) Observer 2 |
|---|---|---|
| Mean | 37.73 | 37.63 |
| Std. Deviation | 11.47 | 11.13 |
| Minimum | 17.68 | 19.12 |
| Maximum | 69.73 | 67.34 |

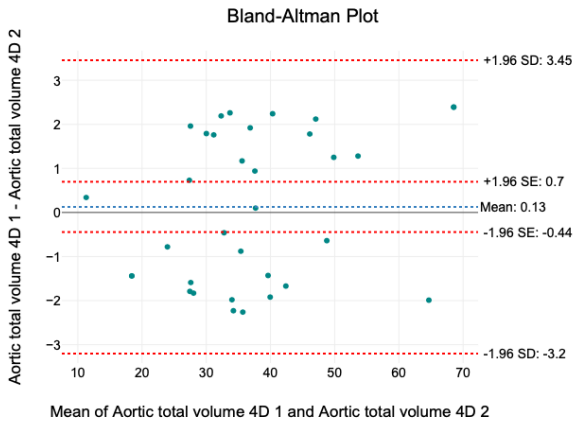


Figure 33 Bland Altman plot for Aortic root total volume (ml) on 4D between observer 1 and 2

**Total vol RPA +LPA (at the vortex)**

Total vol RPA +LPA (at the vortex) was performed by both the observers and Bland Altmann plot was drawn which showed good agreement between two observers with no interobserver variability

Table 35 Interobserver variability related to Total vol RPA +LPA (at the vortex)

| | Total vol RPA +LPA (at the vortex) (observer 1) | Total vol RPA +LPA (at the vortex) (observer 2) |
|---|---|---|
| Mean | 33.97 | 33.30 |
| Std. Deviation | 14.00 | 13.91 |
| Minimum | 11.72 | 13.1 |
| Maximum | 63.56 | 65.9 |

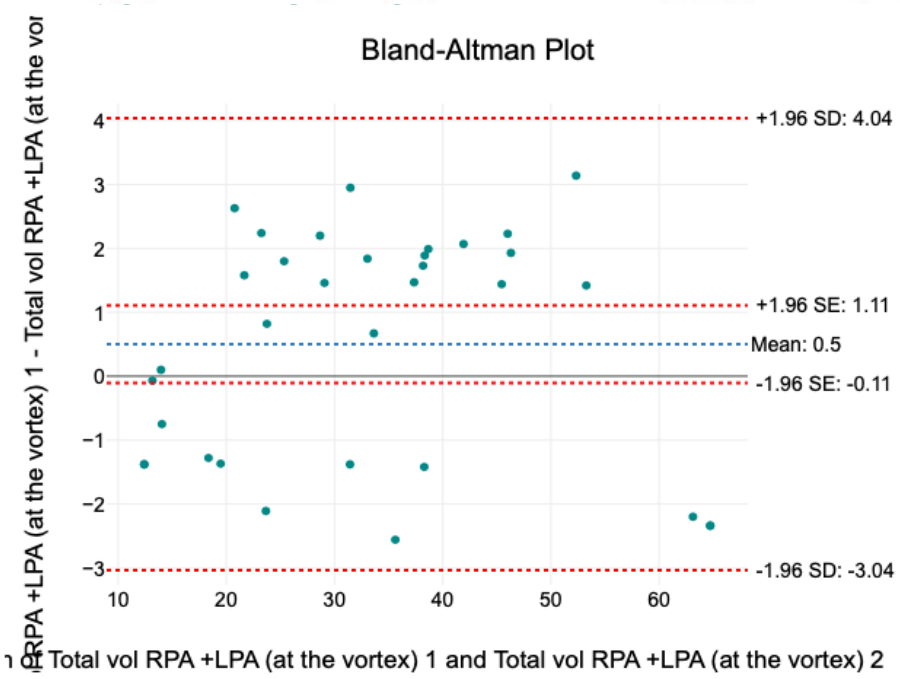


Figure 34 Bland Altman plot for Total vol RPA +LPA (at the vortex) between observer 1 and 2

**Total vol RPA +LPA (distal to the vortex)**

Total vol RPA +LPA (distal to the vortex) was performed by both the observers and Bland Altmann plot was drawn which showed good agreement between two observers with no interobserver variability

Table 36 Interobserver variability related to Total vol RPA +LPA (distal to the vortex)

| | Total vol RPA +LPA (distal to the vortex) (Observer 1) | Total vol RPA +LPA (distal to the vortex) (observer 2) |
|---|---|---|
| Mean | 38.83 | 38.18 |
| Std. Deviation | 11.85 | 11.62 |
| Minimum | 24.53 | 22.76 |
| Maximum | 72.86 | 70.8 |

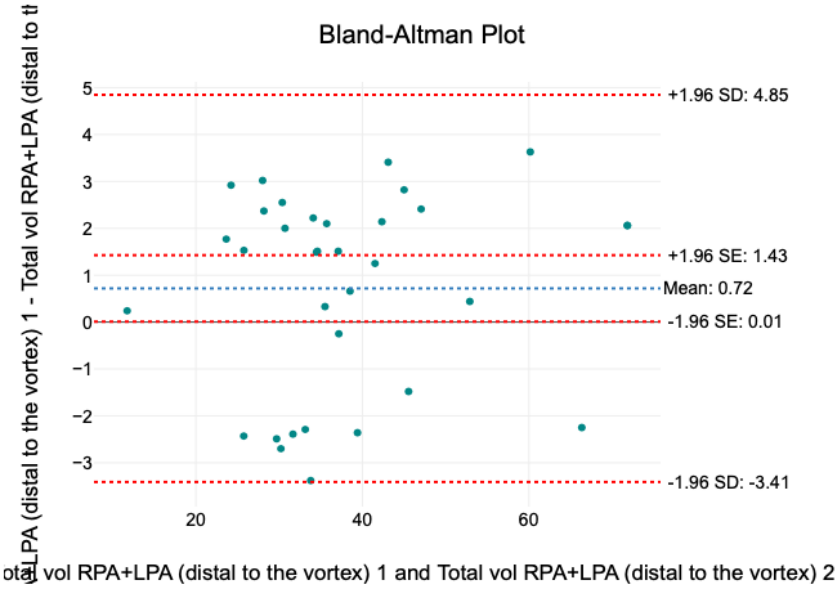


Figure 35 Bland Altman plot for Total vol RPA +LPA (distal to the vortex) between observer 1 and 2

## Representative cases showing differences between 2D PCMRI and 4D flow

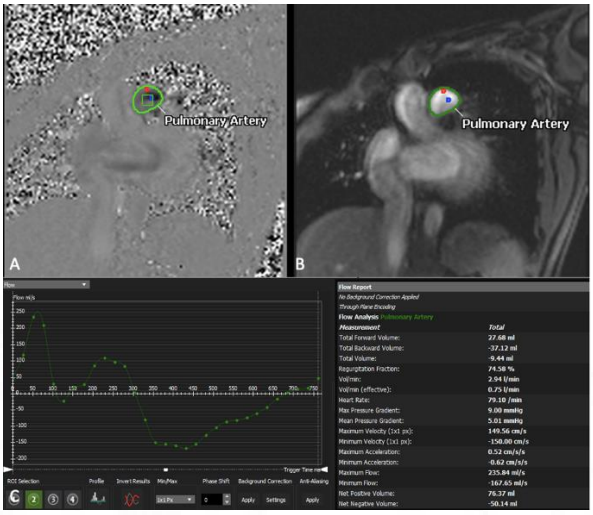


Figure 36 Pulmonary artery flow assessment using 2D PCMRI in a young adult with pulmonary regurgitation 15 years after tetralogy of Fallot repair. A and B phase-contrast and magnitude images in a plane axial to the main pulmonary artery, C showing a pulmonary regurgitation fraction of 74.58%.

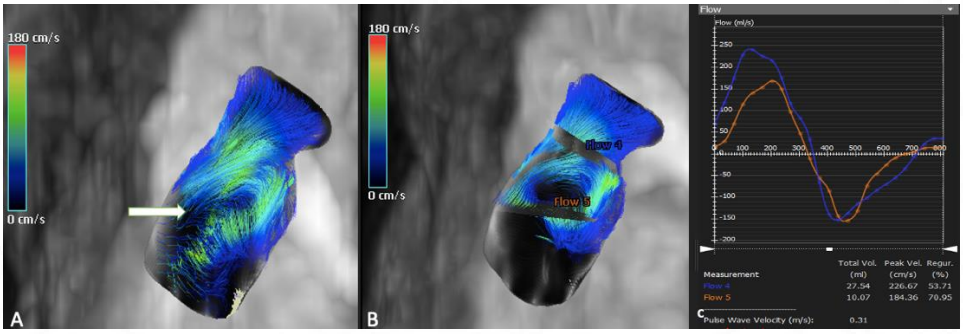


Figure 37 4D flow MRI with streamlines in the same young adult as in Fig with pulmonary regurgitation, demonstrates vortical flow (white arrow in A) in the main pulmonary artery. Streamline visualization allows avoidance of areas of vortical flow (flow 5 in B) , thus improving positioning accuracy for assessment of pulmonary

regurgitation severity. Pulmonary regurgitation (C) was estimated to be 70.95 % (flow 5 in B and C at the vortex) and 53.71% (flow 4 in B and C distal to the vortex)

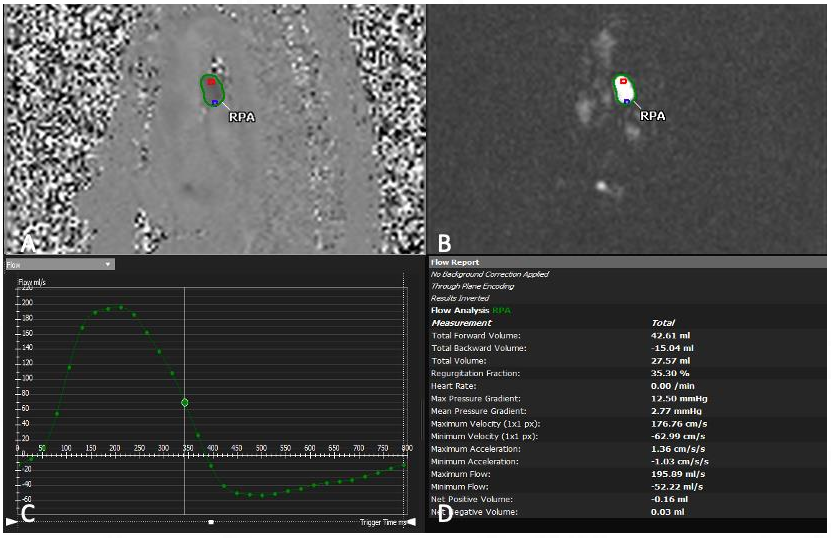


Figure 38 Right pulmonary artery flow assessment using 2D PCMRI in a young adult with pulmonary regurgitation 12 years after tetralogy of Fallot repair. A and B phase-contrast and magnitude images of RPA with C and D showing a regurgitation fraction of 35.30 %.

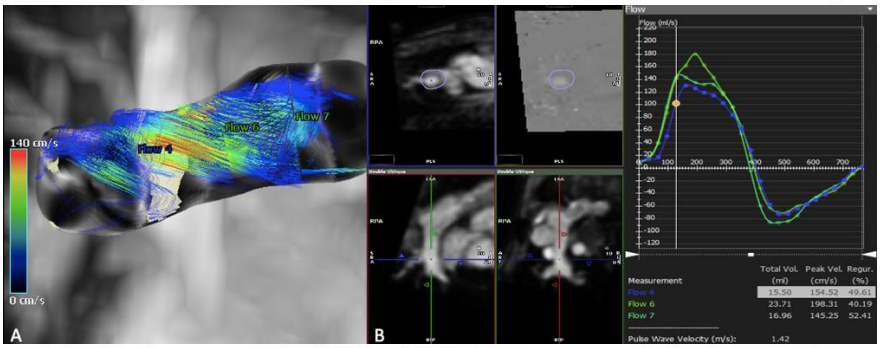


Figure 39 4D flow MRI with streamlines in the same young adult as in Fig demonstrates vortical flow (flow 7 and flow 4 in A) in the proximal and distal segments of RPA, sparing the mid portion. Streamline visualization allows avoidance of areas of vortical flow (flow 7 and flow 4 in A) , thus improving positioning accuracy for assessment of RPA regurgitation severity (flow 6 in A). RPA regurgitation (flow 6 in A) in mid segment (devoid of vortex) was estimated to be 40.19% with total volume of 23.71 ml.

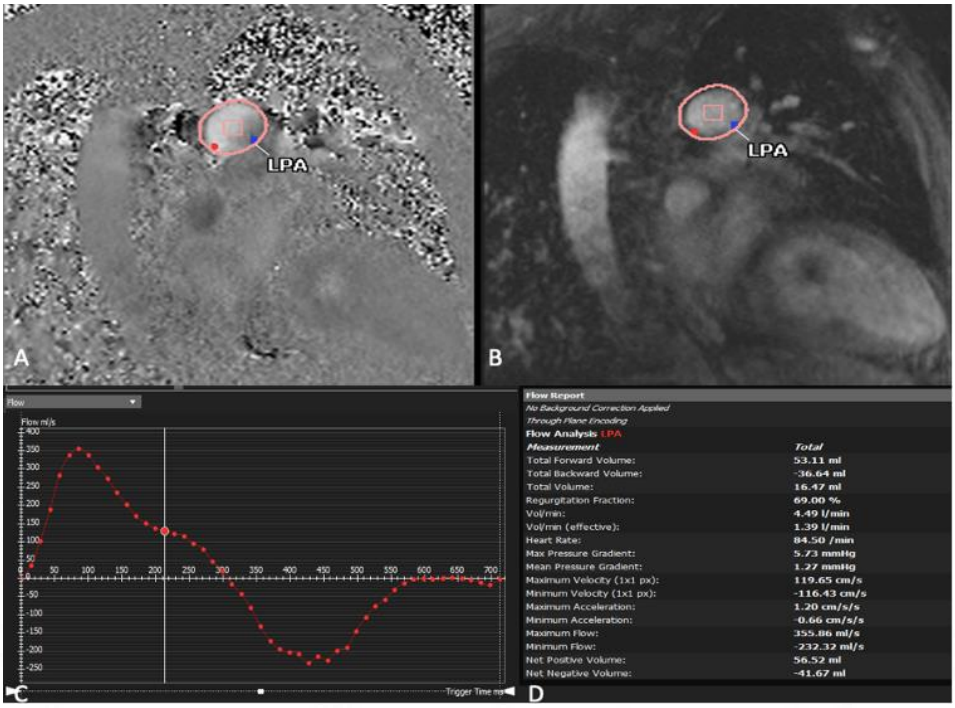


Figure 40 Left pulmonary artery flow assessment using 2D PCMRI in a young adult with pulmonary regurgitation 10 years after tetralogy of Fallot repair. A and B phase-contrast and magnitude images of LPA with C showing a regurgitation fraction of 69 %.

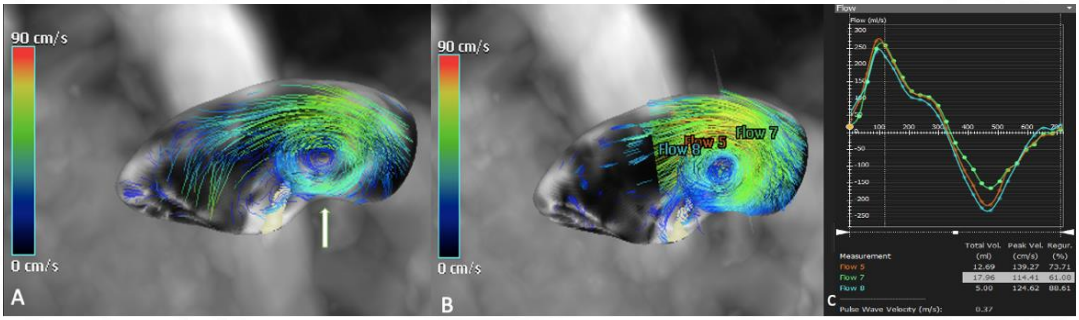


Figure 41 4D flow MRI with streamlines in the same adult as in Fig demonstrates vortical flow (white arrow in A) in the LPA. Streamline visualization allows avoidance of areas of vortical flow (flow 8 and flow 5 in B) , thus improving positioning accuracy for assessment of LPA regurgitation severity (flow 7 in B and C). LPA regurgitation (C) distal to the vortex was estimated to be 61.08% (flow 7 in B and C) with total volume of 17.96 ml.

# DISCUSSION

This single center study aimed to investigate the potential role of 4D flow CMR in a specific pathophysiologic state: PR-induced RV volume overload in a small cohort of repaired TOF patients. The main findings are

- Advanced 4D flow parameters such as WSS and EL were significantly higher in the repaired TOF patients in comparison to the controls (p value <0.001)
- There was a statistically significant difference between the PVR versus non-PVR subjects when PR was measured by 4D flow as compared to 2D PCMRI (p value <0.007)
- This is to our knowledge the first study which has considered internal validation of 4D flow with total volume of pulmonary venous blood flow and total aortic root blood flow.
- Based on the observation of abundance of vortices in the proximal RPA and LPA, our study showed that accurate calculations of 4D flow in the branch pulmonary arteries could be made distal to the vortex thus avoiding vortices and underestimation of blood volume.
- QRS duration showed a medium positive correlation with WSS in the RVOT. Thus this study demonstrated that repaired TOF patients exhibited altered hemodynamics in the pulmonary arteries and RV as characterized by peak velocity, PR, WSS and EL using 4D flow.

- There was high positive correlation and good level of agreement between 2D PCMRI and 4D flow with respect to PR in our study. Earlier 2D PCMRI studies have shown lack of reproducibility in the PR measured in just one transverse cross-section. It is postulated that 2D PCMRI may overestimate the regurgitation and underestimate the volume of blood flow due to vortices in MPA, because of intravoxel dephasing and loss of signal(Zoghbi et al., 2017). Furthermore, it is difficult to accurately scan the orthogonal cross-section of the dilated and tortuous MPA. The indirect calculation method for PRF using RV stroke volume (RVSV) and branch pulmonary flow (RVSV- MPA flow/ RVSV) is unreliable in many repaired TOF cases because of RV dilation and resulting functional TR which is often remarkable. A study by Wald et al (Wald et al., 2008) says that PR volume may be more important, reflecting the severity of regurgitation better than PRF alone. Though, there was a high, positive correlation between RVEDVi and PR on both 2D PCMRI and 4D flow, the correlation coefficient r value was higher on 4D flow, further indicating that 4D flow sequences may be superior in calculation of flow assessment. This is in accordance with a study by Isorni et al(Isorni et al., 2020). In contrast to other studies which showed overestimated results on 4D flow MRI, our study presented with a tendency towards lower values of PR in 4D than in 2D PCMRI (Mean ± Standard Deviation-49.37±14.08 on 4D Vs 50.32 ± 14.42 on 2D PCMRI)(Elsayed et al., 2021). Van der Hulst et al. (Van Der Hulst et al., 2010) also showed that 4D-flow plane measurements are more accurate than single direction 2D PCMRI for valvular flow and assessment of RV diastolic function. Also studies by Hanneman et al(Hanneman et al., 2014) and Wentland et al (Wentland et al., 2013) in other patient groups found

greater inconsistency in 2D PCMRI. Thus, similar to the above studies, our results also showed that 4D flow can retrospectively assess standard flow metrics at any heart location.

- In the present study, there was a statistically significant difference between the two groups (PVR versus subjects not undergoing PVR) when PR was measured by 4D flow (p Value 0.007) as compared to 2D PCMRI (p Value 0.09). The average value of PR by 4D flow was significantly higher in the group who had undergone PVR as compared to those who had not ( 57.53 ± 7.94 versus 43.92±14.25). This may be due to the advantages of 4D flow MRI providing both anatomical and hemodynamic values as well as blood flow visualization, thus resulting in the accurate placement of the imaging plane in MPA avoiding vortices and avoiding overestimation of PRF. Studies by Hirtler et al(Hirtler, 2016) and Geiger et al(Geiger et al., 2011) have also recommended 4D flow over multiple 2D PCMRI acquisitions for evaluating residual pulmonary stenosis, branch artery stenosis, and PR in candidates for PVR.
- Several studies have compared 4D flow with 2D PCMRI as 2D acquisition is historically well validated and standardized. However, 2D slices need to be accurately localized and the results are often inconsistent (e.g. the flows in the RPA and LPA may not add up to the flow in the MPA) due to separate breath-hold acquisitions(Elsayed et al., 2021). Hence, to avoid calculation errors, accuracy was internally validated through employing the 'conservation of mass' principle, comparing volumes that are expected to be equal in absence of valvular malfunction or shunts(Elsayed et al., 2021). All the patients in our study had mild TR and none of them had aortopulmonary collaterals. Hence, total volume of pulmonary venous blood flow was internally validated with total volume of aortic root blood flow on

4D. Similarly, total volume of aortic root blood flow was compared with net pulmonary blood flow on 2D and 4D sequences respectively (Geiger et al., 2011). Total pulmonary venous flow correlated significantly and with good level of agreement with total volume of aortic root flow on 4D. Similarly, the mean differences in the total volume of aortic and pulmonary flows on 4D were lesser as compared to 2D PCMRI. Based on the above results, total pulmonary venous blood flow on 4D was considered as ground truth or benchmark. This is, to our knowledge, the first study that quantified the total volume of pulmonary venous blood flow on 4D flow MRI and analyzed with total volume of flow across MPA on 2D PCMRI versus 4D flow MRI. This analysis showed significantly lower mean differences (Mean 2.5 ± 4.92 on 4D versus -7.2 ± 13.81 on 2D PCMRI), thus further indicating superiority of 4D flow in repaired TOF patients for assessment of total volume of blood across the MPA. In contrast, studies by Nordmeyer et al(Nordmeyer et al., 2010), Gabbour et al(Gabbour et al., 2013) reported no significant differences between 2D PCMRI and 4D flow for both antegrade and retrograde flow in pulmonary artery. Thus with a growing body of studies comparing 4D and 2D PCMRI, both over and underestimation of hemodynamic parameters measured with 4D Flow MRI have been reported for different vendors and systems in literature(Sieren et al., 2019).

- Our study reported higher peak velocities in MPA (p value-0.034), RPA (p value-0.017) and LPA ( p value-0.049) on 4D as compared to 2DPCMRI similar to other studies by Nordmeyer et al(Nordmeyer et al., 2010) and Gabbour et al(Gabbour et al., 2013). The same studies also noted better correlation with echocardiography with 4D flow than 2D PCMRI. This may be due to 4D flow assessment of the entire vessel volume(Elsayed et al., 2021). In contrast, Chelu et al(Chelu et al., 2016) reported

underestimated 4D flow peak systolic velocities.

**Qualitative advanced 4D flow parameters**

- As previously described , an important feature of 4D Flow MRI is the visualization of blood flow patterns in the vessels. With respect to the involvement of the MPA, RPA and LPA by vortices, we found that higher WSS and higher grades of vorticity extended from MPA into the branch pulmonary arteries in all the patients in our study. Pronounced vortices (grade 2) -severe helical or vortical flow(>/= 360 degrees of rotation) in the MPA were seen in 25 patients and moderate vortices (grade 1) in 5 patients. This was in agreement with studies done by Tsuchiya et al(Tsuchiya et al., 2021), Hudani et al(Hudani et al., 2023) and Geiger et al(Geiger et al., 2011). Mean vortices were maximum in MPA (average grading=1.83+_0.379) and LPA (average grading=1.8+_0.406) than RPA (average grading=1.43+_0.504). There was extension of non-laminar flow into mid and distal branch vessels in almost all cases of repaired TOF patients in contrast with a study by Geiger et al (Geiger et al., 2011). However, when vorticity was correlated with the diameter of the branch vessel, no significant p value was noted in our study, could be due to small sample size. This is in contrast to the study by Reiter et al in which he demonstrated that preexisting vortices may lead to pulmonary artery dilation(Reiter et al., 2008). He also detected a correlation between pulmonary hypertension and the appearance of vortex flow, followed by elevated pulmonary arterial pressure. This concept is also confirmed by previous 4D-MRI studies of the aorta, showing that vortices are associated with shear force alterations on the vessel wall, thus leading to changes in endothelial function, which is a predisposing factor for vascular remodelling and aortic dilatation(Frydrychowicz et al., 2008).

**Quantitative advanced 4D flow parameters**

- Advanced 4D flow parameters such as maximum and average WSS were significantly elevated in repaired TOF patients in RVOT, MPA, RPA and LPA in comparison to controls (p value<0.001). This finding is similar to a study done by Hudani et al (Hudani et al., 2023) who also reported similar values of WSS in MPA and branch pulmonary arteries. In our study, WSS was measured in the following three regions – at the proximal MPA above the pulmonary valve, mid MPA and pre bifurcation level. Maximum and average WSS in MPA were found to be of consistently higher values at the prebifurcation level in 24 patients and in proximal MPA in 5 patients. Only 1 patient showed higher WSS in mid MPA. Hudani et al (Hudani et al., 2023) reported in his study of an elevated maximum WSS with greater differences with controls at the pulmonary valve, MPA, and pre-bifurcation (p value<0.001). Average WSS was consistently elevated along the MPA at all plane locations ($p \leq 0.05$) in his study. Though we analysed the location of WSS in the repaired TOF patients, similar analysis was not done for the controls. We also found a statistically significant and positive correlation between the variables RVEDVi (mL/m2) and maximum and average WSS in MPA (p value <0.001).
- When comparing maximum and average EL with controls, repaired TOF patients showed elevated values in MPA, RPA and LPA (p value <0.001) with more significant losses observed at the proximal region of the artery and bifurcation regions. Hudani et al (Hudani et al., 2023) in his study also reported similar values of maximum and average EL in MPA and branch pulmonary arteries.
- Hudani et al (Hudani et al., 2023) reported that higher EL was found to be associated

with higher pulmonary peak velocity, which is expected as peak velocity increasing the energetic dissipation. In our study, we found a statistically significant and positive correlation between the variables RVEDVi (mL/m2) and maximum and average EL in MPA (p value <0.001). Thus, patients with higher EL in MPA tend to have higher RVEDV. As expected, due to constant pulmonary regurgitation, there is a significant expenditure of energy in MPA. Thus, EL can provide meaningful insights into the hemodynamic performance of RV.

- Evaluation of EL which basically reflects the viscous energy dissipation was an important aspect of our study(Barker et al., 2014). On the other hand, Zhao et al(Zhao et al., 2022), Zajac et al (Zajac et al., 2015), Jeong et al(Jeong et al., 2015), Robinson et al (Robinson et al., 2019) had explored the use of turbulent KE instead of EL, with higher KE in repaired TOF patients in MPA as compared to the controls. There are important differences between turbulent KE and EL. KE is given by 0.5× mV2, where m is the mass and V is the velocity and it represents the energy of an object because of its motion.
- However, when EL in MPA, RPA and LPA were compared between patients who underwent PVR versus no PVR, we could not find a statistically significant difference between the two groups. If Higher EL is related to higher RVEDV, then theoretically PVR group should have higher EL, but our analysis showed non-PVR group to have higher EL values and peak systolic velocities in MPA, RPA and LPA. RVEF showed statistically significant difference between the two groups with PVR group showing lower mean values as compared to non-PVR group (48.30±8.20 versus 57.22 ±5.58). As EL is the difference of KE in proximal versus distal aspect of the vessel, if proximal pumping which is represented by RVEF is low, proximal

KE generated will be low. This can also be validated by the lower values of peak systolic velocity in MPA, RPA and LPA in the PVR group. Another possibility of lower EL is conversion to laminar blood flow which is definitely is not the situation in repaired TOF patients due to intracardiac and intravascular vortices. However, statistically significant differences could not be achieved indicating either a study with more participants needs to be done to show the significance or factors other than EL are important in causing RV dilation.

- While assessing WSS in MPA between the patients who underwent PVR versus no PVR, we could not find a statistically significant difference between the two groups. which could be due to smaller sample size. The mean values of maximum and average WSS were comparable between the two groups, thus WSS may not be helpful in differentiating between PVR versus non- PVR group.
- The present assessment of RVOT on 2D sequence relies on its dimension. However, RVOT is a three -dimensional dilated curved structure and the accurate measurement of size can be challenging in the repaired TOF patients due to the anatomic complexity. In the present study, we found that the QRS duration showed a medium positive correlation with maximum and average WSS in the RVOT. However, QRS duration did not show any significant correlation with RVEDVi. This suggests that hemodynamic stress in the RVOT due to constant PR even in asymptomatic repaired TOF patients may be the initiating factor leading to subsequent RV dilation and dysfunction. Thus, alteration in the 4D flow derived hemodynamic parameters such as WSS may be associated with disease severity and may help in predicting patients who are prone to progressive RV failure, thus subjecting them to earlier interventions.

**Branch vessel assessment with 4D flow**

- There was a tendency to higher blood flow in the RPA in repaired TOF patients as compared to the controls ( 2.08±3.86 versus 1.43±0.24), however we could not find a statistically significant difference between the two groups which could be due to smaller sample size. This differential flow to the right and left lungs is similar to findings in previous study by Geiger et al(Geiger et al., 2011). Thus, we postulate that differential flow assessment should be practiced on a regular basis in addition to the PR assessment in MPA. RVEDVi, RVESVi, RVEF and LVEF are used for used for deciding the PVR based on Tal Geva criteria in asymptomatic patients. Differential flow also contributes to development of lung vascular changes, PAH and finally RV remodelling and thus can be included while deciding PVR among the repaired TOF patients.
- Routine 2D PMCRI calculation of blood flows in branch pulmonary arteries is done in the mid aspect where there could be vortices or turbulences. Due to capability of 4D flow to take multiple calculations, we observed the branch pulmonary artery flow analysis in three regions with progressive reduction in the regurgitation fractions and increase in the total volume of flow from proximal to distal aspects. Based on this observation, analysis was made between the total volume of pulmonary venous blood flow on 4D flow MRI and total volume of RPA +LPA flow (at the vortex versus distal to the vortex). Similar analysis was made between the right and left sided pulmonary veins with RPA and LPA (at the vortex and distal to the vortex) respectively. All the above analyses showed significantly lower mean differences with total pulmonary venous as well as ipsilateral pulmonary venous flow in the 4D sequence, as compared to the 2D PCMRI while using the 4D flow distal to vortices.

Thus, 4D flow helps in calculating the measurements in regions devoid of vortices. RPA and LPA showed higher regurgitation fractions in the proximal aspect with lower total volumes of blood flow in the region of vortices. Most of the vortices with heterogeneous flow patterns were noted in the proximal and distal segments of RPA. In our study, 24 patients showed relatively lesser degrees of vortex formation in the mid segment of RPA. Remaining 6 patients had lesser degrees of vortex formation in the distal segments of RPA. LPA showed higher vortices in the proximal segment with equal distribution of vortices in the mid and distal aspects.

# SUMMARY AND CONCLUSION

- In this single-center retrospective cross-sectional, observational study 30 repaired TOF patients were included. The symptomatology, QRS duration and associated results of cardiopulmonary exercise test (CPET) of the enrolled patients were recorded. All the patients underwent standard clinical TOF CMR protocol followed by 4D flow study of whole heart. Qualitative 4D flow analysis included gross visualization of the flow, velocity vectors, streamlines, and path lines. Quantitative analysis involved flow calculation, calculation of wall shear stress (WSS) and viscous energy loss (EL).Advanced 4D flow parameters such as maximum and average WSS were significantly elevated in repaired TOF patients in RVOT, MPA, RPA and LPA in comparison to controls (p value<0.001). When comparing maximum and average EL with controls, repaired TOF patients showed elevated values in MPA, RPA and LPA (p value <0.001) with more significant losses observed at the proximal region of the artery and bifurcation regions. A medium positive and a statistically significant correlation between QRS duration and Maximum WSS (p value=0.001) and average WSS RVOT (p value=0.002) was noted. A Pearson correlation showed a high, positive correlation between PR by 2DPCMRI and 4D flow , $r(28) = 0.87$, $p = <0.001$. A statistically significant and positive correlation was found between RVEDV and PR by 2D PCMRI (p value 0.015) and 4D flow (p value <0.001).However the correlation coefficient was higher for 4D as compared to 2D PCMRI (r=0.835 on 4D versus 0.442 on 2D). Internal validation was done between aortic root total volume and total Pulmonary venous flow on 4D. Spearman Rank correlation analysis showed a statistically significant and positive

correlation between these variables (r = 0.861, p value <0.001). Correlation analysis between aortic root total volume and total Volume of MPA blood flow on 2D and 4D sequences showed a stronger correlation (r = 851) and a much higher coefficient of determination ($R^2$ = 0.819) on 4D flow as compared to the 2D sequence (r = 670, $R^2$ = 0.508). The mean difference was significantly lower in the 4D flow, as compared to the 2D PCMRI. (Mean 2.5 ± 4.92 on 4D versus -7.2 ± 13.81 on 2D PCMRI) while assessing the total pulmonary venous blood flow via MPA total volume. While assessing the total pulmonary venous blood flow on 4D via RPA+LPA total volumes by 4D flow, the mean difference was significantly lower distal to the vortex, as compared to at the vortex (Mean -0.32 ± 5.83 versus 4.55+_13.49).There was a statistically significant difference between the PVR versus non-PVR subjects when PR was measured by 4D flow as compared to 2D PCMRI. The average value of PR by 4D flow was significantly higher in the group who had undergone PVR as compared to those who had not (Mean 57.53 versus 43.92, p value- 0.007). However, the average value of PR by 2D PCMRI was comparable in both the groups ( p value 0.09). When EL in MPA, RPA and LPA were compared between patients who underwent PVR versus no PVR, we could not find a statistically significant difference between the two groups. Our analysis showed non-PVR group to have higher EL values and peak systolic velocities in MPA, RPA and LPA. RVEF showed statistically significant difference between the two groups with PVR group showing lower mean values as compared to non-PVR group (48.30±8.20 versus 57.22 ±5.58). As EL is the difference of KE in proximal versus distal aspect of the vessel, if proximal pumping which is represented by RVEF is low, proximal KE generated will be low. This can also be validated by the lower values of peak

systolic velocity in MPA, RPA and LPA in the PVR group. However, statistically significant differences could not be achieved.

Thus, to conclude, 4D flow is highly applicable to repaired TOF patients in a single free-breathing 10–15 min acquisition. Particular strengths are better volumetric and velocity quantification. Calculations by 4D flow scores over 2D PCMRI as seen by our 4D flow analysis of total pulmonary venous blood flow and comparison between the total volume of blood in MPA on 2D PCMRI versus 4D flow. This method has the potential to compensate for the limitations of conventional PR measurements. Identification of lower EL in the PVR group in comparison with non-PVR group was a new finding and may need better evaluation with larger samples to find if lower EL corresponds to early onset RV dysfunction. Positive correlation of QRS duration with WSS in the RVOT but no significant correlation with RVEDVi may suggest that hemodynamic stress in the RVOT due to constant PR even in asymptomatic repaired TOF patients may be the initiating factor leading to subsequent RV dilation and dysfunction. Thus, alteration in the 4D flow derived hemodynamic parameters such as WSS may be associated with disease severity and may help in predicting patients who are prone to progressive RV failure, thus subjecting them to earlier interventions. More prospective, randomized, multi-centered studies are required to investigate the application of these methods in patient management.

**Strength of the study:**

- This is, to our knowledge, the first study that quantified the total volume of pulmonary venous blood flow on 4D flow MRI and analyzed with total volume of flow across MPA on 2D PCMRI versus 4D flow MRI.
- Another novel finding of this study was the observation of abundance of the vortices in proximal RPA and LPA, leading to calculation of quantitative parameters in RPA and LPA at level of vortex (proximal aspect of artery) and distal to the vortex (could be either mid or distal aspects of artery) and comparing them with total pulmonary venous blood flow.
- Another strength of the study was age matched controls for comparison.
- Analysis of the data by two observers

**Limitations**

- All the patients in our study underwent CMR in 1.5 T. Further studies are required to compare 1.5 vs 3 T in accuracy or visualization of flow parameters on 4D flow MRI.
- Limited number of subjects in our study
- Majority of the patients belonged to FC I, hence comparison of 4D flow parameters to exercise capacity and clinical outcomes in a larger cohort with heterogeneous FC is warranted.
- This was a cross sectional observational study. As Vortex flow has been corelated with pulmonary hypertension, and turbulent flow to the development of RV remodeling in repaired TOF, further follow up is required to assess significant events in such patients.

- Valve tracking at the valve locations and ventricular flow analysis and ventricular turbulent KE were not taken into consideration.
- A VENC of 200 cm/s was kept in all the patients and controls, keeping a balance between lower and higher velocities. Dual and triple VENC sequences have been developed recently to avoid aliasing in fast velocities and retain high SNR in low flow regions may be better for flow quantification.

# REFERENCES


Azarine A, Garçon P, Stansal A, et al. (2019) Four-dimensional Flow MRI: Principles and Cardiovascular Applications. *RadioGraphics* 39(3): 632–648. DOI: 10.1148/rg.2019180091.

Bailliard F and Anderson RH (2009) Tetralogy of Fallot. *Orphanet Journal of Rare Diseases* 4(1): 2. DOI: 10.1186/1750-1172-4-2.

Barker AJ, Van Ooij P, Bandi K, et al. (2014) Viscous energy loss in the presence of abnormal aortic flow: Energy Loss in the Presence of Abnormal Aortic Flow. *Magnetic Resonance in Medicine* 72(3): 620–628. DOI: 10.1002/mrm.24962.

Bédard E, McCarthy KP, Dimopoulos K, et al. (2009) Structural Abnormalities of the Pulmonary Trunk in Tetralogy of Fallot and Potential Clinical Implications. *Journal of the American College of Cardiology* 54(20): 1883–1890. DOI: 10.1016/j.jacc.2009.06.040.

Bissell MM, Raimondi F, Ait Ali L, et al. (2023) 4D Flow cardiovascular magnetic resonance consensus statement: 2023 update. *Journal of Cardiovascular Magnetic Resonance* 25(1): 40. DOI: 10.1186/s12968-023-00942-z.

Bock J, Frydrychowicz A, Stalder AF, et al. (2010) 4D phase contrast MRI at 3 T: Effect of standard and blood-pool contrast agents on SNR, PC-MRA, and blood flow visualization. *Magnetic Resonance in Medicine* 63(2): 330–338. DOI: 10.1002/mrm.22199.

Burchill LJ, Wald RM, Harris L, et al. (2011) Pulmonary Valve Replacement in Adults With Repaired Tetralogy of Fallot. *Seminars in Thoracic and Cardiovascular Surgery: Pediatric Cardiac Surgery Annual* 14(1): 92–97. DOI: 10.1053/j.pcsu.2011.01.016.

Carlsson M, Töger J, Kanski M, et al. (2011) Quantification and visualization of cardiovascular 4D velocity mapping accelerated with parallel imaging or k-t BLAST: head to head comparison and validation at 1.5 T and 3 T. *Journal of Cardiovascular Magnetic Resonance* 13(1): 55. DOI: 10.1186/1532-429X-13-55.

Chelu RG, Wanambiro KW, Hsiao A, et al. (2016) Cloud-processed 4D CMR flow imaging for pulmonary flow quantification. *European Journal of Radiology* 85(10): 1849–1856. DOI: 10.1016/j.ejrad.2016.07.018.

Cheng JY, Hanneman K, Zhang T, et al. (2016) Comprehensive motion-compensated highly accelerated 4D flow MRI with ferumoxytol enhancement for pediatric

congenital heart disease: Motion-Compensated Accelerated 4D Flow. *Journal of Magnetic Resonance Imaging* 43(6): 1355–1368. DOI: 10.1002/jmri.25106.

Dyverfeldt P, Bissell M, Barker AJ, et al. (2015) 4D flow cardiovascular magnetic resonance consensus statement. *Journal of Cardiovascular Magnetic Resonance* 17(1): 72. DOI: 10.1186/s12968-015-0174-5.

Elsayed A, Gilbert K, Scadeng M, et al. (2021) Four-dimensional flow cardiovascular magnetic resonance in tetralogy of Fallot: a systematic review. *Journal of Cardiovascular Magnetic Resonance* 23(1): 59. DOI: 10.1186/s12968-021-00745-0.

Farina S, Bruno N, Agalbato C, et al. (2018) Physiological insights of exercise hyperventilation in arterial and chronic thromboembolic pulmonary hypertension. *International Journal of Cardiology* 259: 178–182. DOI: 10.1016/j.ijcard.2017.11.023.

Fogel MA, Sundareswaran KS, de Zelicourt D, et al. (2012) Power loss and right ventricular efficiency in patients after tetralogy of Fallot repair with pulmonary insufficiency: Clinical implications. *The Journal of Thoracic and Cardiovascular Surgery* 143(6): 1279–1285. DOI: 10.1016/j.jtcvs.2011.10.066.

François CJ, Lum DP, Johnson KM, et al. (2011) Renal Arteries: Isotropic, High-Spatial-Resolution, Unenhanced MR Angiography with Three-dimensional Radial Phase Contrast. *Radiology* 258(1): 254–260. DOI: 10.1148/radiol.10100443.

François CJ, Srinivasan S, Schiebler ML, et al. (2012) 4D cardiovascular magnetic resonance velocity mapping of alterations of right heart flow patterns and main pulmonary artery hemodynamics in tetralogy of Fallot. *Journal of Cardiovascular Magnetic Resonance* 14(1): 16. DOI: 10.1186/1532-429X-14-16.

François CJ, Markl M, Schiebler ML, et al. (2013) Four-dimensional, flow-sensitive magnetic resonance imaging of blood flow patterns in thoracic aortic dissections. *The Journal of Thoracic and Cardiovascular Surgery* 145(5): 1359–1366. DOI: 10.1016/j.jtcvs.2012.07.019.

Fratz S, Chung T, Greil GF, et al. (2013) Guidelines and protocols for cardiovascular magnetic resonance in children and adults with congenital heart disease: SCMR expert consensus group on congenital heart disease. *Journal of Cardiovascular Magnetic Resonance* 15(1): 51. DOI: 10.1186/1532-429X-15-51.

Fredriksson A, Trzebiatowska-Krzynska A, Dyverfeldt P, et al. (2018) Turbulent kinetic energy in the right ventricle: Potential MR marker for risk stratification of adults with repaired Tetralogy of Fallot. *Journal of Magnetic Resonance Imaging* 47(4): 1043–1053. DOI: 10.1002/jmri.25830.

Frydrychowicz A, Berger A, Russe MF, et al. (2008) Time-resolved magnetic resonance angiography and flow-sensitive 4-dimensional magnetic resonance imaging at 3

Tesla for blood flow and wall shear stress analysis. *The Journal of Thoracic and Cardiovascular Surgery* 136(2): 400–407. DOI: 10.1016/j.jtcvs.2008.02.062.

Gabbour M, Rigsby C, Markl M, et al. (2013) Comparison of 4D flow and 2D PC MRI blood flow quantification in children and young adults with congenital heart disease. *Journal of Cardiovascular Magnetic Resonance* 15(S1): E90, 1532-429X-15-S1-E90. DOI: 10.1186/1532-429X-15-S1-E90.

Gatzoulis MA, Balaji S, Webber SA, et al. (2000) Risk factors for arrhythmia and sudden cardiac death late after repair of tetralogy of Fallot: a multicentre study. *The Lancet* 356(9234): 975–981. DOI: 10.1016/S0140-6736(00)02714-8.

Geiger J, Markl M, Jung B, et al. (2011) 4D-MR flow analysis in patients after repair for tetralogy of Fallot. *European Radiology* 21(8): 1651–1657. DOI: 10.1007/s00330-011-2108-4.

Geva T (2011) Repaired tetralogy of Fallot: the roles of cardiovascular magnetic resonance in evaluating pathophysiology and for pulmonary valve replacement decision support. *Journal of Cardiovascular Magnetic Resonance* 13(1): 9. DOI: 10.1186/1532-429X-13-9.

Giese D, Wong J, Greil GF, et al. (2014) Towards highly accelerated Cartesian time-resolved 3D flow cardiovascular magnetic resonance in the clinical setting. *Journal of Cardiovascular Magnetic Resonance* 16(1): 42. DOI: 10.1186/1532-429X-16-42.

Ha H, Kim GB, Kweon J, et al. (2016) Hemodynamic Measurement Using Four-Dimensional Phase-Contrast MRI: Quantification of Hemodynamic Parameters and Clinical Applications. *Korean Journal of Radiology* 17(4): 445. DOI: 10.3348/kjr.2016.17.4.445.

Hanneman K, Sivagnanam M, Nguyen ET, et al. (2014) Magnetic Resonance Assessment of Pulmonary (QP) to Systemic (QS) Flows Using 4D Phase-contrast Imaging. *Academic Radiology* 21(8): 1002–1008. DOI: 10.1016/j.acra.2014.04.012.

Hess AT, Bissell MM, Ntusi NAB, et al. (2015) Aortic 4D flow: Quantification of signal-to-noise ratio as a function of field strength and contrast enhancement for 1.5T, 3T, and 7T: Quantification of SNR in Aortic 4D Flow. *Magnetic Resonance in Medicine* 73(5): 1864–1871. DOI: 10.1002/mrm.25317.

Hirtler D (2016) Assessment of intracardiac flow and vorticity in the right heart of patients after repair of tetralogy of Fallot by flow-sensitive 4D MRI. *Eur Radiol*.

Hofman MBM, Visser FC, Van Rossum AC, et al. (1995) In Vivo Validation of Magnetic Resonance Blood Volume Flow Measurements with Limited Spatial Resolution in Small Vessels. *Magnetic Resonance in Medicine* 33(6): 778–784. DOI: 10.1002/mrm.1910330606.

Hsiao A, Alley MT, Massaband P, et al. (2011) Improved cardiovascular flow quantification with time-resolved volumetric phase-contrast MRI. *Pediatric Radiology* 41(6): 711–720. DOI: 10.1007/s00247-010-1932-z.

Hudani A, Ihsan Ali S, Patton D, et al. (2023) 4D-Flow MRI Characterization of Pulmonary Flow in Repaired Tetralogy of Fallot. *Applied Sciences* 13(5): 2810. DOI: 10.3390/app13052810.

Isorni MA, Martins D, Ben Moussa N, et al. (2020) 4D flow MRI versus conventional 2D for measuring pulmonary flow after Tetralogy of Fallot repair. *International Journal of Cardiology* 300: 132–136. DOI: 10.1016/j.ijcard.2019.10.030.

Jacobs KG, Chan FP, Cheng JY, et al. (2020) 4D flow vs. 2D cardiac MRI for the evaluation of pulmonary regurgitation and ventricular volume in repaired tetralogy of Fallot: a retrospective case control study. *The International Journal of Cardiovascular Imaging* 36(4): 657–669. DOI: 10.1007/s10554-019-01751-1.

Jeong D, Anagnostopoulos PV, Roldan-Alzate A, et al. (2015) Ventricular kinetic energy may provide a novel noninvasive way to assess ventricular performance in patients with repaired tetralogy of Fallot. *The Journal of Thoracic and Cardiovascular Surgery* 149(5): 1339–1347. DOI: 10.1016/j.jtcvs.2014.11.085.

Knauth AL, Gauvreau K, Powell AJ, et al. (2008) Ventricular size and function assessed by cardiac MRI predict major adverse clinical outcomes late after tetralogy of Fallot repair. *Heart* 94(2): 211–216. DOI: 10.1136/hrt.2006.104745.

Lee S, Kim YJ, Jung JW, et al. (2019) Evaluation of Flow Pattern in the Ascending Aorta in Patients with Repaired Tetralogy of Fallot Using Four-Dimensional Flow Magnetic Resonance Imaging. *Korean Journal of Radiology* 20(9): 1334. DOI: 10.3348/kjr.2019.0096.

Marelli AJ, Mackie AS, Ionescu-Ittu R, et al. (2007) Congenital Heart Disease in the General Population: Changing Prevalence and Age Distribution. *Circulation* 115(2): 163–172. DOI: 10.1161/CIRCULATIONAHA.106.627224.

Markl M, Frydrychowicz A, Kozerke S, et al. (2012) 4D flow MRI. *Journal of Magnetic Resonance Imaging* 36(5): 1015–1036. DOI: 10.1002/jmri.23632.

Mbbs SB (2008) Review Article Indications for Electrophysiology Study in children. *Indian Pacing and Electrophysiology Journal*.

Neuhaus E, Weiss K, Bastkowski R, et al. (2019) Accelerated aortic 4D flow cardiovascular magnetic resonance using compressed sensing: applicability, validation and clinical integration. *Journal of Cardiovascular Magnetic Resonance* 21(1): 65. DOI: 10.1186/s12968-019-0573-0.

Nordmeyer S, Riesenkampff E, Crelier G, et al. (2010) Flow-sensitive four-dimensional cine magnetic resonance imaging for offline blood flow quantification in multiple

vessels: A validation study. *Journal of Magnetic Resonance Imaging* 32(3): 677–683. DOI: 10.1002/jmri.22280.

Reiter G, Reiter U, Kovacs G, et al. (2008) Magnetic Resonance–Derived 3-Dimensional Blood Flow Patterns in the Main Pulmonary Artery as a Marker of Pulmonary Hypertension and a Measure of Elevated Mean Pulmonary Arterial Pressure. *Circulation: Cardiovascular Imaging* 1(1): 23–30. DOI: 10.1161/CIRCIMAGING.108.780247.

Robinson JD, Rose MJ, Joh M, et al. (2019) 4-D flow magnetic-resonance-imaging-derived energetic biomarkers are abnormal in children with repaired tetralogy of Fallot and associated with disease severity. *Pediatric Radiology* 49(3): 308–317. DOI: 10.1007/s00247-018-4312-8.

Schnell S, Markl M, Entezari P, et al. (2014) *k-t* GRAPPA accelerated four-dimensional flow MRI in the aorta: Effect on scan time, image quality, and quantification of flow and wall shear stress: *k-t* GRAPPA Acceleration and Hemodynamics. *Magnetic Resonance in Medicine* 72(2): 522–533. DOI: 10.1002/mrm.24925.

Sieren MM, Berlin C, Oechtering TH, et al. (2019) Comparison of 4D Flow MRI to 2D Flow MRI in the pulmonary arteries in healthy volunteers and patients with pulmonary hypertension. *PLOS ONE* Chen X (ed.) 14(10): e0224121. DOI: 10.1371/journal.pone.0224121.

Smith CA, McCracken C, Thomas AS, et al. (2019) Long-term Outcomes of Tetralogy of Fallot: A Study From the Pediatric Cardiac Care Consortium. *JAMA Cardiology* 4(1): 34. DOI: 10.1001/jamacardio.2018.4255.

Sträter A, Huber A, Rudolph J, et al. (2018) 4D-Flow MRI: Technique and Applications. *RöFo - Fortschritte auf dem Gebiet der Röntgenstrahlen und der bildgebenden Verfahren* 190(11): 1025–1035. DOI: 10.1055/a-0647-2021.

Tariq U, Hsiao A, Alley M, et al. (2013) Venous and arterial flow quantification are equally accurate and precise with parallel imaging compressed sensing 4D phase contrast MRI. *Journal of Magnetic Resonance Imaging* 37(6): 1419–1426. DOI: 10.1002/jmri.23936.

Tsuchiya N, Nagao M, Shiina Y, et al. (2021) Circulation derived from 4D flow MRI correlates with right ventricular dysfunction in patients with tetralogy of Fallot. *Scientific Reports* 11(1): 11623. DOI: 10.1038/s41598-021-91125-2.

Valente AM and Geva T (2017) How to Image Repaired Tetralogy of Fallot. *Circulation: Cardiovascular Imaging* 10(5): e004270. DOI: 10.1161/CIRCIMAGING.116.004270.

Valvano G, Martini N, Huber A, et al. (2017) Accelerating 4D flow MRI by exploiting low-rank matrix structure and hadamard sparsity: Accelerating 4D Flow MRI by

Low-Rank Sparse Decomposition. *Magnetic Resonance in Medicine* 78(4): 1330–1341. DOI: 10.1002/mrm.26508.

Van Der Hulst AE, Westenberg JJM, Kroft LJM, et al. (2010) Tetralogy of Fallot: 3D Velocity-encoded MR Imaging for Evaluation of Right Ventricular Valve Flow and Diastolic Function in Patients after Correction. *Radiology* 256(3): 724–734. DOI: 10.1148/radiol.10092269.

Vasanawala SS, Hanneman K, Alley MT, et al. (2015) Congenital heart disease assessment with 4D flow MRI: CHD Assessment for 4D Flow. *Journal of Magnetic Resonance Imaging* 42(4): 870–886. DOI: 10.1002/jmri.24856.

Wald RM, Redington AN, Pereira A, et al. (2008) Refining the assessment of pulmonary regurgitation in adults after tetralogy of Fallot repair: should we be measuring regurgitant fraction or regurgitant volume? *European Heart Journal* 30(3): 356–361. DOI: 10.1093/eurheartj/ehn595.

Wentland AL, Grist TM and Wieben O (2013) Repeatability and Internal Consistency of Abdominal 2D and 4D Phase Contrast MR Flow Measurements. *Academic Radiology* 20(6): 699–704. DOI: 10.1016/j.acra.2012.12.019.

Wymer DT, Patel KP, Burke WF, et al. (2020) Phase-Contrast MRI: Physics, Techniques, and Clinical Applications. *RadioGraphics* 40(1): 122–140. DOI: 10.1148/rg.2020190039.

Zajac J, Eriksson J, Dyverfeldt P, et al. (2015) Turbulent kinetic energy in normal and myopathic left ventricles: Turbulent Flow in Normal and Myopathic Hearts. *Journal of Magnetic Resonance Imaging* 41(4): 1021–1029. DOI: 10.1002/jmri.24633.

Zhao X, Hu L, Leng S, et al. (2022) Ventricular flow analysis and its association with exertional capacity in repaired tetralogy of Fallot: 4D flow cardiovascular magnetic resonance study. *Journal of Cardiovascular Magnetic Resonance* 24(1): 4. DOI: 10.1186/s12968-021-00832-2.

Zoghbi WA, Adams D, Bonow RO, et al. (2017) Recommendations for Noninvasive Evaluation of Native Valvular Regurgitation. *Journal of the American Society of Echocardiography* 30(4): 303–371. DOI: 10.1016/j.echo.2017.01.007.

## ANNEXURES

**Patient Information Sheet**

**TITLE OF THE STUDY:** Four-Dimensional Cardiovascular Magnetic Resonance flow analysis and velocity mapping of alterations of right heart flow patterns and main pulmonary artery hemodynamics in patients with repaired Tetralogy of Fallot

Study number**:** .....

Participant's name: .....

Date of Birth / Age (in years): .....son/daughter of .....

You have been informed that you are suffering from a congenital heart disease Tetralogy of Fallot for which surgery had been done. You have been asked for three yearly follow-up by Cardiac MRI which provides information regarding velocities and amount of blood flowing through the cardiac chamber and arteries. 4D flow by MRI is a new technique which takes an additional time of five minutes for evaluating the hemodynamic parameters at an earlier stage where in timely intervention can be done and condition of the patient can be improved. Also, MRI is advantageous as there is no radiation and the contrast used in MRI is safe. You are being requested to participate in a study to evaluate Four-Dimensional Cardiovascular Magnetic Resonance flow analysis and velocity mapping of alterations of right heart flow patterns and main pulmonary artery hemodynamics in patients with repaired Tetralogy of Fallot. Participating in this study, in which only data from the investigations you have undergone for your treatment will be used, may influence treatment decisions.

**What is 4D flow MRI and does it have any harmful effects?**

MRI is an imaging technique in which radio waves are used. A powerful magnet linked to a computer is used to make detailed pictures of areas inside the body. 4D flow is an advanced imaging technique in which blood flow in the heart chambers will be assessed. Speed of the blood, the amount of blood flowing in the right ventricle and main pulmonary artery and pressure exerted by the flowing blood will be assessed. This MRI is a safe imaging technique and there are no harmful effects. This study is vital in assessing complications post-surgery and planning for further treatment.

**If you take part what will you have to do?**

For this study, we will be using some of the data like history, other clinical details, Imaging and treatment details. No additional cost will be incurred /no additional drugs will be used and there are no additional risks as a part of the research. Analysis of these data may or may not be useful for you later, but this is likely to give more understanding of the alteration in various hemodynamic parameters in patients with repaired TOF. This will help in guiding timely interventions. It would also be of help to the future generations. You understand that strict confidentiality will be maintained

**Can you withdraw from this study after it starts?**

Your participation in this study is entirely voluntary and you are also free to decide to withdraw permission to participate in this study. If you do so, this will not affect your usual treatment at this hospital in any way.

**What will happen if you develop any study related injury?**

This study only analyses the results of your investigation and treatment details and thus we do not expect any injury to happen to you but if you do develop any side effects or problems due to the study, these will be treated at this institute by the experienced team of medical professionals. We are unable to provide any monetary compensation, however.

**Will you have to pay for the study?**

The study will only analyse the results of the investigations and treatment which you will undergo in natural process of your treatment at this institute and no extra cost will be borne by you for this particular study.

**What happens after the study is over?**

You may or may not benefit from this study. After the study we will be able to assess the hemodynamic parameters by 4D flow MRI. If any abnormality is detected by MRI, it will help in deciding treatment options at an earlier stage. It may also benefit other patients with similar illness.

**Will your personal details be kept confidential?**

The results of this study may be published in a medical journal but you will not be identified by name in any publication or presentation of results. However, your medical notes may be reviewed by people associated with the study, without your additional permission, should you decide to participate in this study.

**If you have any further questions, please ask Dr. Karmakar Deepmala Kalyankumar (Tel: 8355994050) or email: kardeepmala@sctimst.ac.in/ contact IEC member secretary (Tel: 0471- 2524689)**

**Patient Consent Form**

**CONSENT FORM**

**TITLE OF THE STUDY**: Four-Dimensional Cardiovascular Magnetic Resonance flow analysis and velocity mapping of alterations of right heart flow patterns and main pulmonary artery hemodynamics in patients with repaired Tetralogy of Fallot

Study number: .....

Participant's name: .....

Date of Birth / Age (in years): .....

I..... Son/daughter of ..... (Please tick boxes)

- Declare that I have read the above information provided to me regarding the study: "Four-Dimensional Cardiovascular Magnetic Resonance flow analysis and velocity mapping of alterations of right heart flow patterns and main pulmonary artery hemodynamics in patients with repaired Tetralogy of Fallot and have clarified any doubts that I had. [ ]
- I also understand that my participation in this study is entirely voluntary and that I am free to withdraw permission to continue to participate at any time without affecting my usual treatment or my legal rights. [ ]
- I also understand that study investigators will be using some of the data like history and other clinical details, Imaging details (Cardiac MRI) delayed follow up clinical and radiological regarding the disease and treatment which I undergo in hospital. [ ]
- I also understand that no additional cost will be incurred /no additional drugs will be used and there are no additional risks as a part of the research. [ ]

- I understand that the study staff and institutional ethics committee members will not need my permission to look at my health records even if I withdraw from the trial. I agree to this access. []
- I understand that my identity will not be revealed in any information released to third parties or published. [ ]

- I voluntarily agree to take part in this study. [ ]
- I received a copy of this signed consent form. [ ]

Name:

Signature:

Date:

Name of witness:

Relation to participant:

Date:

(Person Obtaining Consent) I attest that the requirements for informed consent for the medical research project described in this form have been satisfied. I have discussed the research project with the participant and explained to him or her in nontechnical terms all of the information contained in this informed consent form, including any risks and adverse reactions that may reasonably be expected to occur. I further certify that I encouraged the participant to ask questions and that all questions asked were answered.

.....

Name and Signature of Person Obtaining Consent Principal Investigator.

For any clarifications regarding the study's ethics clearance you may contact the Member Secretary of the SCTIMST-IEC. The phone number is: 0471-2524689 and the email id is iec.mem.sec@sctimst.ac.in

श्री चित्रा तिरुनाल आयुर्विज्ञान और प्रौद्योगिकी संस्थान, त्रिवेन्द्रम
तिरुवनन्तपुरम - ६९५०११, केरल, इंडिया
SREE CHITRA TIRUNAL INSTITUTE FOR MEDICAL SCIENCES AND TECHNOLOGY, TRIVANDRUM
Thiruvananthapuram - 695 011, Kerala, India
*(An Institute of National Importance under Govt. of India)*
Grams : Chitramet, Phone : +91-471-2443152, Fax : +91-471-2550728 / 2446433, E-mail : sct@sctimst.ac.in, Website : www.sctimst.ac.in

## Institutional Ethics Committee
(IEC Regn No. ECR/189/Inst/KL/2013/RR-21)

SCT/IEC/1790/DECEMBER-2021 30.12.2021

**Dr. Karmakar Deepamala Kalyankumar**
Senior Resident
Department of IS & IR
SCTIMST, Thiruvananthapuram

Dear Dr. Karmakar Deepamala Kalyankumar,

The project proposal with the title "**FOUR-DIMENSIONAL CARDIOVASCULAR MAGNETIC RESONANCE FLOW ANALYSIS AND VELOCITY MAPPING OF ALTERATIONS OF RIGHT HEART FLOW PATTERNS AND MAIN PULMONARY ARTERY HEMODYNAMICS IN PATIENTS WITH REPAIRED TETRALOGY OF FALLOT**" submitted to Institutional Ethics Committee (IEC) has been reviewed in the IEC Meeting held on 18th December, 2021 and assigned number as IEC/1790.

**List of documents submitted:**
1. Covering letter addressed to the Chairperson, IEC, SCTIMST dated 12.11.2021
2. IEC Application form
3. Declaration form
4. Consent Form in English and Malayalam
5. CV of PI and Co-PIs
6. Project Proposal
7. Proforma
8. Information Sheet in English and Malayalam
9. Checklist Form
10. SRC Approval Letter

**IEC Recommendations**

- Patient identifiers from the proforma have to be removed.
- Prospective Case control Study- (tick in appropriate box needed in study design in IEC form)
- Better to exclude patients with low GFR. (IEC form protocol and exclusion criteria is mentioned differently)
- Control may be totally normal. Control cases selection not mentioned in IEC forms and in the consent forms and patient information sheet. Data on that is being compared is not mentioned.
- Dr Deepa in the Department of Cardiology has been wrongly mentioned as Department of IS & IR. Please correct it.
- Age group of patients is not clear. Are pediatric patients included? If so Ascent is required.

One set of all the documents including those revised may be submitted. The covering letter should indicate the revisions made.

Sincerely,

**G. Srinivas**
Member Secretary, IEC

SREE CHITRA TIRUNAL INSTITUTE FOR MEDICAL SCIENCES & TECHNOLOGY
INSTITUTIONAL ETHICS COMMITTEE (IEC) SCTIMST THIRUVANANTHAPURAM

## CURRICULUM VITAE

Address : Dosti Vasudha, Dosti Vihar, Vartak Nagar, Thane(W)-400606, Maharashtra

Ph : 8355994050

Email: kardeepmala@gmail.com

Languages : English , Bengali, Marathi, Hindi, Gujrati, Malayalam

Academic Qualification:

- MBBS : Lokmanya Tilak Municipal Medical College and Sion Hospital, Mumbai ( 2010-2016)
- MD Radiodiagnosis: Seth GSMC and KEM hospital, Mumbai (2016-2019)
- Senior Resident in Topiwala National Medical College and Nair Hospital, Mumbai (2019-2020)
- DNB Radiodiagnosis (Dec 2019)
- DM Cardiovascular Imaging and Vascular Interventional Radiology (pursuing) : Sree Chitra Tirunal Institute for MedicalSciences and Technology, Trivandrum

Submitted Manuscripts for Publications :

- Case report on Persistent fifth aortic arch with aortic coarctation and bicuspid aortic valve

  -role of CT Cinematic rendering
- Case report on Left Pulmonary Artery Sling- Why is virtual CT bronchoscopy important?
- Review article on Imaging and endolymphatic interventions in lymphatic diseases

Conferences and Presentations

- Bailout DIPSS in Acute Budd Chiari Syndrome (BCS) presenting with acute liver failure and hepatic encephalopathy: A shunt road less travelled- CIRSE September 2021 (E poster)
- Imaging and interventions in endoleaks- CIRSE September 2021
- Won 2nd prize in GE Radaspire quiz 2021 (E poster)
- Comparison between 2D Phase contrast (PC) MRI and Dynamic contrast Perfusion to assess differential lung perfusion in patients with corrected Tetralogy of Fallot, IACI 12th Annual Conference, Goa October 2022, Oral Paper Presentation
- Pictorial review of congenital anomalies with tracheobronchial and esophageal compression in IACI 12th Annual Conference, Goa October 2022, educational exhibit
- Won 1st prize in CT Quiz in IACI 12th Annual Conference, Goa October 2022.
- Won Sirius ISVIR 2023, Kerala- Percutaneous closure of a congenital intrahepatic portosystemic shunt using a novel technique
- Prediction of tumor response via a pretreatment MRI radiomics-based nomogram(T2WI) in HCC treated with TACE- A retrospective study- Oral paper presentation in ISVIR Feb 2023
- Interventional management of congenital and acquired lymphatic disorders- E poster in ISVIR Feb 2023.
- SAFARI technique to treat chronic critical limb ischemia- CMC Vellore CME in April 2023
- Case presentation on Spinal cord ischemia in Crawford Type 1 TAAA in ISVIR Midterm CME 2023

RE-2022-164591-plag-report

ORIGINALITY REPORT

| 9 % | 4% | 4% | 1% |
|---|---|---|---|
| SIMILARITY INDEX | INTERNET SOURCES | PUBLICATIONS | STUDENT PAPERS |

PRIMARY SOURCES

| | | |
|---|---|---|
| 1 | Kotomi Iwata, Tetsuro Sekine, Junya Matsuda, Masaki Tachi et al. "Measurement of Turbulent Kinetic Energy in Hypertrophic | <1% |
| 2 | Cardiomyopathy Using Triple-velocity Encoding 4D Flow MR Imaging", Magnetic Resonance in Medical Sciences, 2022<br>Publication | <1% |
| 3 | Ashifa Hudani, Safia Ihsan Ali, David Patton, Kimberley A. Myers, Nowell M. Fine, James A. White, Steven Greenway, Julio Garcia. "4D-Flow MRI Characterization of Pulmonary Flow in Repaired Tetralogy of Fallot", Applied Sciences, 2023<br>Publication | <1% |
| 4 | "Multimodality Imaging Innovations In Adult Congenital Heart Disease", Springer Science and Business Media LLC, 2021<br>Publication | <1% |